2019

THERMODYNAMIC MODELING AND EQUILIBRIUM SYSTEM DESIGN OF A SOLVENT EXTRACTION PROCESS FOR DILUTE RARE EARTH SOLUTIONS

Alind Chandra
University of Kentucky, alind.chandra@outlook.com
Digital Object Identifier: https://doi.org/10.13023/etd.2020.004

STUDENT AGREEMENT:

I represent that my thesis or dissertation and abstract are my original work. Proper attribution has been given to all outside sources. I understand that I am solely responsible for obtaining any needed copyright permissions. I have obtained needed written permission statement(s) from the owner(s) of each third-party copyrighted matter to be included in my work, allowing electronic distribution (if such use is not permitted by the fair use doctrine) which will be submitted to UKnowledge as Additional File.

I hereby grant to The University of Kentucky and its agents the irrevocable, non-exclusive, and royalty-free license to archive and make accessible my work in whole or in part in all forms of media, now or hereafter known. I agree that the document mentioned above may be made available immediately for worldwide access unless an embargo applies.

I retain all other ownership rights to the copyright of my work. I also retain the right to use in future works (such as articles or books) all or part of my work. I understand that I am free to register the copyright to my work.

REVIEW, APPROVAL AND ACCEPTANCE

The document mentioned above has been reviewed and accepted by the student's advisor, on behalf of the advisory committee, and by the Director of Graduate Studies (DGS), on behalf of the program; we verify that this is the final, approved version of the student's thesis including all changes required by the advisory committee. The undersigned agree to abide by the statements above.

Alind Chandra, Student

Dr. Rick Honaker, Major Professor

Dr. Zach Agioutantis, Director of Graduate Studies

THERMODYNAMIC MODELING AND EQUILIBRIUM SYSTEM DESIGN OF A SOLVENT EXTRACTION PROCESS FOR DILUTE RARE EARTH SOLUTIONS

DISSERTATION

A dissertation submitted in partial fulfillment of the
requirement for the degree of Doctor of Philosophy in the
College of Engineering at the University of Kentucky

By

Alind Chandra

Lexington, Kentucky

Co-Directors : Dr. Rick Q. Honaker, Professor of Mining Engineering

and : Dr. Joshua Werner, Assistant Professor of Mining Engineering

Lexington, Kentucky

2019

ABSTRACT OF DISSERTATION

THERMODYNAMIC MODELING AND EQUILIBRIUM SYSTEM DESIGN OF A SOLVENT EXTRACTION PROCESS FOR DILUTE RARE EARTH SOLUTIONS

Rare earth elements (REEs) are a group of 15 elements in the lanthanide series along with scandium and yttrium. They are often grouped together because of their similar chemical properties. As a result of their increased application in advanced technologies and electronics including electric vehicles, the demand of REEs and other critical elements has increased in recent decades and is expected to significantly grow over the next decade. As the majority of REEs are produced and utilized within the manufacturing industry in China, concerns over future supplies to support national defense technologies and associated manufacturing industries has generated interest in the recovery of REEs from alternate sources such as coal and recycling.

A solvent extraction (SX) process and circuit was developed to concentrate REEs from dilute pregnant leach solutions containing low concentrations of REEs and high concentrations of contaminant ions. The separation processes used for concentrating REEs from leachates generated by conventional sources are not directly applicable to the PLS generated from coal-based sources due to their substantially different composition. Parametric effects associated with the SX process were evaluated and optimized using a model test solution produced based on the composition of typical pregnant leach solution (PLS) generated from the leaching of pre-combustion, bituminous coal-based sources. Di-2(ethylhexyl) phosphoric acid (DEHPA) was used as the extractant to selectively transfer the REEs in the PLS from the aqueous phase to the organic phase. The tests performed on the model PLS found that reduction of Fe^{3+} to Fe^{2+} prior to introduction to the SX process provided a four-fold improvement in the rejection of iron during the first loading stage in the SX circuit. The performances on the model system confirmed that the SX process was capable of recovering and concentrating the REEs from a dilute PLS source. Subsequently, the process and optimized parametric values were tested on

a continuous basis in a pilot-scale facility using PLS generated from coal coarse refuse. The continuous SX system was comprised of a train of 10 conventional mixer settlers having a volume of 10 liters each. A rare earth oxide (REO) concentrate containing 94.5% by weight REO was generated using a two- stage (rougher and cleaner) solvent extraction process followed by oxalic acid precipitation.

The laboratory evaluations using the model PLS revealed issues associated with a third phase formation. Tributyl Phosphate (TBP) is commonly used as a phase modifier in the organic phase to improve the phase separation characteristics and prevent the formation of a third phase. The current study found that the addition of TBP affected the equilibrium extraction behavior of REE as well as the contaminant elements., The effect on each metals was found to be different which resulted in a significant impact on the separation efficiency achieved between individual REEs as well as for REEs and the contaminant elements. The effect of TBP was studied using concentrations of 1% and 2% by volume in the organic phase. A Fourier Transform Infrared (FTIR) analysis on the mixture of TBP and DEHPA and experimental data quantifying the change in the extraction equilibrium for each element provided insight into their interaction and an explanation for the change in the extraction behavior of each metal. The characteristic peak of P-O-C from 1033 cm^{-1} in pure DEHPA to 1049 cm^{-1} in the 5%DEHPA-1%TBP mixture which indicated that the bond P-O got shorter suggesting that the addition of TBP resulted in the breaking of the dimeric structure of the DEHPA and formation of a TBP-DEHPA associated molecule with hydrogen bonding.

The experimental work leading to a novel SX circuit to treat dilute PLS sources was primarily focused on the separation of REEs from contaminant elements to produce a high purity rare earth oxide mix product. The next step in the process was the production of individual REE concentrates. To identify the conditions needed to achieve this objective, a thermodynamic model was developed for the prediction of distribution coefficients associated with each lanthanide using a cation exchange extractant. The model utilized the initial conditions of the system to estimate the lanthanide complexation and the non-idealities in both aqueous and organic phases to calculate the distribution coefficients. The non-ideality associated with the ions in the aqueous phase was estimated using the Bromley activity coefficient model, whereas the non-ideality in the organic phase was computed as the ratio of the activity coefficient of

the extractant molecule and the metal extractant molecule in the organic phase which was calculated as a function of the dimeric concentration of the free extractant in the organic phase. To validate the model, distribution coefficients were predicted and experimentally determined for a lanthanum chloride solution using DEHPA as the extractant. The correlation coefficient defining the agreement of the model predictions with the experimental date was 0.996, which is validated the accuracy of the model. As such, the developed model can be used to design solvent extraction processes for separation of individual metals without having to generate a large amount of experimental data for distribution coefficients under different conditions.

KEYWORDS: rare earth elements, solvent extraction, distribution coefficient modeling, DEHPA, TBP

Alind Chandra

(Author's Name)

12/04/2019

(Date)

THERMODYNAMIC MODELING AND EQUILIBRIUM SYSTEM DESIGN OF A SOLVENT EXTRACTION PROCESS FOR DILUTE RARE EARTH SOLUTIONS

By

Alind Chandra

Dr. Rick Honaker

(Co-Director of Dissertation)

Dr. Joshua Werner

(Co-Director of Dissertation)

Dr. Zacharias Agioutantis

(Director of Graduate Studies)

12/04/2019

(Date)

ACKNOWLEDGMENTS

I want to express my most sincere gratitude to my advisor Dr. Rick Honaker, for guiding and supporting me in my Ph.D. He always encouraged me to achieve my goals and dreams throughout my Ph.D. and motivated me by his dedication towards research and excellence. He has played the most significant role in shaping my professional career, and I will always be grateful to him for this opportunity. I would also like to thank my co-advisor, Dr. Joshua Werner, for always pushing my boundaries and challenging me to work outside my comfort zone. His enthusiasm and zeal for excellence inspired me to achieve my personal goals.

I want to extend gratitude to Dr. John Groppo, Dr. Chad Risko, and Dr. Matthew Beck for dedicating their time and energy to serve on my advisory committee. Dr. Groppo taught me about the fundamentals of surface chemistry and hydrometallurgy, as well as gave me insights about experimental techniques and laboratory setup, which helped me immensely during the initial period of my grad school. I would like to especially thank Dr. Risko for giving me insights about the fundamentals of thermodynamics, not only by welcoming me to sit in his class but also by having numerous discussions after classes, which helped me understand the nuances of the solution chemistry.

I want to thank John May and Megan Combs at the Environmental Research and Training Laboratory for teaching me valuable analytical techniques and helping me analyze thousands of samples to support my study. I would also like to thank Jason Backus at KGS for providing various analytical support, which helped me much in my research.

I want to express my gratitude to all the faculty and staff at the Department of Mining Engineering for supporting me and guiding me for the last four and a half years. I would like to especially thank my colleagues, Dr. Wencai Zhang, Dr. Xinbo Yang, and Dr. Honghu Tang, for providing valuable insights and help for my research efforts. I would also like to thank my fellow graduate students and friends I made during my stay at Lexington. I acknowledge Tushar Gupta, Anand Kumar, Kayla Mayfield, Douglas Addo, and Dr. Ashish Kumar, among others who made my stay in Lexington very enjoyable and fun.

I want to dedicate this dissertation to Ms. Murchhana Roy for tolerating my endless tantrums and helped me get through this agonizing period in the most positive way.

At last, I would like to express my deepest love and appreciation to my parents, Mr. Anoop Raj and Mrs. Rachna Raj, along with my sister Mrs. Anindya Verma. They have been nothing but supportive of all my choices for career development to pursue an advanced degree overseas. Their unconditional love is one of my greatest power whenever I go through any difficulties.

TABLE OF CONTENTS

LIST OF TABLES

LIST OF FIGURES

1 INTRODUCTION

1.1 Background

The rare earth elements (REEs) are a group of 15 lanthanide series elements and two transition elements, scandium (atomic number 21) and Yttrium (atomic number 39). The demand for high purity REEs has grown exponentially in recent years and is used in advanced electronics, the lighting industry, energy generation, and military equipment. The majority of the REE resources currently being exploited are natural resources (primary resources). However, due to the current low market values for the REEs and the relatively high cost for recovery and concentration, substantial research is being undertaken to evaluate the technical and economic feasibility of recovering REEs such as coal-based sources.

Coal has been shown to be a potential alternative source of REEs with certain coal seam sources having REE concentrations in the range of 0.1 to 0.5% by weight[1, 2]. The REE concentrations typically associated with coal are low relative to rare earth mineral ore feeding REE commercial plants. However, due to the vast amounts of coal which is mined annually, the absolute amount of REEs makes coal a viable source, Based on a study conducted by Luttrell et al. [3]U.S. coal plants produce coarse reject material containing enough REEs to meet the U.S. annual demand. Given that the worldwide demand is around 120,000 tons, only around 200 coal preparation plants having an average throughput capacity equal to 20 plants in the survey would be needed to meet this demand. This observation, coupled with the fact that the REEs typically found in the coal sources are higher in value than those found in the conventional sources, makes coal a very attractive resource for REE production.

Given that the REEs are difficult to recover from coal using conventional physical processing technologies[2], hydrometallurgical processing of coal is the most promising avenue for the economic recovery of REEs from coal sources. REEs can be extracted from coal sources into an aqueous phase using acid leaching followed by separation processes to recover the REEs and reject contaminants to produce high-grade rare earth oxide (REO) concentrates that can be further processed to produce high purity individual REEs.

Solvent extraction (SX) is a separation technique that is commonly used to separate the individual REEs from a pregnant leach solution (PLS) produced from leaching of a mixed REO

concentrate[4-7]. The process utilizes differences in the relative solubilities of a solute in two immiscible liquid phases (i.e., typically an organic and an aqueous phase) to make the separation between ions, molecules, or complexes. Solvent extraction has been the preferred method by industrial practitioners since the 1960's due to its capability to separate individual REEs based on small differences in their basicity. The elemental composition of the PLS produced from coal is significantly different from those produced from conventional sources. The coal-based PLS contain significantly high concentrations of the contaminant elements such as aluminum, calcium, and iron, while having relatively low concentrations of REEs. As such, the separation of REEs from the contaminant elements is significantly difficult for coal-based leachates using separation processes used for leachates generated from conventional sources.

The current study focused on the system design of an SX process using di(2-ethylhexyl) phosphoric acid (DEHPA) as the extractant to concentrate the REEs from dilute PLS having high concentrations of contaminants. The extraction characteristics of the REEs and the contaminant species were studied in a model test solution prepared from the salts of the RE and contaminant metals. A continuous SX process circuit was designed based on batch laboratory experiments and implemented on a continuous scale on PLS generated from coal-based sources. The impact of tributyl phosphate (TBP) was studied in a series on batch extraction tests and further evaluated in the continuous system. TBP is commonly used as a phase modifier to improve the organic-aqueous phase disengagement on the extraction behavior of REE, and their separation factors with respect to contaminant species were studied using extraction tests. Finally, a thermodynamic model was developed to predict the distribution coefficient of the REEs using the initial system condition taking the lanthanide complexation and the lanthanide ion activity into consideration. Using this information, the distribution data, which is required for the development of an SX process for separation of REEs from contaminants, as well as individual REEs from PLS, can be generated without performing the time-intensive equilibrium shake-out tests in the laboratory.

1.2 **Objectives**

The overall goal of the current study was to design the SX process and circuit capable of efficiently recovering and concentrating REEs dilute PLS containing high concentrations of

contaminants and based on the data obtained from a thermodynamic model to predict the distribution coefficient for each of the REEs and the contaminants. The specific objectives of the study included:

1. Review the i) fundamentals in the literature associated with the application of the SX for lanthanides, ii) processes for concentration of REEs from PLS, iii) synergistic behavior of phase modifiers, and iv) predictive models for distribution coefficients;
2. Experimentally quantify the extraction behavior of individual REE ions with DEHPA in a model test solution created from pure salts of the metals in the presence of contaminant metals;
3. Study the effect of oxidation potential on the extraction behavior of iron with DEHPA and the related effect on the selectivity of SX;
4. Develop a batch process for concentrating REEs from dilute leachates and determine the optimum parameters of the process using leachates generated from coal-based sources;
5. Develop a continuous process for concentrating REEs from dilute leachates;
6. Evaluate the effect of the addition of the phase modifier TBP and DEHPA blend on the extraction equilibria of the REEs and the major contaminants generally present in acid leachates; and
7. Develop a predictive thermodynamic model for the distribution coefficient of the lanthanide chlorides in the DEHPA system based on the lanthanide complexation and the lanthanide ion activity in the organic and aqueous phase.

1.3 Organization

The dissertation is organized into eight chapters. The first chapter consists of a brief introduction to the background and objectives of the study. The second chapter provides a comprehensive review of the existing literature describing hydrometallurgical processing techniques for recovering and concentrating REEs as well as the fundamental understanding of the lanthanide extraction, and the mechanism of the synergism achieved using phase modifiers. It also consists of a review of the existing work done on the predictive models used to obtain distribution coefficients by empirical, semi-empirical, and chemical techniques.

The third chapter covers the experimental techniques used for testing, including the sample preparation and characterization, extraction setup, and the experimental procedures used for the study. The chapter also describes the analytical tools and instruments used for quantitative elemental analysis, activity, and potential measurement. Analysis of the test results and a detailed discussion of the studies are covered in chapters four, five, and six. Chapter four describes the studies performed for the development of a continuous SX process. Chapter five focuses on the impact that phase modifiers have on the extraction behavior of REE. Chapter six included the development of the predictive thermodynamic model for the distribution coefficients of the REEs using DEHPA. Chapters seven and eight provides a summary and conclusions from the study and recommendations for future studies related to this topic respectively.

2 LITERATURE REVIEW

2.1 Rare Earth Elements

2.1.1 Chemical properties

The rare earth elements (REE) are a group of 15 elements from lanthanide series from lanthanum (La) to lutetium (Lu) and two transition elements, scandium (Sc) and yttrium (Y)[4, 5, 8, 9]. Most of the REEs are not rare as the name suggests, rather the elements are rarely concentrated in the natural occurrence and were discovered in the eighteenth century as part of minerals which are rare in the crust. Many REEs like cerium and lanthanum are more abundant in the earth's crust than elements like silver or mercury [10-12].

The REEs share similar chemical properties due to their electronic configuration [4, 13]. REEs exhibit an electronic configuration in the form of $6s_2 5d_1 4f_{n-1}$ or $6s_2 4f_n$. The chemistry of the lanthanides is, therefore, predominantly ionic as most of the lanthanides exist as M^{3+}, with the notable exception of cerium, which has a stable +4 valence state occurring naturally along with the +3 state. The chemistry of the REEs is defined by its two characteristics, lanthanide contraction and their high basicity, which are explained in further detail in the following paragraphs[14].

The size of the lanthanide atom, as well as their corresponding ions, decreases by a value that is greater than expected with the atomic number. This phenomenon is called lanthanide contraction [4, 13, 15]. The phenomenon is attributed to less than perfect shielding of the electrons in the 4f shell on the electrons in the 6s shell. This contraction is a very important factor for the unique features of rare earth elements. The lanthanum trivalent ion is significantly bigger than the yttrium trivalent ion. However, due to the large lanthanide contraction, the yttrium ion is similar to the holmium-erbium size range. The similarity in ionic radius explains the strong association of the yttrium with the group of heavy REEs (HREE) [4]. The ionic radius of the scandium ion is smaller than the lanthanides even after lanthanide contraction, which explains the significantly different chemistry and different mode of occurrence of scandium than the rest of REEs [16].

One of the most important properties of the REEs for hydrometallurgy is the basicity of the elements of the group[17, 18]. The property is directly related to its ionic radius and its charge density. Basicity is defined as the tendency of the ion to act as a proton acceptor. Therefore, the lower the charge density of the ion, the higher its basicity. The basicity of the REEs decreases with the atomic number. The basicity of the ions dictates the extent of hydrolysis of the ions in solution, the solubilities of different salts, and the stability of different complexes formed by the ions in solution. Almost all the separation processes for individual REEs utilize the difference in the basicity of REE ions[6, 19-23].

Owing to their very similar chemical behavior and occurrence in natural sources, REEs are often grouped together as a single group. There are, however, several schemes that are used for the classification of REEs. International Union for Pure and Applied Chemistry (IUPAC) classifies REEs according to atomic numbers as light rare earth elements (LREE), which include elements from lanthanum to samarium, and heavy rare earth elements (HREE) which include elements from europium to lutetium[24]. In this classification, yttrium is considered an HREE, while scandium is considered an LREE. REEs are also categorized based on the solubility of the REE salts as the insoluble group, which includes scandium and lanthanides from lanthanum to samarium, the slightly soluble group which includes lanthanides from europium to dysprosium, and the soluble group which includes lanthanides from holmium to lutetium and yttrium [22]. REEs may also be classified based on Oddo-Harkins rule into odd atomic number and even atomic number elements. According to the rule, the even atomic number element is more abundant than the odd atomic number elements adjacent to it [25].

2.1.2 Occurrence of Rare Earth Elements

The natural sources of REEs can be categorized according to the geological association as deposits formed by high-temperature processes, which include carbonatites and alkaline igneous rocks, and low-temperature processes, which include mineral sands and ion-adsorption clays [4, 26-28].

2.1.2.1 Carbonatites

Carbonatites are igneous rocks containing more than 50% carbonates [29]. They are the largest source of current global REE production as the source for the four largest mines in the world: Bayan Obo [26] and Maoniuping [30, 31] in China, Mt Weld in Australia [32] and Mountain

Pass [33] in the USA are all carbonatites in nature. Carbonatites mostly include REE containing carbonates like bastnaesite, parasite, and synchysite. However, many carbonatite sources also contain REE-bearing phosphates, including monazite and apatite [27]. One of the key features of carbonatite sources is that proportionately, a very large amount of lanthanum and cerium is produced in the process of recovering the desired REEs, i.e., neodymium or dysprosium, which in turn creates an excess supply of lanthanum and cerium [1].

2.1.2.2 Alkaline Igneous Rocks

A large variety of rare earth ores fall under the alkaline igneous rocks category. The ores in this category are comprised of aluminum silicates, with some ores having magmatic origins, while others originated from hydrothermal activity [34]. The only active REE mining in this group takes place in the Lovozero agpaitic nepheline syenite complex in Russia[35]. The REE distribution in this group is much better as compared to that of the carbonatite group. The production of a significant amount of neodymium also produces a commercially attractive amount of dysprosium with relatively low amounts of cerium and lanthanum. Another key feature of these deposits is the relatively low quantities of uranium and thorium [36, 37].

2.1.2.3 Placer deposits

The placer deposits have been a major source of REEs in India and Australia[7, 38-40]. The deposits typically form due to erosion of the igneous rocks containing REEs. The placer deposits, which are commonly used for extraction of other elements like tin and titanium, are also reported to have a significant potential for REEs [41]. The biggest concern in extracting REEs from these sources is the generation of large quantities of radioactive byproducts like uranium and thorium in monazite and xenotime [27].

2.1.2.4 Ion Exchanged Clay Sources

The ion-exchanged clay deposits were formed by chemical weathering decomposition, and the dissolution of granite followed by adsorption and enrichment on clay minerals during the migration and penetration process of rare earth mineral solutions[4, 42, 43]. The minerals are, therefore, also called weathering crust elution-deposited REEs. They typically contain lower concentrations of REE (4000 ppm) as compared to rare earth mineral sources (8-9% by weight). Despite this fact, they are considered to be a very important REE source, as a large proportion of the REEs present in the source are HREEs and are relatively easily extractable

[44]. These deposits have been found in southern China in 7 districts of Jiangxi, Guangdong, Fujian, Zhejiang, Hunan, Guangxi, and Yunnan. Because of the ease of extraction, they currently comprise around 35% of the total REE production from China [43].

2.1.3 End-Use of Rare Earth Elements

The demand for the REEs has been growing steadily over recent years. Initially, the principal use of REEs was in the manufacturing of the flint for the lighters as rare earth mischmetal (an alloy of lanthanum, cerium, and neodymium). However, with the rapid technological advancement, the high purity REEs have found use in advanced electronics, power generation, and lighting, as summarized in Table 2.1. Consequently, the production for REEs has increased rapidly in recent years. The production of REO has increased from 75,500 tons in 2000 to 123,100 tons in 2016 [27]. The growth in demand in the coming years is expected to mainly come from neodymium, praseodymium, and dysprosium due to their use in electric vehicles and wind power generation [45]. According to various estimates, the demand for REEs is expected to increase to 190,000 tons by 2026 [27].

Table 2.1 List of REEs and their major end-use in the industry [46].

[46]Light REE	**Major end-use**	**Heavy REE**	**Major end-use**
Lanthanum	Hybrid engines, metal alloys	Gadolinium	Magnets
Cerium	Auto catalysts, petroleum refining	Terbium	Phosphors, permanent magnets
Praseodymium	Magnets	Dysprosium	Permanent magnets, hybrid engines
Neodymium	Auto catalysts, hybrid engines, magnets	Erbium	Phosphors
Samarium	Magnets	Yttrium	Alloy agent, fluorescent lamps
Europium	Television and computer screens	Holmium	Glass coloring
		Thulium	Medical x-ray units
		Lutetium	Catalysts

Ytterbium	Lasers, steel alloys	

2.2 Recovery of Rare Earth Elements

The extraction process of the REEs after mining is carried out in three steps 1. Physical beneficiation using flotation, gravity magnetic, and electrostatic processes. 2. Hydrometallurgical extraction of metals using acidic and/or basic leaching and 3. Separation and purification using solvent extraction and ion-exchange [47].

2.2.1 Physical Beneficiation

2.2.1.1 Bastnaesite

Bastnaesite has replaced monazite as the chief mineral source for REEs since the 1950s, as the two biggest mines in the world, Bayan Obo in China and Mountain Pass in the USA, have been discovered and developed [48]. The separation of bastnaesite may employ multiple magnetic and gravity separation techniques. However, the most common process which is used for the physical beneficiation of bastnaesite is froth flotation using fatty acids (oleic) or hydroxamates [4, 49]. Sodium silicate, sodium hexafluorosilicate, and lignin sulfonate have been used as a depressant in these situations [50]. As shown in Figure 2.1, the unprocessed ore having 7% REO by weight is upgraded to a concentrate containing 70% REO by weight using froth flotation[51].

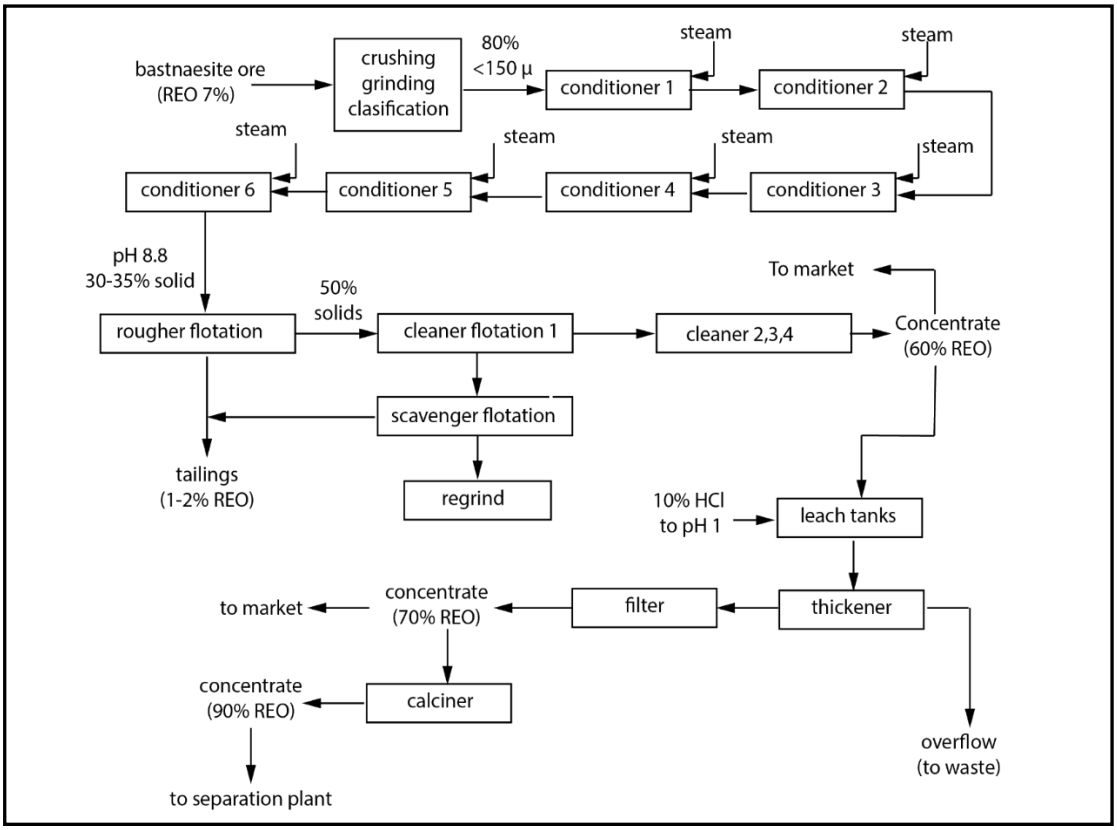

Figure 2.1 Simplified flowsheet for the physical beneficiation of bastnaesite at the Molycorp plant [51].

2.2.1.2 Monazite

Monazite is a rare-earth phosphate which, like bastnaesite, contains around 70% REEs by wt. However, it also contains 4-12% of thorium and variable amounts of uranium.[4, 52]. Monazite is found mostly as a placer deposit or beach sand. It is also one of the components of the ore in Bayan Obo mine in China. As shown in Figure 2.2, Monazite deposits are usually preconcentrated using high capacity gravity separators such as spiral or table concentrators. The individual minerals occurring in the placer deposits are then separated by exploiting small differences in the magnetizability and surface ionization potential [4]. Sometimes, froth flotation is also used to concentrate monazite from gangue minerals like rutile and ilmenite.

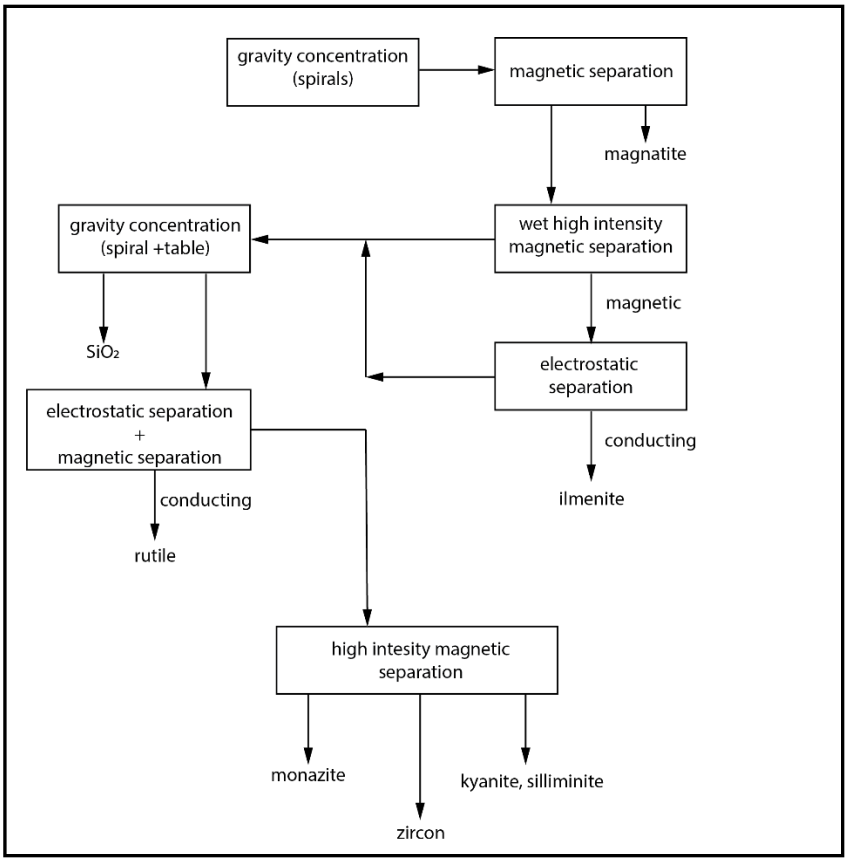

Figure 2.2 Simplified flowsheet for the physical beneficiation of the monazite at Congolone, Mozambique [53].

2.2.1.3 Xenotime

Xenotime is an yttrium-rich rare-earth phosphate that typically occurs with monazite as it undergoes a similar mode of weathering, transportation, and concentration during its formation. Its concentration varies from 0.5 – 5% of the weight of monazite in the source. However, some sources have reported 50% xenotime by weight of monazite. Despite its scarcity, it is considered one of the most essential sources of REEs because of the high proportions of HREE present in the mineral and is the primary source of HREEs apart from the ion-exchanged clays in China. It is most often associated with monazite and is produced as a by-product of monazite processing. Therefore, there are no processes developed specifically for the physical beneficiation of xenotime mineral[4, 49].

2.2.2 Leaching

2.2.2.1 Bastnaesite

Multiple processes have been developed to leach both the crude bastnaesite ore or the concentrate from froth flotation that are summarized in Figure 2.3. The bastnaesite concentrate containing 60% REO can be upgraded to 70% REO by leaching by 10% HCl and removing the calcium and strontium carbonates. The concentrate can either by upgraded to 90% by calcination and driving off CO_2 or leached by 30% HCl followed by neutralization to produce mixed rare earth chlorides.

Bastnaesite processing in China is done by roasting the concentrate with 98% H_2SO_4 to digest the ore, which releases the CO_2 and hydrofluoric gases. The REEs are then precipitated as double sulfates ($Na.REE(SO_4)_2$) by leaching with water and sodium chloride. The rare-earth sulfates are subsequently converted to hydroxides using strong NaOH solution and separated into individual REEs using solvent extraction[4, 54, 55].

In the Molycorp process developed for europium recovery, the bastnaesite concentrate is calcined at 620^oC, which displaces CO_2 and oxidizes cerium to an insoluble tetravalent oxide state. It is then leached with 30% HCl to dissolve the rest of the soluble REEs, which leaves the CeO_2 rich residue, which is sold in the market separately. The leach solution is treated to separate europium from the rest of the REEs using solvent extraction. The other REEs are precipitated as hydroxides using caustic treatment [4].

A process was developed at the Ames laboratory to directly treat the bastnaesite ore by calcining the crude ore at 800^oC followed by grinding to less than 10 mesh. The ground ore was digested in concentrated HNO_3, and the REEs were recovered from the solution by solvent extraction using tributyl phosphate, recovering around 98% of the total REE content in the ore.

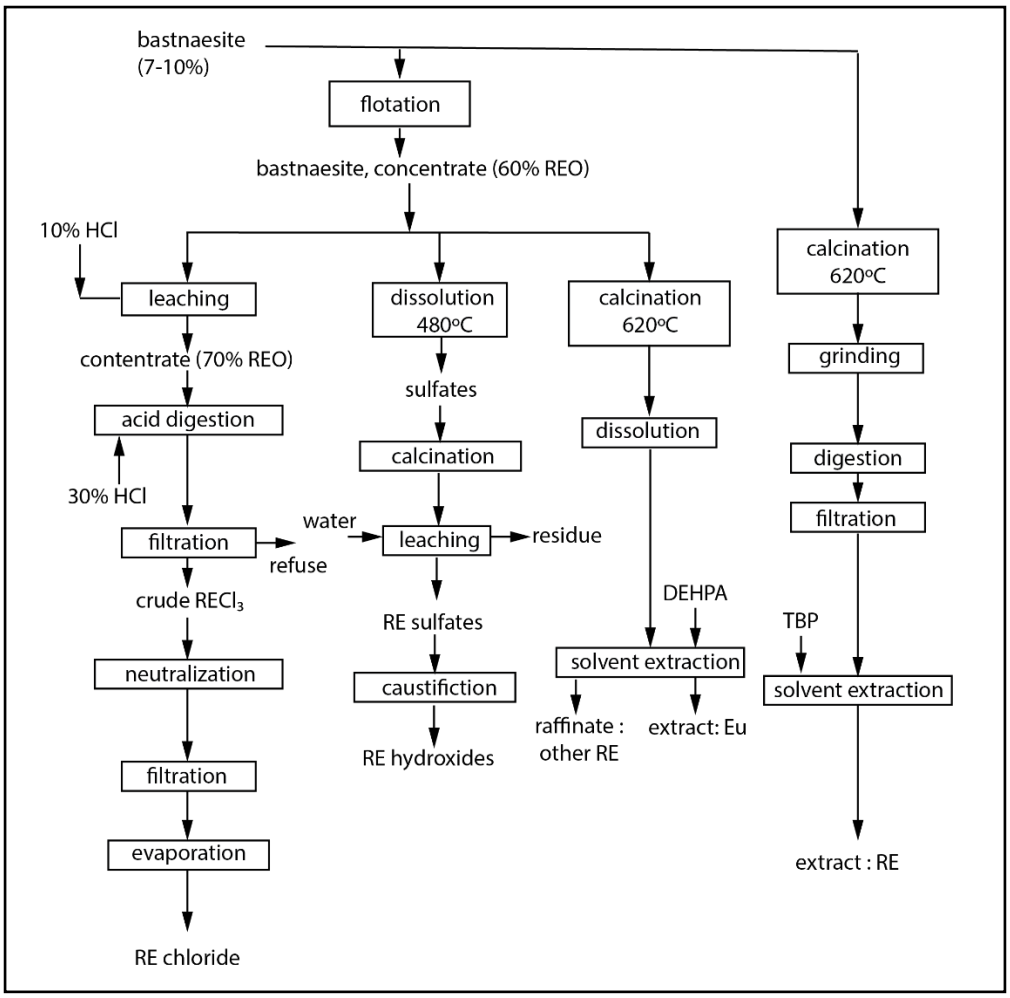

Figure 2.3 Various methods of chemically processing of bastnaesite ore to recover rare earth elements in different forms[4].

2.2.2.2 Monazite

Multiple processes have been developed for the extraction of REEs and separation of thorium from monazite[4] [53, 56]. The two most commonly used methods are acid treatment [57] and alkali treatment [47]. As shown in Figure 2.4, in the acid treatment process, monazite is subjected to concentrated H_2SO_4 at high temperature to dissolve either the REEs, thorium, or both based on the ore-to-acid ratio, temperature, and acid concentration. The REEs and thorium are subsequently recovered from the solution using different techniques. The REEs can be recovered using double sulfate precipitation, in which cerium and other light REEs precipitate, whereas yttrium and other heavy REEs stay in solution with thorium. The HREEs are very difficult to separate from thorium, and even fractional precipitation (separation of different salts based on their solubilities) causes the thorium to precipitate with the heavy REEs. The

thorium, however, can be separated from REEs by solvent extraction using TBP. The LREE precipitate is converted to rare earth hydroxide by NaOH and further purified by fractional precipitation.

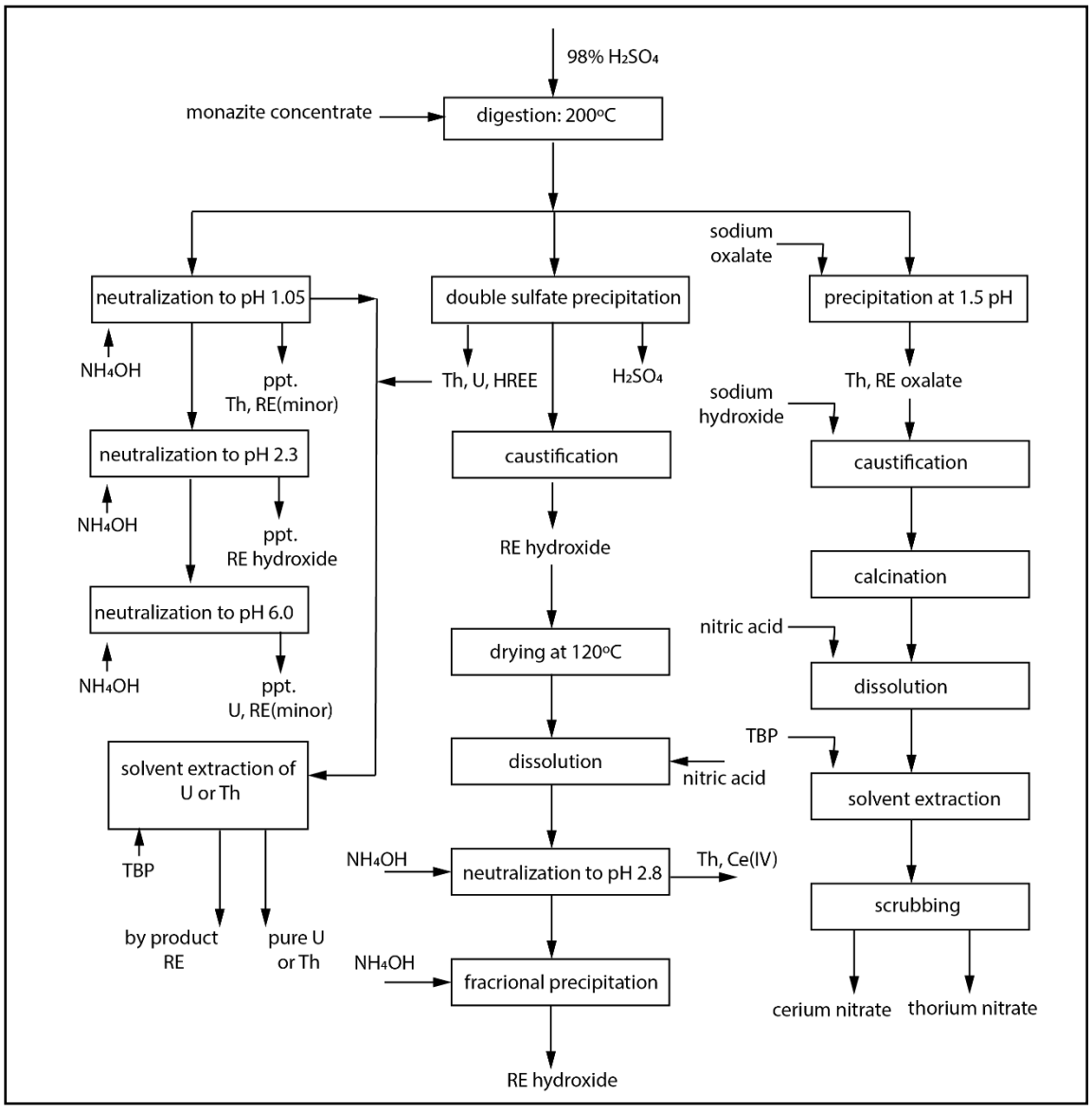

Figure 2.4 Schematic for acid treatment of monazite to recover rare earth elements using different processes[58].

The alkali method has been more popular in commercial practice for monazite processing as the process enables the production of a phosphate product at the beginning of the flowsheet as shown in Figure 2.5.

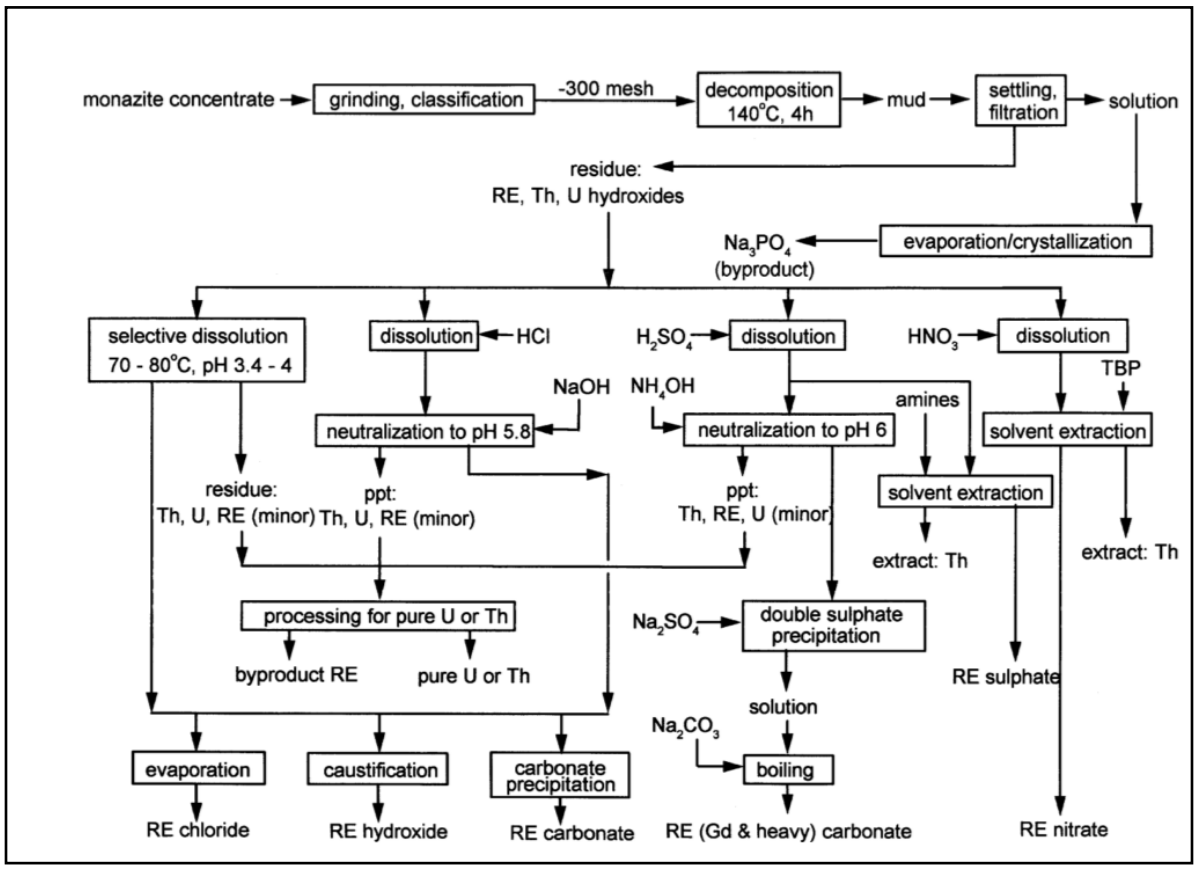

Figure 2.5 Schematic for alkali treatment of monazite to recover rare earth elements using different processes [4].

2.2.2.3 Xenotime

Chemical treatment of xenotime is achieved in the industry by multiple processes (Figure 2.6). The most popular process attacks the mineral with concentrated sulfuric acid at 250°C for 1-2 h. This reaction converts the phosphates into more soluble rare earth sulfates, which are then leached using water. The acid leaching for xenotime is feasible for sources containing more than 10% xenotime by mass. REEs from the leachate are recovered either by oxalic precipitation or directly processing the sulfate solution for individual separation. The alternate methodologies for chemical treatment include fusing it with caustic soda at 400°C or roasting it with sodium carbonate at 900°C, which helps to leach the phosphates leaving rare earth hydroxides, which can be leached with an appropriate amount of HCl or HNO_3.

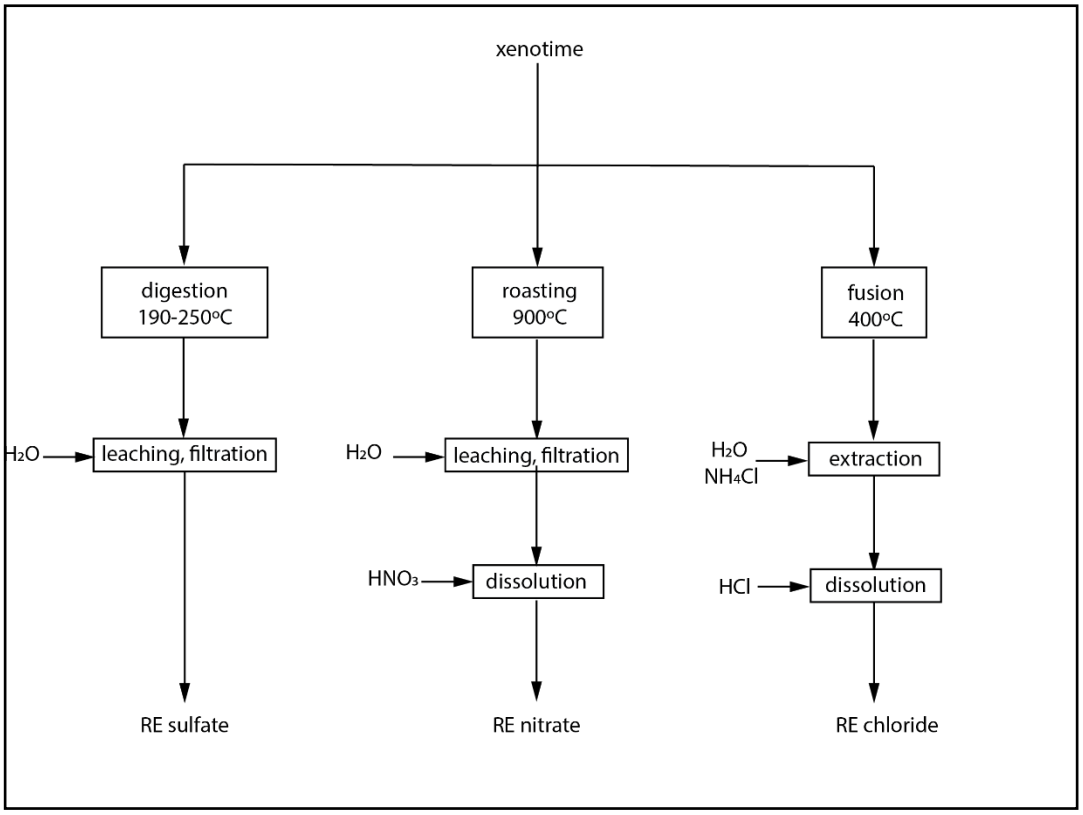

Figure 2.6 Schematic for different methods for processing of Xenotime for recovery of rare earth elements [4].

2.2.2.4 Ion exchanged Clays

Ion exchange clay source, also known as weathered crust elution deposit, is a very important source of REEs as 60% of the REEs present in the source are HREE. They contributed 35% of the total REE production of China in 2013. The ion exchange clays contains 0.05-0.3% REEs by weight, of which 60% occurs as a physically adsorbed species, which can be recovered by simple ion-exchange leaching [59]. There are three successive generations of technologies which have been employed by China for leaching REE from these sources as described by Chi et al [60].

i. Batch leaching with NaCl (first generation leaching);
ii. Heap leaching with $(NH_4)_2SO_4$ (second generation leaching); and
iii. In-situ leaching with $(NH_4)_2SO_4$ (third generation leaching).

The in-situ leaching is currently applied for the recovery of very low-grade ores and the tailings of the older batch and heap leaching plants [59]. The benefit of the in-situ leaching is reduced

environmental impact and soil disturbance [43]. The lixiviant (0.3M $(NH_4)_2SO_4$) is pumped at high pressure directly into the orebody and returned through the recovery well. Depending on the ore characteristics, the entire process can take up to 400 days [59].

2.2.3 Solvent Extraction

Solvent extraction (also known as Liquid-Liquid Extraction (LLE)) is a technique that separates solutes or metal-complexes based on the relative solubilities of the complexes in two different phases, typically organic and aqueous phases. Solvent extraction has been the industrial process of choice for the production of large quantities of REEs since the 1960s. Solvent extraction is preferred over different separation techniques like ion-exchange because of its capability to treat large volumes of pregnant liquors and producing high purity individual REOs.

Separation and extraction of REEs by solvent extraction is achieved by modifying the REE ions by forming a hydrophobic complex so that they get extracted in the organic phase. This is typically achieved by three ways by three categories of extractants, i.e.:

i. Replacement of the hydrated water molecule by an organic solvating reagent (solvating extractants);
ii. Formation of ion-pair (basic extractants);
iii. Reaction of the metal cation with a suitable anion to form the neutral species (acidic extractants).

2.2.3.1 Cation exchange extractants

The general reaction for the cation exchange extraction is represented by:

$$RE^{3+} + 3HA \rightleftharpoons REA_3 + 3H^+ \quad (2.1)$$

where RE denotes the REE, and A represents the organic anion. Two different categories of cation exchange extractants are commonly used in the extraction of REEs, i.e., carboxylic acids and organo-phosphoric acids.

The key feature of carboxylic acid extractants for REE extraction is the different behavior of yttrium with different carboxylic acids. Yttrium extraction by Versatic acid follows the middle rare earth elements (samarium, europium, and gadolinium) closely, whereas the yttrium

extraction follows the extraction of light rare earth elements with naphthenic acid. Naphthenic acid has been reported to be used for the separation of yttrium with other rare earth elements in China. One of the significant shortcomings of carboxylic acid as an extractant is its high solubility in water, which leads to high extractant losses in the continuous operation[4, 5, 61].

Organophosphorus acid extractants are the most extensively studied for the separation and extraction of REEs. DEHPA (di(2-ethylhexyl) phosphoric acid) and HEHEHP (2-ethylhexyl phosphonic acid mono-2-ethylhexyl) are the two main extractants that are used in the industry for REE separation. The extraction of REE by DEHPA and EHEHPA was studied by Bautista [61] and Sato [62]. As shown in Figure 2.7, the distribution coefficients of the REEs increased in the order of the atomic number as the distribution coefficients of La<Ce<Pr<Nd<Sm<Eu<Gd<Tb<Dy<Ho<Er<Tm<Yb<Lu. Therefore, it was shown that organophosphorus extractants can be used to make a separation between the rare earth elements exploiting the differences in the distribution coefficients. Additionally, it was seen that there is a tetrad effect i.e. the elements can be grouped together into groups of four (tetrads) with the inflexions at neodymium, gadolinium and holmium. Gadolinium was seen to be common to the second and third tetrad.

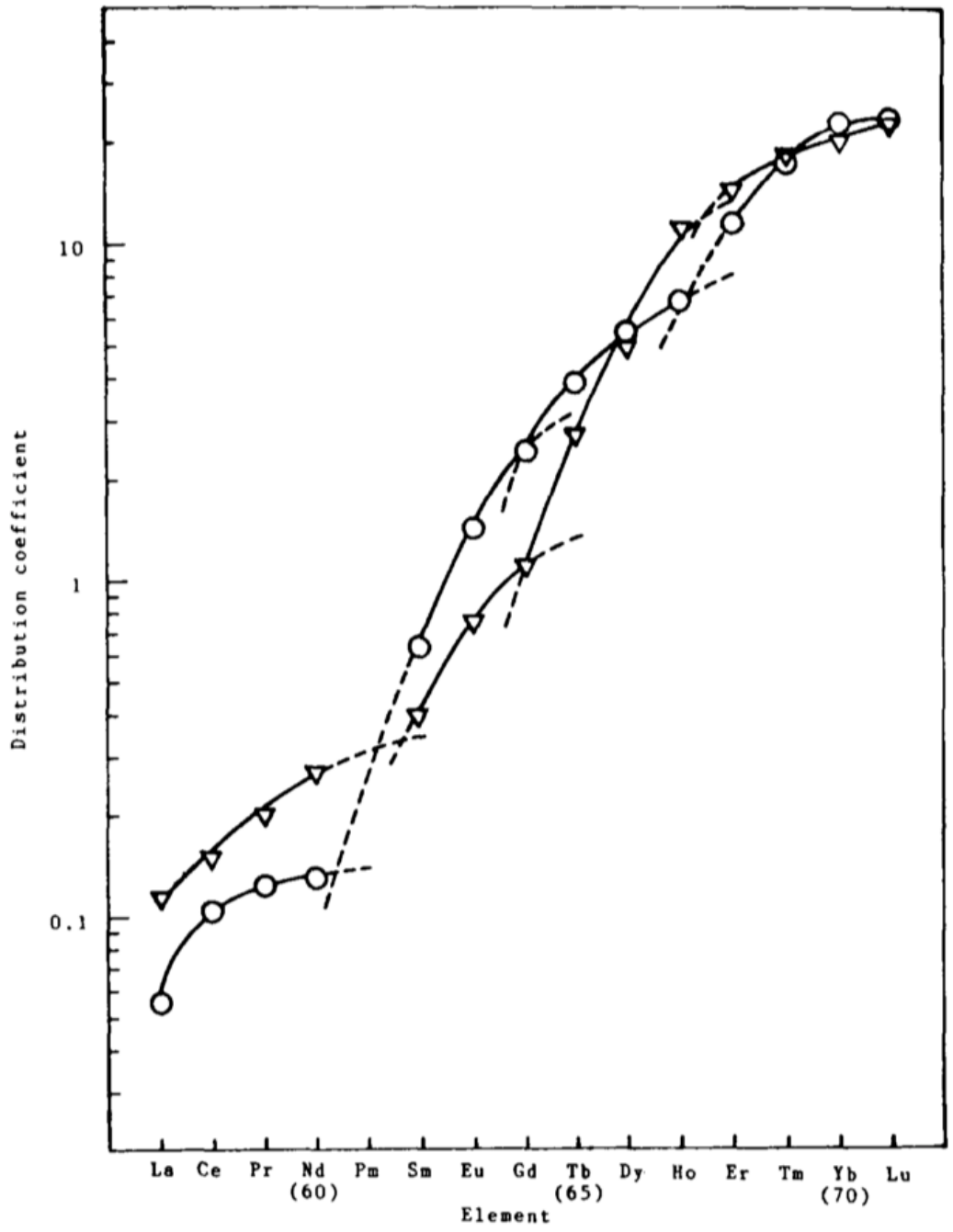

Figure 2.7 Dependence of the distribution coefficient of the rare earth elements with 0.05 mol/liter DEHPA solution in kerosene with the atomic numbers showing the tetrad effect Δ represents the distribution curve from EHEHPA and O represents the distribution curve from DEHPA[62].

2.2.3.2 Solvation Extractant

A solvation extractant replaces the water molecules which hydrolyze the REE ion in solution to form an organic soluble species. One of the most important solvation extractants is TBP (tributyl phosphate). The effective reaction by TBP can be represented as

$$RE(NO_3)_3.xH_2O + 3TBP = RE(NO_3)_3(TBP)_3 + xH_2O \quad (2.2)$$

Peppard [63] showed that the distribution coefficients of the REEs with pure TBP increase with the increase in the atomic number due to the reduced ionic radius of the lanthanide ion in the solution resulting in stronger electrostatic interaction between the cation and ligand. As the size of the cation increases beyond a certain size, the steric conditions begin to overrule the electrostatic interaction, resulting in a maxima in the plot of extraction efficiency with the atomic number, as shown in Figure 2.8.

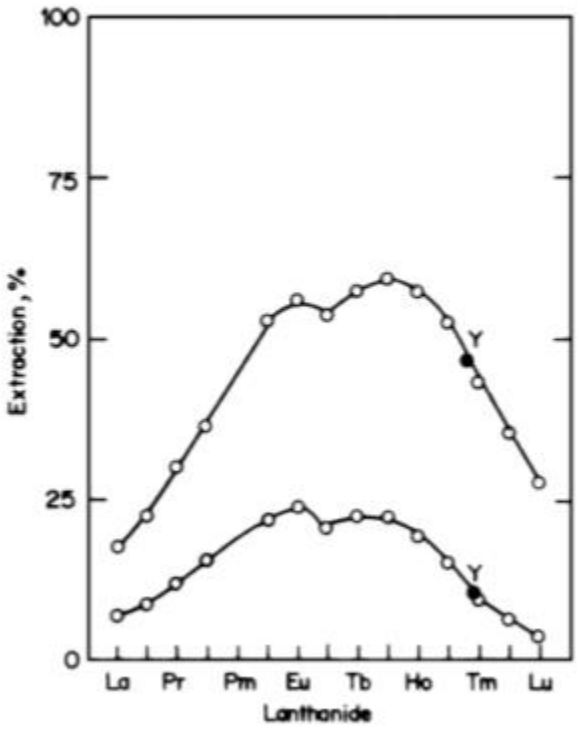

Figure 2.8 Variation of the extraction efficiency with the atomic number of metals [54].

2.2.3.3 Anion Exchange Extractants

Anion exchanges extract metal ion as organic soluble anionic complexes in the presence of strong ligand present in the aqueous phase. Long-chain quaternary ammonium salts are useful for REE separation and extraction[4, 5, 61]. The reaction mechanism through which the REE get extracted can be represented using the following equation

$$R_4N.X + RE^{3+} + 3X^- = R_4N.RE(X)_4 \quad (2.3)$$

The extraction of REE with ammonium salts exhibits different trends in thiocyanate and nitrate systems. In the thiocyanate system, the extraction of REE increases with the atomic number, while it decreases with the atomic number in the nitrate system. This is explained by the difference in the complexes formed by both the ligands in the aqueous phase and their stability and subsequent extractability in the organic phase.

As shown in Figure 2.9, yttrium exhibits an anomalous behavior with anion exchange extraction as it extracts with the LREEs in the thiocyanate media and extracts with the HREE in the nitrate media which indicates that the amine extractants in thiocyanate media can be used to separate yttrium with the HREE, with which it is typically extracted using the cation exchange extractants.

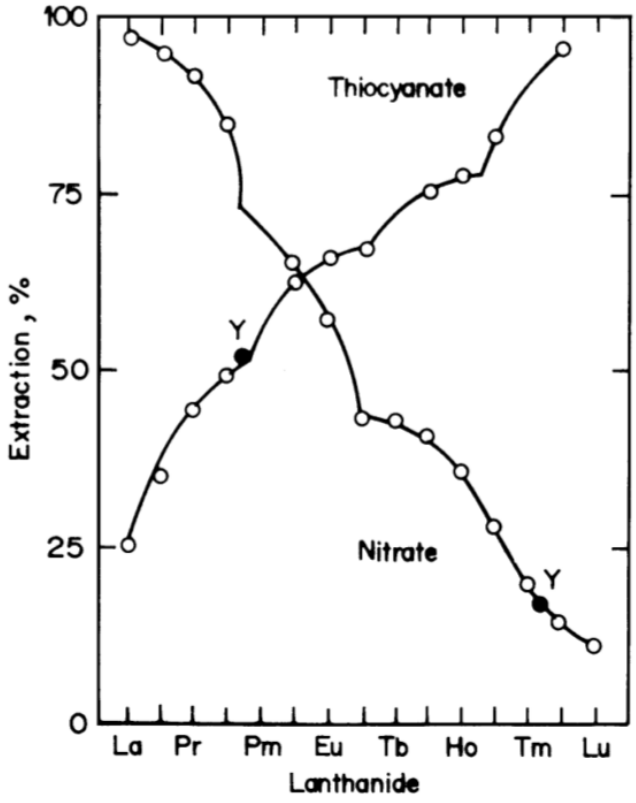

Figure 2.9 Variation of the extraction efficiency of rare earth elements by quaternary ammonia salts with the atomic number in thiocyanate and nitrate media [58].

2.2.4 Definition of basic terms related to solvent extraction

There are several terms which are used for describing the extraction of a metal by solvent extraction process and its separation characteristics

1. Distribution coefficient: The distribution coefficient (D) is the ratio of the metal concentration in the organic phase at equilibrium to that in aqueous phase in molar terms. A high distribution coefficient indicates high affinity of a metal to get extracted in the organic phase.

$$\mathrm{D} = \frac{[\mathrm{metal}]_{\mathrm{organic}}}{[\mathrm{metal}]_{\mathrm{aqueous}}} \tag{2.4}$$

2. Extraction efficiency: The extraction efficiency (E) is the % metal present in the feed solution which is extracted in the organic phase at equilibrium

$$E\% = \frac{[\text{metal}]_{\text{organic}}}{[\text{metal}]_{\text{feed}}} \times 100 \tag{2.5}$$

3. Separation factor: The separation factor or separation efficiency (S) of a metal A with respect to another metal B is defined as the ratio of the distribution coefficients of the two metals for the same condition.

$$S_{A/B} = \frac{D_A}{D_B} \tag{2.6}$$

4. Decontamination factor: The decontamination factor (DF) is used to describe the efficiency of the process at rejecting the contaminants from the desired metal. It is defined as the ratio of the relative concentration of the contaminants in the feed to that in the product (organic phase in this case)

$$DF = \frac{([\text{Contaminant}]/[\text{metal}])_{\text{feed}}}{([\text{Contaminant}]/[\text{metal}])_{\text{product}}} \tag{2.7}$$

5. $pH_{0.5}$: The $pH_{0.5}$ or $pH_{1/2}$ is used to the compare two different extractants for extraction of a metal. It is defined as the pH value at which the extraction efficiency of a metal is 50% or the distribution coefficient is 1.

2.3 Rare Earth Elements in Coal

2.3.1 Abundance and occurrence of REE in coal

The average concentration of the REEs in global coal is 68.5 ppm, as reported by Zhang et al. [2] The concentration of the REEs in US coals, on the other hand, is 62 ppm, which is very close to the average of the global coal. The average concentration is, however, 2.5 times lower than the average concentration of the REEs in the rocks in the upper continental crust, which is 168.4 ppm. The REEs in the coal are shown to be associated with the incombustible fraction

of the coal. The average concentration of the REEs in the incombustible fraction of the coal is 404 ppm globally and 512 ppm in the US coals, which is around 3 times the concentration of REEs in the UCC[64]. The concentration of the REEs in the coal is much lower than a typical REE ore like monazite and bastnaesite, in which the cut-off grade is 1.5%-2.0% [1]. The concentration of REEs in the incombustible component of coal is, however, comparable to the concentrations found in the ion adsorbed clays for which the cut-off grade is 0.06%-0.15%. Given the large amount of coal, which is mined globally every year, coal can be considered to be a valuable alternate reserve of REEs even if a part of the REEs present in the coal are recovered efficiently. According to estimates, the total amount of REEs which are present in the global coal is 50 million tons, which represent around 50% of the total REE reserve in the world [2, 65-67].

The occurrence of REEs in coal sources can be classified as the following forms [64]

1. Pyroclastic minerals which are derived from the explosive volcanic activity like monazite and xenotime
2. Diagenetic and epigenetic minerals which are formed by precipitation or recrystallization
3. Organic compounds

The REEs are present in many of the REE rich coals as finely disseminated pyroclastic minerals, the existence of which has been proved by Scanning Electron Microscope-Energy Dispersive X Ray (SEM-EDX) analysis [68]. The minerals of this nature are mainly associated with the clay component of the coal or in the parting section of the coal seam, while the organic portion of the coal is devoid of such minerals. Many low ash low-rank coals which are rich in REEs do not have REE minerals, but the REEs are associated with the combustible organic matter. The REE content in the humic acid component of such coals is much higher as compared to the raw coal. The organic association of the REEs was proved by indirect evidence such as the negative correlation of REEs and ash and direct evidence like sequential extraction of REEs from raw coal [64].

2.3.2 Physical Beneficiation of REEs from coal

Due to the complexity of the composition and distribution of the REEs in coal coupled with the limits of existing physical processing methods like gravity and flotation, the recovery of the REEs was not well explored until recently. The technologies which are typically used for traditional REE minerals do not apply directly to the recovery of REEs from coal. The processes which have been explored for REE recovery are physical separation, leaching and solvent extraction.

Gravity separation can be used to recover the higher density rare earth minerals from the lighter density gangue minerals. The rare earth minerals in the coal matrix are very finely disseminated, with the maximum particle size not exceeding a few microns. Therefore, to liberate the minerals, fine grinding is required, which reduces the size of the particles to below the capabilities of current gravity separation processes. Hence, it is challenging to produce a separation between the coal and rare earth minerals based on the difference in their densities.

Similarly, for the magnetic separation, the entrapment of gangue particle magnetic flocculation inhibits its use below 74-micron particles. There are several gravity-based separators like the Knelson Concentration, Falcon concentrators, and Kelsey Jig, which have the capability of treating large capacity of ultrafine minerals. However, there is no study in the literature to investigate the feasibility of these concentrators for the recovery of REEs from coal.

The recovery of ultrafine minerals using froth flotation is also restricted to the particle size of around 10 microns because of the mechanism of the collision between the bubbles and the particles. A study showed that REE could be concentrated from coal using froth flotation using MIBC as the frother and sodium oleate as the collector to produce an REE concentrate of 4700 ppm from a feedstock having 256 ppm of REE.

2.3.3 Hydrometallurgical Extraction of REEs from coal

Extensive studies have been carried out at the University of Kentucky[69-72] to explore the hydrometallurgical extraction of REEs from coal sources using ion exchange and acid leaching. The impact of chemical and thermal activation on the leaching performance was studied in detail. It was seen that the particle size of the coal had a significant effect on the leaching recovery of the LREEs while having little to no effect on the recovery of the HREEs.

Ion exchange leaching was explored as a possible method of extraction of REEs from coal. Ion exchange using 0.1 M ammonium sulfate at pH value of 5.0 resulted in poor recovery of around 9-10% TREEs. Interestingly the recovery of the HREE was twice that of LREEs, as shown in Figure 2.10. The difference in recovery was the indirect evidence of a difference in the mode of occurrence of light and heavy REEs. However, the recovery of TREE as a group is very low to be economically viable in industrial applications [73].

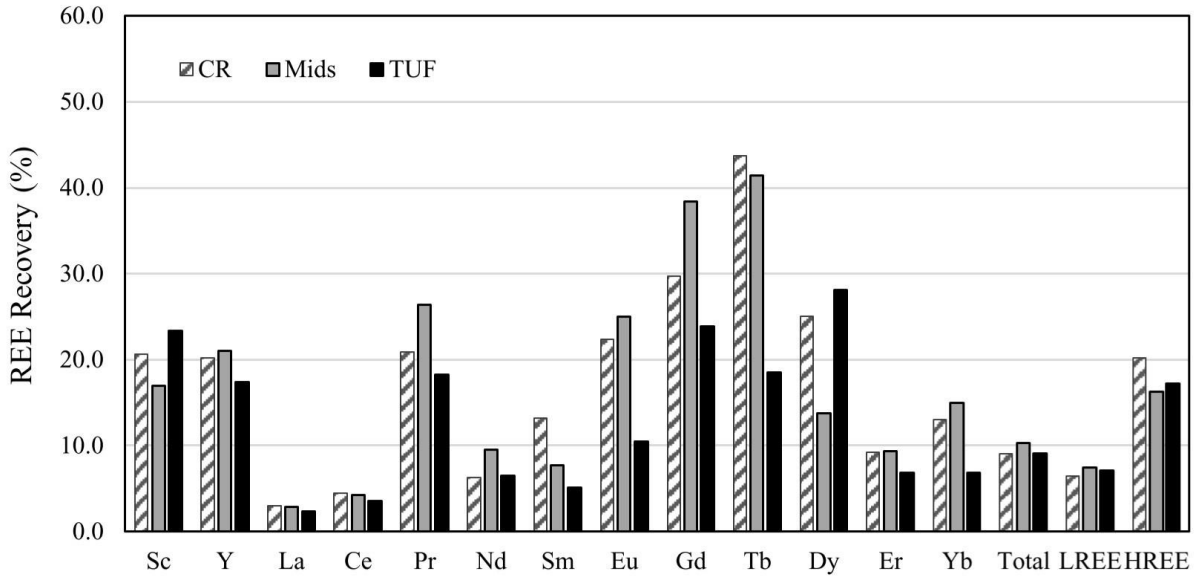

Figure 2.10 Leaching recovery of selective rare earth elements from different plant samples after 24 hours of leaching using 1.2 mol/L sulfuric acid [73].

Thermal and chemical activation in the form of roasting before leaching was explored to enhance the leaching performance of the REE from coal. The recovery of the REEs increased from 31% to 74% upon blank roasting of coal samples at 750^{o}C for 2 hours. The increase of recovery was more pronounced on the LREEs for which the recovery increased by 45% points compared to HREEs for which the increase was only 8%, as shown in Figure 2.11. The treatment of thickener underflow material with 8 M NaOH before acid leaching with sulfuric acid was also shown to be very effective. The activation resulted in an increase in the REE recovery from 22% to 75%, as shown in Figure 2.12. For both roasting and alkaline pretreatment, the increase in the recovery of LREEs was more than the increase in the recovery of the heavy REEs [73].

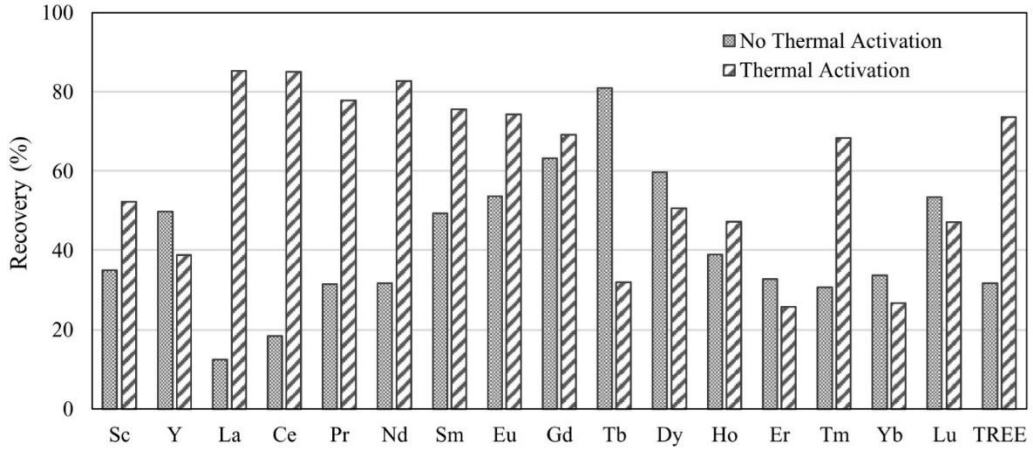

Figure 2.11 Improvement in the leaching recovery of rare earth elements after thermal pretreatment of the de-carbonized -180 micron middling material and five hours of leaching using 1.2 mol/L sulfuric acid solution at 75^{o}C [62].

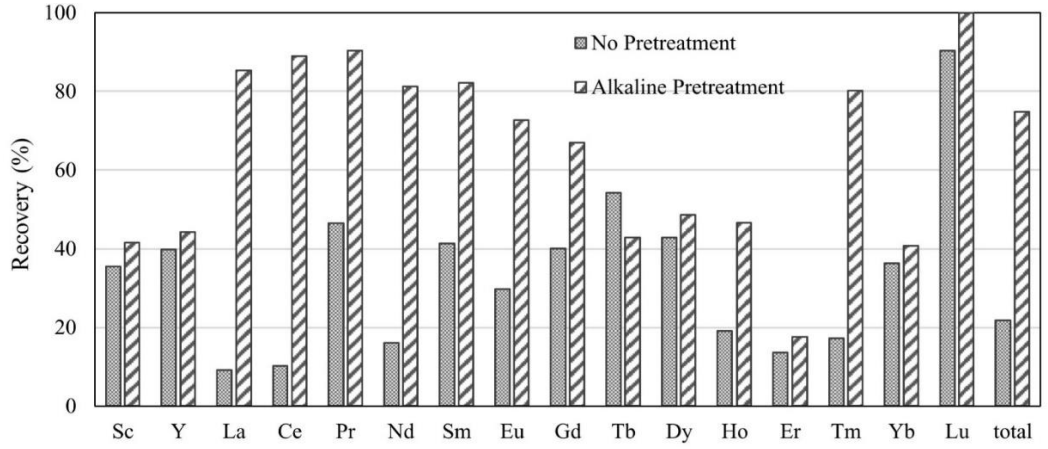

Figure 2.12 Improvement in the leaching recovery of rare earth elements after alkaline pretreatment of the de-carbonized -180 micron middling material and five hours of leaching using 1.2 mol/L sulfuric acid solution at 75^{o}C [73].

The composition of leachates generated from coal sources is significantly different from the leachates obtained from acid leaching of conventional sources as well as secondary sources like the recycling of magnets, etc., as shown in Table 2.2. The difference in the leachates arises from the fact that the concentration of the REEs in the conventional sources is much higher

than the coal sources, whereas the concentration of the contaminant elements is much lower than the coal sources. The high concentration of the contaminant, coupled with the low concentration of the REEs, makes the separation of the REEs very challenging.

Table 2.2 Elemental compositions of PLS from different sources comparing the concentration of rare earth elements with the concentration of major contaminants in the solution.

Source	**TREE (g/L)**	**Iron (g/L)**	**Aluminum (g/L)**	**Calcium (g/L)**
Manganese nodule leaching[23]	0.094	0.20	0.735	N/A
Calcium sulphate sludge leaching[74]	20.3	N/A	0.300	16.1
Phosphate rock leaching[75]	5.0	N/A	N/A	240.0
NdFeB magnet leaching[76]	28.1	9.80	N/A	N/A
Bastnaesite leaching[20]	58.5	7.75	N/A	1.23
Monazite leaching[57]	37.8	0.54	N/A	N/A
Magnetic scrap leaching[77]	4.74	3.03	N/A	N/A
Coal acid leaching	0.034	0.80	1.2	0.60

The separation techniques which are used for producing mixed REO concentrate from conventional sources cannot be effectively applied in the coal-based leachates because of the significantly different compositions. Solvent extraction has been used widely for the separation of individual REEs from mixed REO concentrates. However, there is a significant gap in the literature regarding the applicability of the solvent extraction process to generate an REO concentrate by removing the contaminants from the leachate, specifically from leachates having low concentrations of REE and high concentration of contaminant ions such as those generated from coal-based sources.

2.4 Effect of TBP on REE Recovery with DEHPA

DEHPA is one of the most common extractants used for the extraction of several metals, including zinc, cadmium copper, and REEs. One of the problems associated with the extractant

DEHPA is that a significant amount of DEHPA is wasted in industrial use because of poor phase separation characteristics [78]. Tributyl phosphate (TBP) is frequently used as a phase modifier in the various processes where DEHPA and other organo-phosphoric acids are the active extractants. The primary purpose of TBP as a phase modifier is to improve the phase separation characteristics of the organic and aqueous phase reducing the waste of extractant during the operation [79]. The addition of TBP to organo-phosphoric acids has a synergistic effect on the extraction behavior of metals, as reported by several researchers [62, 80-87].

The reason for the change in the extraction behavior of the metals with DEHPA in the presence of TBP was studied by Barnard et al. [88]. The study revealed that TBP and DEHPA reacted to form butyl-bis(2-ethylhexyl) phosphate (DEHPA-OBu) and dibutyl phosphate (DBP). The reaction mechanism was shown to progress by a nucleophilic substitution mechanism. The nucleophilic attack of TBP by the DEHPA acid occurs, resulting in the breaking of the C-O bond and formation of DBP anion, as shown in Figure 2.13.

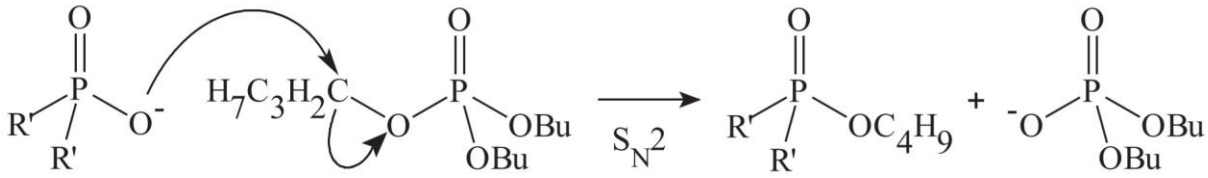

Figure 2.13 The S_N2 reaction proposed by Bernard et al.[80] for the formation of butyl phosphinate due to the reaction of phosphinic acid with tributyl phosphates [88].

Cheraghi et al. [85] studied the interaction of DEHPA and TBP during the extraction of vanadium using FTIR spectroscopy. The analysis showed that the P=O vibration band of TBP impacted the P=O vibration band of DEHPA, as shown in Figure 2.14. It was further observed that the extraction of vanadium had no impact on the P=O vibration band, and the extraction affects the P-O-H characteristic vibration band only, as shown in Figure 2.15. It was therefore concluded that TBP does not actively participate in the extraction of vanadium by DEHPA, and the organometallic compounds are formed only with DEHPA. The study showed that at lower temperatures (25^{o}C to 40^{o}C), the synergistic effect of TBP on DEHPA for vanadium was negligible, which showed that the synergistic effect was dependent on the metal extracted.

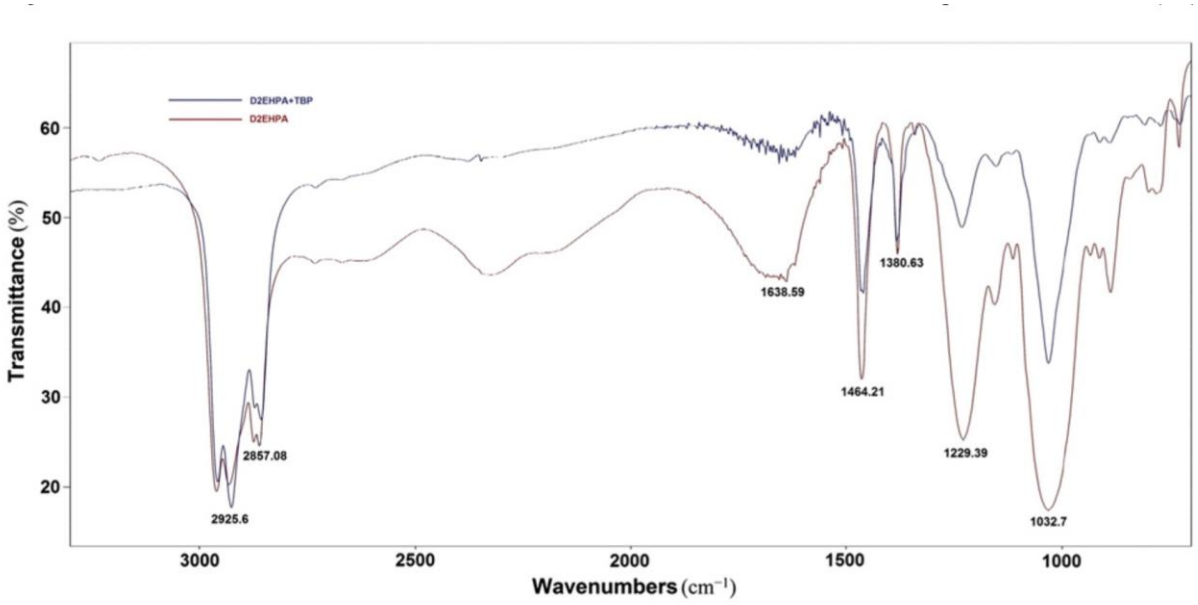

Figure 2.14 Comparison of FT-IR spectra of pure DEHPA and a mixture of DEHPA and TBP [85].

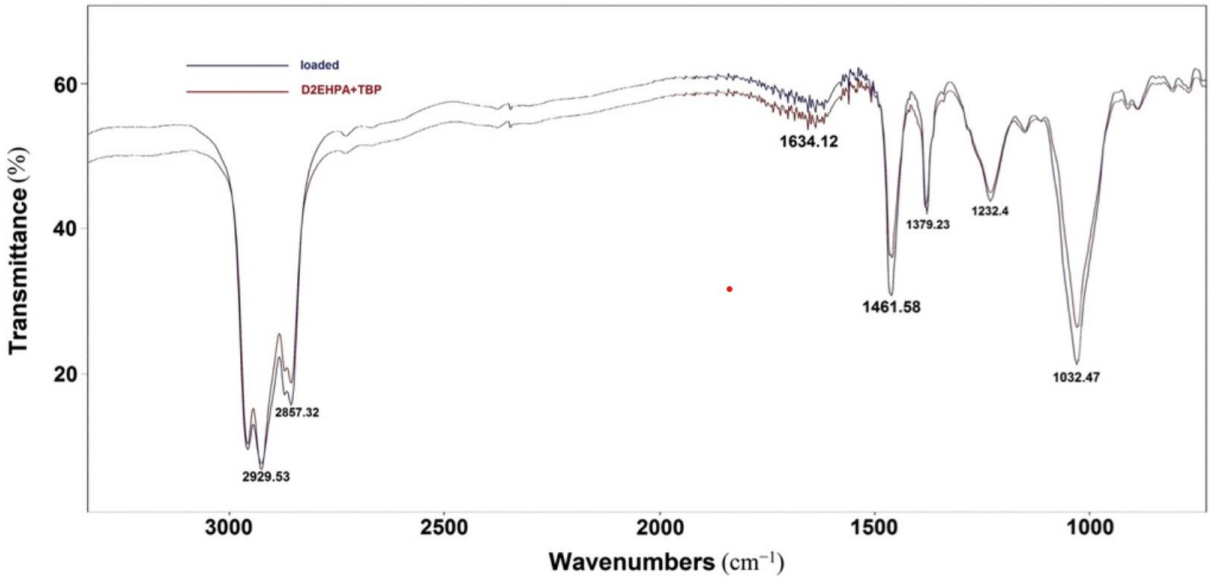

Figure 2.15 Comparison between the FT-IR spectra of the pure organic phase and organic phase loaded with vanadium at pH=1.7 [85].

Fatmeshari et al. [81] studied the effect of TBP on the extraction behavior of zinc and cadmium using DEHPA. The study showed that better separation of zinc and cadmium could be achieved

by the addition of a small amount of TBP to DEHPA, which results in effective separation in fewer stages. The impact of TBP on the extraction curve of cadmium is more than the impact on the extraction curve of zinc as shown in Figure 2.16.

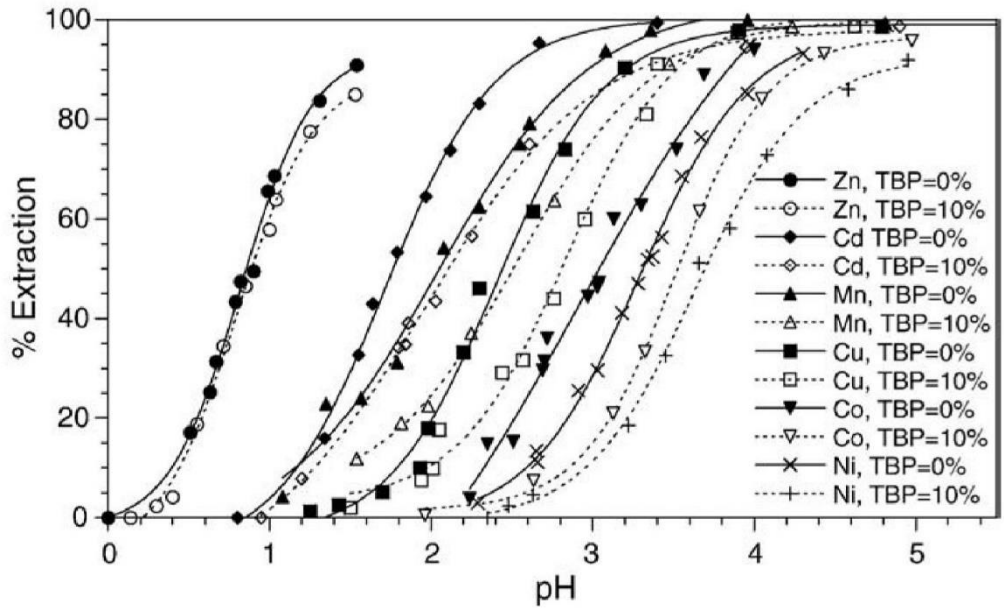

Figure 2.16 Extraction curves of Zn, Cd, Mn, Cu, Co, and Ni by 20% DEHPA solution with different concentrations of TBP in the organic phase [81].

Azizitobarghi et al. [84] reported that the addition of TBP to DEHPA for selective extraction of iron over zinc resulted in reduced extraction for both metals. As shown in Figure 2.17 the extraction efficiency (quantified by $pH_{0.5}$) of both zinc and iron decreased with increase in the mole fraction of TBP in the organic phase (XTBP). The mole fraction XTBP is defined as the moles of TBP per total moles of DEHPA and TBP. However, the reduction in the extraction efficiency was not equal for both the metals which resulted in better efficiency of the separation of the process.

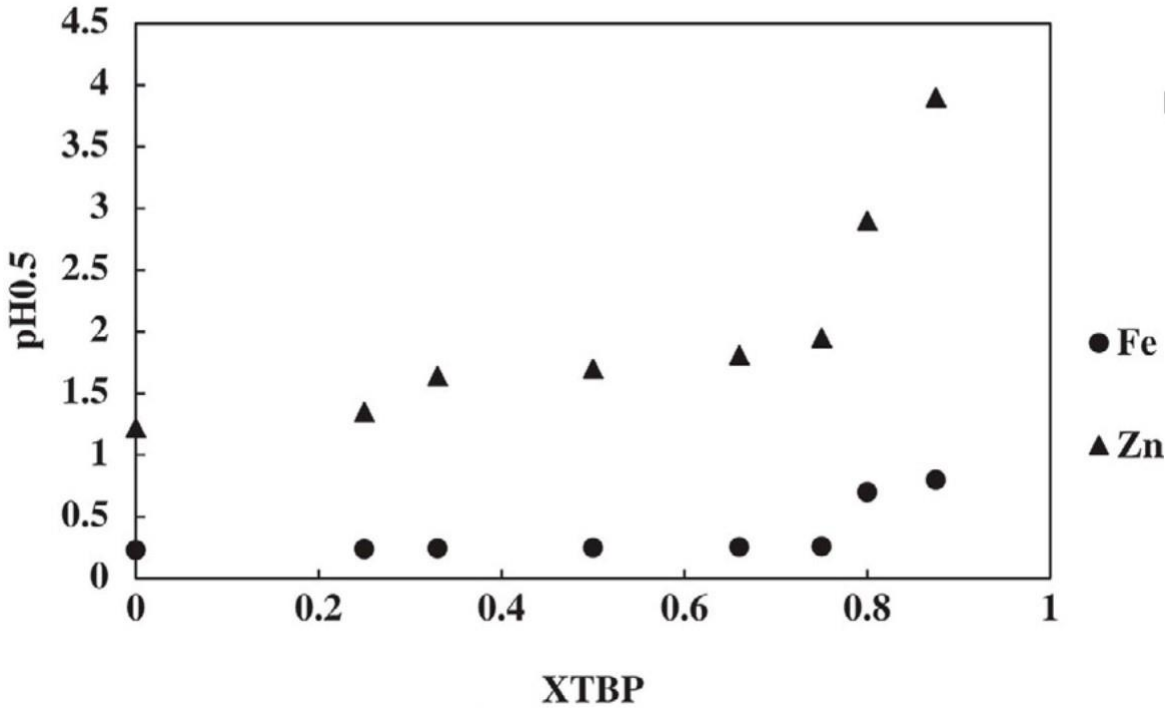

Figure 2.17 Effect of addition of different mole fractions of TBP-to-DEHPA (XTBP) on the $pH_{0.5}$ of Fe^{2+} and Zn^{2+} at 25ºC and O/A ratio of 1:1 [84].

Sato[89] reported a positive synergism of TBP and DEHPA for the extraction of uranium. The partition coefficient (distribution coefficients) increased sharply with an increase in TBP concentration followed by a slow decline with further TBP additions as shown in Figure 2.18.

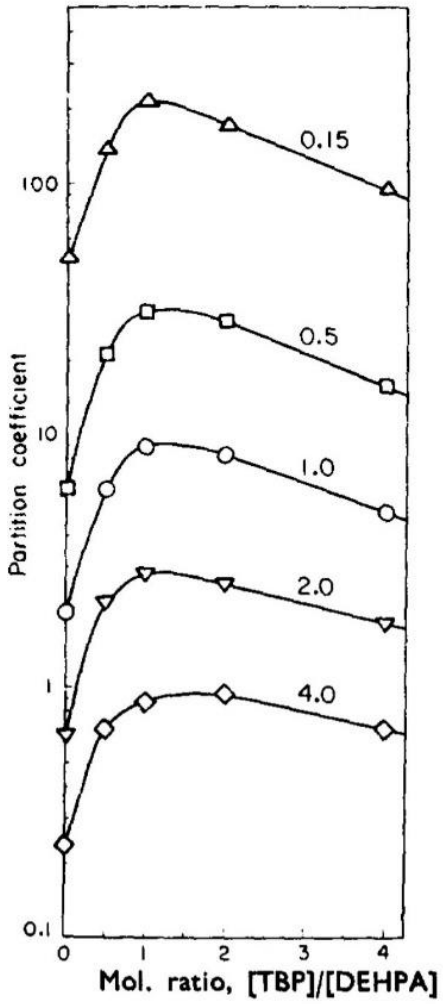

Figure 2.18 Variation of the distribution coefficient of with molar ratio of TBP to DEHPA for the extraction of uranium (VI) from sulfuric acid solutions by DEHPA + TBP in kerosene [89].

While there have been no comprehensive studies that evaluated the effect of TBP on the separation characteristics of the REEs and the contaminants to best of the author's knowledge, there are a few studies that have studied the effect of TBP on the distribution coefficients of the individual REEs. Ferdowsi et al. [80] conducted a study on the impact of TBP on the distribution coefficients of REEs present in the leachate generated from mineral apatite. 0.8 M organic solution of DEHPA was used for extraction of REE from the aqueous solutions. As shown in Figure 2.19, distribution coefficient of yttrium was reduced drastically when

additional TBP was added to the solution, which indicated that better separation could be achieved by optimizing the composition of the organic phase.

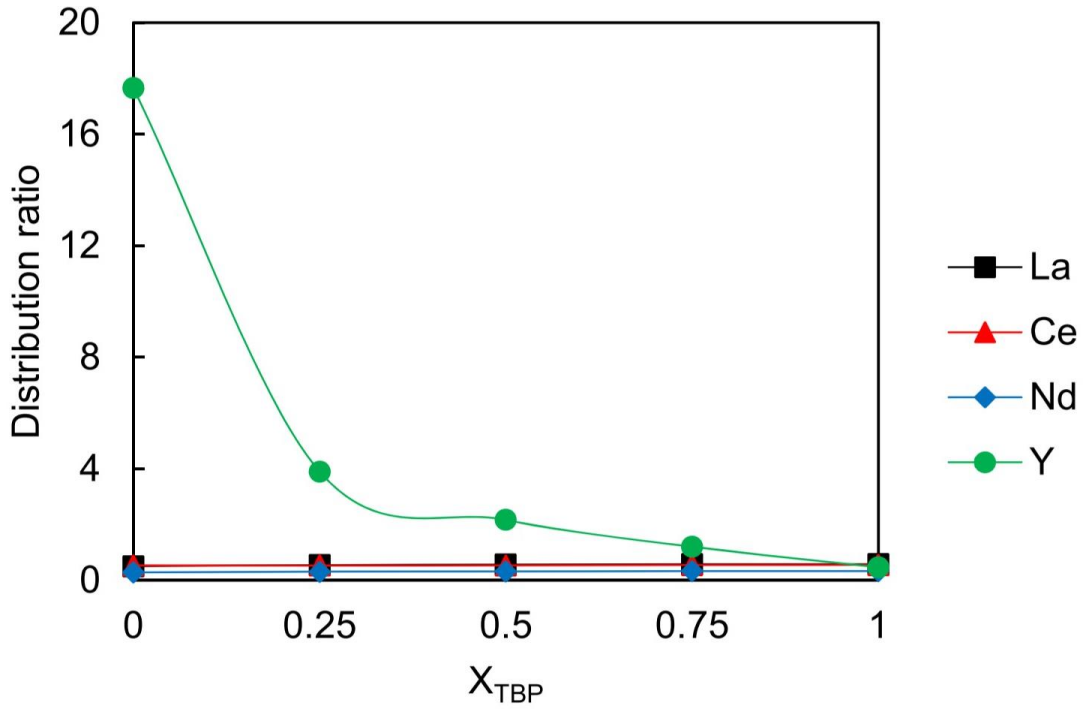

Figure 2.19 Effect of composition of organic phase on the distribution ratio of La, Ce, Nd, and Y over a range of mole fractions of TBP with DEHPA (X_{TBP}) [80].

Another study by Krakaew et al. [90] studied the impact of TBP on the synergistic number defined as

$$Sy = \frac{D_{1,2}}{D_1 . D_2} \tag{2.8}$$

Where $D_{1,2}$ is the distribution coefficient of the metal in a mixture of two extractants 1 and 2, while D_1 and D_2 are distribution coefficients in the pure solutions of the extractants. The study was done on a mixed rare earth nitrate solution, and it was shown that lanthanum has a synergism number of <1, indicating that the addition of TBP had an antagonistic effect on the extraction of lanthanum.

The results of the studies are inconsistent in that the results are dependent on the composition of the test solution. A systematic study has yet to be conducted on the impact of TBP on the separation efficiency between individual REEs as well as the major contaminants commonly found in leachates generated from coal-based sources.

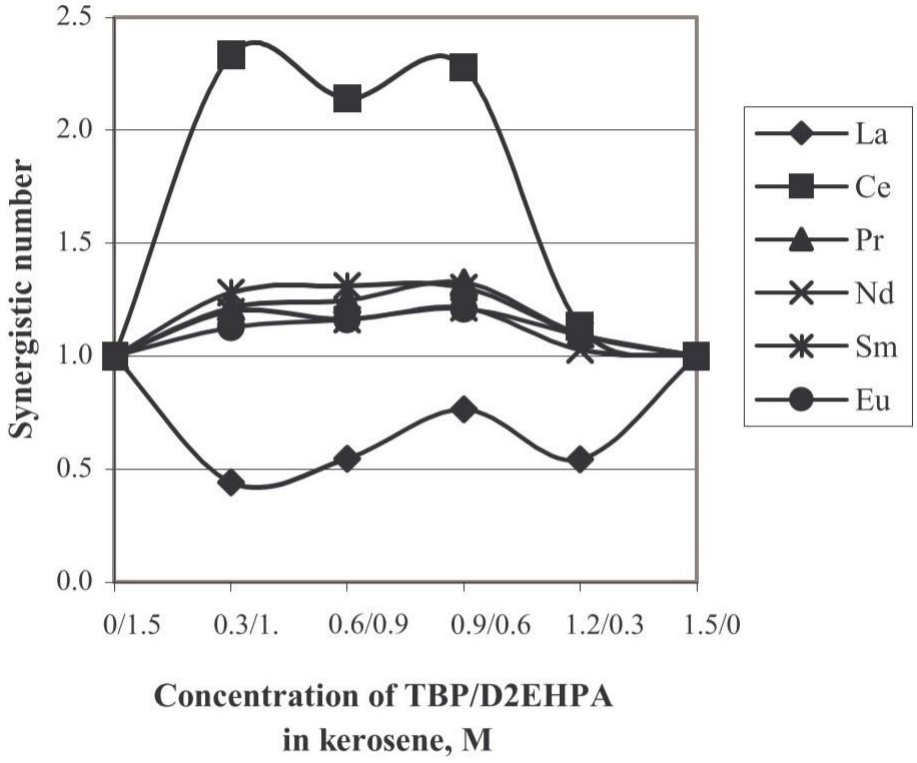

Figure 2.20 Variation in the synergistic numbers of the rare earth elements as a function of the TBP/DEHPA ratio in kerosene [90].

2.5 Thermodynamic Model of Distribution Coefficient of Rare Earth Elements

2.5.1 Reaction mechanism of extraction of lanthanides by DEHPA

The common use of DEHPA for the concentration and separation of REEs began with the seminal study by Peppard et al. [91] in 1957 in which REEs were effectively separated from each other by fractional extraction. The extraction efficiency of the REE solutions by DEHPA increased with a rise in the atomic number of the element (Figure 2.21). The study used the tracer technique to show that the extraction efficiency was also dependent on the third order of

the concentration of extractant in the organic phase as well as inversely dependent on the third power of acid concentration of the aqueous phase. By slope analysis, the following reaction mechanism was proposed:

$$M^{3+}|_A + 3HG|_o = 3M(G)_3|_o + 3H^+|_A \tag{2.9}$$

where HG represents a monomeric DEHPA molecule and M is the lanthanide in the solution.

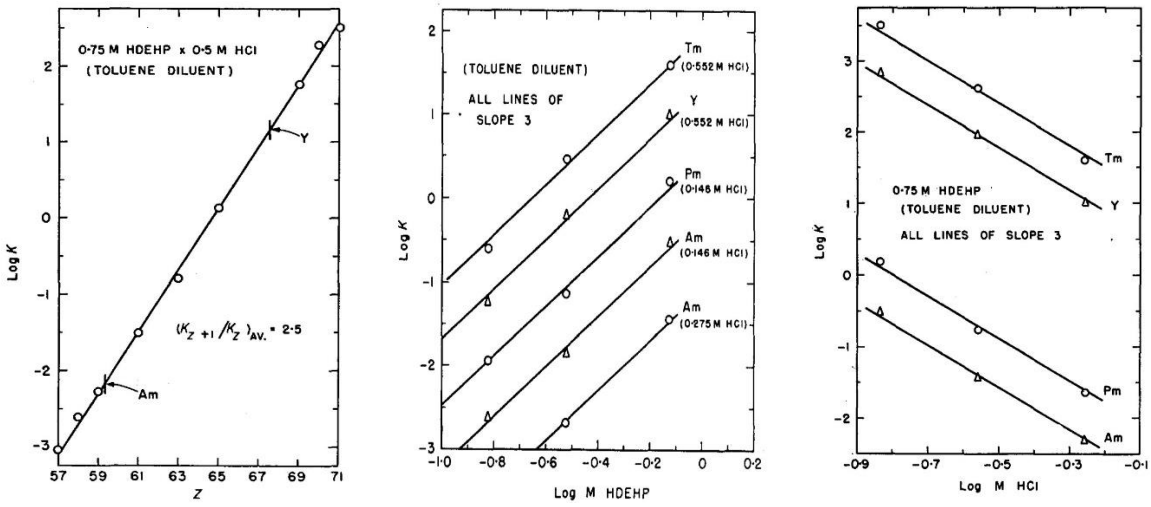

Figure 2.21 Variation of the log of the distribution coefficient of Tm, Y, Pm, and Am with atomic number (Z) log of the concentration of DEHPA and free concentration of acid in the solution[91].

A subsequent study by Peppard et al. [92] reported using cryoscopic and IR spectroscopy in which the molecule of DEHPA was strongly dimerized in benzene and naphthalene. Based on the extraction data in these solvents, the study suggested a revised reaction mechanism as shown by the expression:

$$M^{3+}|_A + 3(HG)_2|_o = 3M(HG_2)_3|_o + 3H^+|_A \tag{2.10}$$

where $(HG)_2$ represents the dimer molecule of DEHPA and M^{3+} represents the metal ion.

An isopiestic study performed by Baker et al. [93] supported the findings of the previous study and showed that, with the exception of the high molecular weight carboxylic acid, DEHPA exists as a dimer especially in non-polar diluents such as octane and kerosene.

A detailed study of lanthanum extraction by DEHPA over a range of concentrations in the aqueous phase by Kosinski et al. [94] showed that, at high lanthanum concentrations, the extracted species is not solely La^{3+} ions but also complexes formed by the ligand present in the aqueous phase as well. The study suggested that the extraction took place by three simultaneous reactions, which are shown as the following equations.

$$La^{3+}|_A + 3(HG)_2.H_2O|_o = 3La(HG_2)_3|_o + 3H^+|_A + 3H_2O \quad (2.11)$$

$$La + 2(HG)_2 \cdot 2H_20 = La(NO_3)(HG_2)_2 + 2H_2O + 2H^+ \quad (2.12)$$

$$La + 3(HG)_2|_o = 3La(HG_2)_3|_o + 3H^+|_A \quad (2.13)$$

The existence of DEHPA as a dimer and the extraction of metals as complexes has been validated by subsequent studies [95-98]. It is imperative to describe the complexing behavior of the metal in the aqueous phase to model the distribution coefficient accurately.

2.5.1.1 Basic Theory of Mononuclear Complexation

The aqueous solutions comprising of two different species A and B will theoretically form a range of complexes in the form of A_aB_b where a≥1 and b≥0. In the dilute solutions as studied in the present research, a large number of complexes for which a = 1 and b ≠ 0 are formed, which are called mononuclear complexes. The solutions under this study typically form metal complexes in which the central group (A) is a metal, and the surrounding groups (B) are ligands. The formation of these complexes is denoted by the following equilibrium reaction

$$A + nB = AB_n \quad (2.14)$$

The equilibrium constant for this reaction, also known as the overall thermodynamic stability constant, is given by

$$T_{kn} = \frac{|AB_n|}{|A||B|^n} \quad (2.15)$$

The quantities in the relation are thermodynamic activities of the respective species. In the case the preceding complex (AB_{n-1}) is also present in the system, the formation of the complex can be described by the stepwise stability constants T_{sn} which are described by the following equations

$$AB_{n-1} + B = AB_n \tag{2.16}$$

$$T_{sn} = \frac{|AB_n|}{|AB_{n-1}||B|} \tag{2.17}$$

Based on the definitions of the stepwise and the overall stability constants, the relation between the two can be depicted as

$$T_{kn} = \Pi_{n=1}^{m} T_{sn} \tag{2.18}$$

For weak complexing ions like the REE ions in chloride media, the mononuclear complexation occurs for all the complexes possible, i.e., R^{3+}, RCl^{2+}, RCl_2^{+}, and RCl_3. The total concentration of the central group species (REE) is calculated by the equation

$$(R)_T = (R^{3+}) + (RCl^{2+}) + (RCl_2^{+}) + (RCl_3) \tag{2.19}$$

Whereas the total concentration of the ligand species(chloride) can be calculated by the equation

$$(Cl)_T = (Cl^{-}) + (RCl^{2+}) + 2(RCl_2^{+}) + 3(RCl_3) \tag{2.20}$$

The more general form of these relations which are true for all the complexes can be written as

$$(A)_T = (A) + (AB) + (AB_2) + (AB_3) + \ldots \tag{2.21}$$

$$(B)_T = (B) + (AB) + 2(AB_2) + 3(AB_3) + \ldots \tag{2.22}$$

The concentration of any complex based on equation 11 can be calculated as

$$(AB_n)=T_{kn}(A)(B)^n \quad (2.23)$$

Substituting in the equations X and Y the total concentration can be expressed as a function of overall stability constants as follows

$$B_T=(B) + (A)\Sigma\, nk_n(B)^n \quad (2.24)$$

$$A_T=(A)(1 + \Sigma k_n(B)^n) \quad (2.25)$$

The degree of formation(a_i) is defined as the contribution of the complex in the total concentration of the central group i.e.

$$a_i=(AB_i)/((A)_T \quad (2.26)$$

rearranging the equation, the degree of formation can be defined as the

$$a_i = \frac{k_i(B)^i}{a + \sum_{n=1}^{m} k_n(B)^n} \quad (2.27)$$

2.5.2 The complex chemistry of the REEs in aqueous solution

There are several studies regarding the calculation of the stability constants of the metal complexes formed by the REEs, specifically the lanthanides in different acid media[17, 99-102]. In general, the stability constant of a complex of metal M in ligand X can be calculated by measuring a property of either M^{b+} or $MX^{(b-1)+}$ as a function of the concentration of X^-[103]. Choppin and Strazik [104] showed that the complexes formed by the REEs in the aqueous phase are of the outer sphere in nature, due to the monolayer of the water molecule between the metal and ligand ions. It also follows that the neutral species are absent in the solution except in the highly concentrated solution where the salt concentrations reach the solubility limits.

There are several methods to determine the stability constants of metal complexes most frequently used in the literature are ion spectrophotometry, potentiometric method, and distribution method.

The spectrophotometric method of calculating the stability constant involves measuring the impact of ligand species on the absorption spectra of the central group species and the change in the shape of the absorption band of the bonds. Coward and Kiser [105] studied the complexation behavior of the neodymium nitrate system at high concentrations of 0.5 M Nd concentrations and 4 M NO_3 concentrations. The study used a differential spectrophotometric method in the visible wavelength range (325-800 mμ). The association constant was calculated to be 0.77 at the ionic strength of 4.2 M. Krumholz [100] in a similar spectrophotometric study on the neodymium nitrate solution, determined the stability constants and the degree of formation, for the system for a range of ionic strengths from 0.6M to 2.0 M.

Mckay did a similar study using a similar methodology to estimate the stability constants of uranium complex in nitrate media using the spectra of 0.014M Uranium (IV) solutions [106]. The absorption spectra for different H^+ concentrations and NO_3^- concentrations were determined at room temperature with a double beam recording spectrophotometer (Figure 2.22). The study showed that the formation of the uranium nitrate complexes up to $U(NO_3)_6^{+2}$ occurred at successive concentrations of nitrate ion in the solution. The stability constants hence calculated, were verified by partition methodology, and the numbers from both the methods were in close agreement with each other.

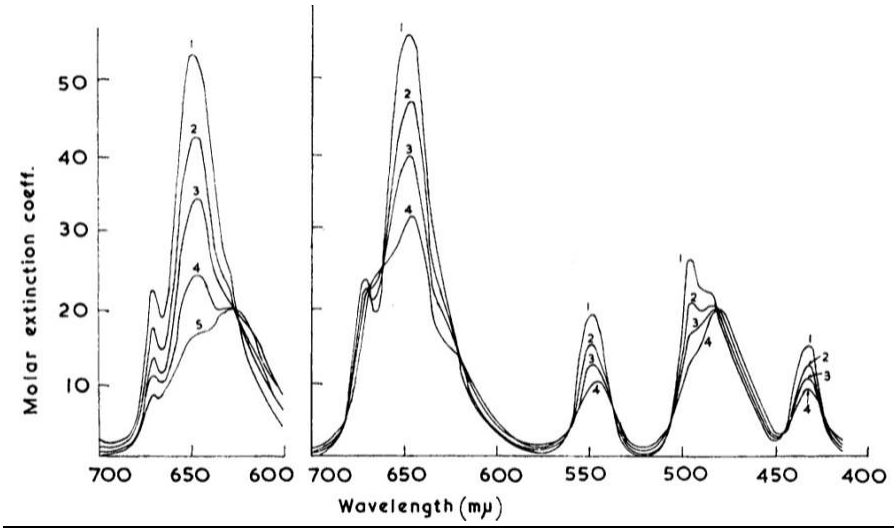

Figure 2.22 The changes in the uranium (IV) spectra due to hydrolysis and nitrate complex formation at different concentrations of H^+ ions and NO_3^- ions in the solution [106].

The potentiometric method for calculation of stability constants involves changing the concentration of metal ion, keeping the ligand concentration constant, and computing the ligand number by measuring the free ligand concentration and verifying the value by keeping the metal ion constant and varying the concentration of ligand in the aqueous phase. Goto and Smutz [101] calculated the stability constants of lighter REE, i.e., lanthanum, praseodymium, neodymium, and samarium using the potentiometric method. They reported the values to be 1.60, 1.58, 1.62, and 1.62, respectively, with 95% confidence levels [101]. A similar study was conducted by Ahrland and Larsson [107] for studying uranium complexation. The increase in the acidity of the solution when a known quantity of anhydrous uranium chloride salt was dissolved in the solution was less than one mole of the acid liberated per mole of uranyl ion liberated. The study determined the complexity of the U(IV) system by measuring the redox potential of the U(VI) and U(IV) couple in solutions of known acidity and different ligand concentration.

Peppard et al. [103] used the distribution method to study the complex chemistry of lanthanides and actinides. Perchloric acid was used to adjust the ionic concentration as well as the H^+ concentration of the solution. The variation of the distribution coefficient with the concentration of nitrate ligand was used to calculate the value of stability constants of $M(NO3)^{2+}$ for lanthanum, yttrium, scandium, actinium, and americium. The extractant, di[para(1,1,3,3 tetramethyl butyl)phenyl] phosphoric acid, was used in this study for calculation of the stability constants. Using the distribution method (Figure 2.23), the stability coefficients for nitrate complexes of lanthanum, cerium, praseodymium, and europium were calculated to be 1.3, 1.3, 1.7, and 2.0. The ionic strength was maintained at 1.0 using perchlorate salts for all the calculations.

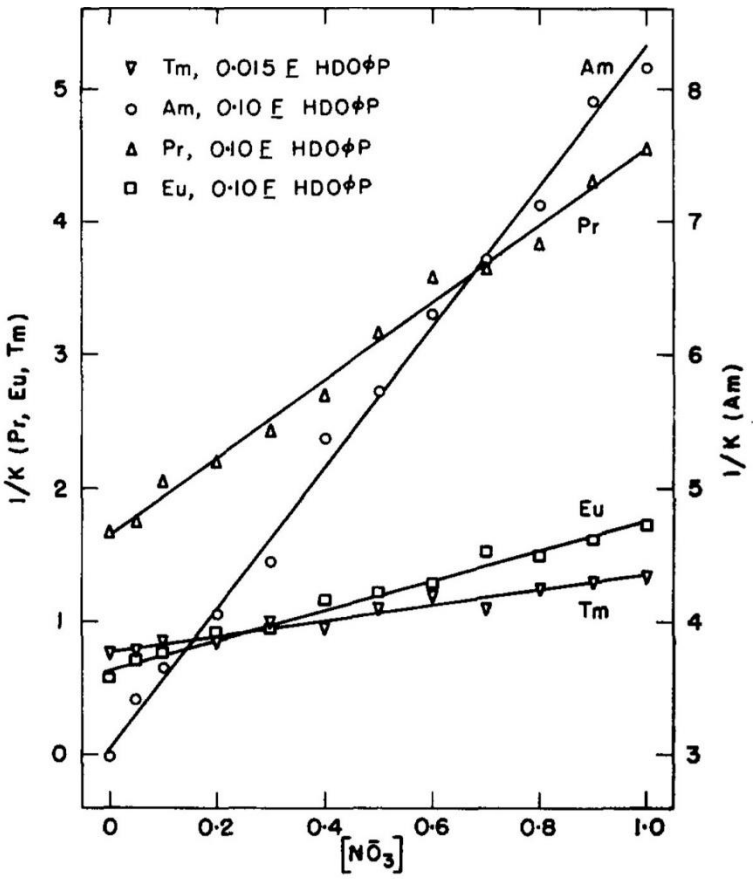

Figure 2.23 Variation of (1/K) (K = Distribution coefficient) for Tm, Am, Pr, and Eu with NO_3^- concentrations in the solution with ionic strength [108].

2.5.3 Modeling of Distribution Coefficients of REEs

Due to their similar nature as well as their high tendency to interact with each other, it is notoriously difficult to predict the extraction behavior of REEs in different systems. As a result, despite having a well-established industry for extraction and separation of REEs, there is a lack of a general model to predict their extraction behavior in various systems and conditions. A comprehensive review of the existing models was carried out by Forrest and Hughes [109], which categorized the models in to broadly 3 categories, fully empirical, semi-empirical, and chemical model.

A basic regression model to compare the extraction of REEs in nitrate and sulfate media was carried out by Alstad et al. [110] to predict the effect of complexation on the distribution

coefficient across the phases. Sharp and Smutz [108] developed a fully empirical mathematical model for predicting the extraction behavior of a five solute system consisting of the REEs associated with monazite mineral. The model used experimental data for two-component and extrapolated the data for more complex systems. The calculation method employed by Sharp et al. [108] had two basic assumptions,

i. Separation factors between two rare earth nitrates are a function of the total nitrate molarity and relatively independent of the phase composition
ii. The separation factor data obtained using 2 solute system could be extrapolated to multi-solute systems.

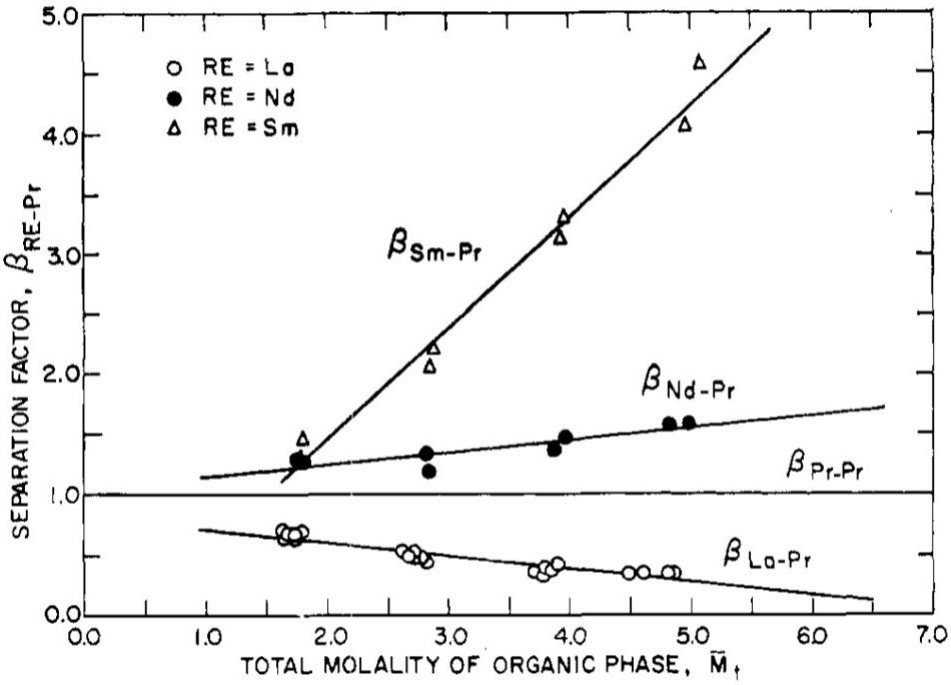

Figure 2.24 Separation factor between different $RE(NO_3)_3$ (Sm, Nd, Pr, and La) and $Pr(NO_3)_3$ for binary systems as a function of the total molal concentration of the organic phase [108].

A similar approach was tried by Goto [111], where he modeled the extraction of copper in LIX on a three-variable polynomial. There was a good agreement in the predicted and experimental

calculated; however, the polynomial was fitted using separate parameters on separate parts of the extraction curve. In a separate study by Ioannou [97] the same extraction curve was fitted on a different polynomial of the form

$$y = a_1 x^{a_2} e^{a_3 H^{(a_4 + a_5 H + a_5 H^2)}} \tag{2.28}$$

Where a_1, a_2, a_3, a_4, a_5 are the empirical constants calculated by curve fitting.

The average error in all the empirical models was reported to be less than 5%. However, the models did not have a thermodynamic basis, and the prediction was made solely on mathematical regression.

The extraction of metals between two immiscible phases in a liquid-liquid equilibrium can be modeled on a semi-empirical basis by making use of the equations which are used to model other analogous equilibriums, for instance, solid-gas equilibria or vapor-liquid equilibria. Lloyd and Ortel [112] used the power relation analogous to the Freundlich adsorption theorem which is depicted by the following equation

$$\frac{y}{x} = \varepsilon(M - ny)^d \tag{2.29}$$

where *y* is the molarity of the metal in the organic phase, *x* the molarity of the metal in the aqueous phase, *M* the total extractant concentration, and *n* the number of amine molecules reacting with a metal ion. Therefore, (M-ny) represents the available extractant concentration. The study correlated around 100 extraction isotherms using amines, and most of the curves were correlated using the linear form of the power equation, i.e., d=1.

Ioannou et al. [97]. attempted to correlate the extraction of lanthanide chlorides by DEHPA using a series of linear terms derived from Raoult's law and Dalton's law for vapor-liquid equilibria. The total concentration of REEs in the organic phase was modeled as given in the following equations for binary and ternary systems, respectively:

$$Y_T = y\ddot{S}\ddot{m}N_{Sm,aq} + y\ddot{N}\ddot{d}N_{Nd,aq} + \Delta y_{Sm} + \Delta y_{Nd} \tag{2.30}$$

$$Y_T = y\ddot{S}\ddot{m}N_{Sm,aq} + y\ddot{N}\ddot{d}N_{Nd,aq} + y\ddot{C}\ddot{e}N_{Ce,aq} + \Delta y_{Sm} + \Delta y_{Nd} + \Delta y_{Ce} \tag{2.31}$$

where Y_T is the total REE concentration in the organic phase, Δy_{sm}, Δy_{Nd}, *and* Δy_{Ce} the deviations from ideality for their respective elements, i.e., the fugacity of the extraction. The $y\ddot{S}m, yNd, \ddot{a}nd\ y\ddot{C}e$ represent the molarity of the metals in the organic phase. The predicted equilibrium values are in close agreement with the experimental data. However, the models in this category are not calculated on the actual reaction mechanism and have no basis on the thermodynamics of the reaction taking place in the extraction.

The first notable attempt to model the distribution coefficients of metals thermodynamically was reported by W.G. O Brien [113]. The study used the reaction mechanism developed by Kosinski and Baustian [94]. The developed model was a function of the activity of hydrogen ions in the solution, activity of the nitrate ion, and the stability constants for the nitrate complexes in the solution. The model calculated the extraction constants for each complex using the least-squares method. The predicted values were close to the experimental values; however, the extraction constants calculated were negative in value, which negated any physical significance of the thermodynamic model. The author acknowledged that the model transgressed into an empirical model.

Nevarez and Bautista[114] used a similar methodology to model the extraction of cobalt from a cobalt chloride solution using TBP. The primary assumption in Nevarez's approach, which was different from O'Brien's method, was that the ratio of the activity coefficient was represented by a constant, which simplified the model significantly. A similar assumption was applied by Hoh and Bautista [115] in their model copper-LIX system, and the model predicted published experimental data accurately with a correlation coefficient value (R^2) of 0.99 which reflects the differences between the predicted and experimental data. Hoh [95] developed a thermodynamic model to predict the liquid-liquid extraction of lanthanides and actinides from aqueous acidic solutions, which extended the work done by previous researchers and applied it to binary and ternary systems. The study covered both DEHPA and TBP as the extractant. One of the main shortcomings of the aforementioned models is that each model required equilibrium data of some species in the system to predict the distribution coefficient of the metal. While the estimation is based on a thermodynamic calculation, it is impossible to predict the distribution coefficients from these models using just the initial conditions of the extraction, which is required for designing a solvent extraction circuit.

In recent studies carried out by Giles et al. [116], an artificial neural network was used to predict the distribution coefficients of the lanthanides. The principal variables selected for this study were the concentration of the dimeric extractant, aqueous pH value, initial aqueous rare earth concentration, the concentration of spectator anion, the phase ratio, and the polarity of the diluent. The regression of the function was performed by the back-propagation network of an input layer with eight processing units, one hidden layer with two nodes and a sigmoidal output layer with one node corresponding to the output, i.e., the % extraction of the metal. Though the model predicted the distribution coefficients accurately; it did not incorporate the impact of metal complexation on its extraction behavior.

Han et al. [117] developed a thermodynamic model that predicted the distribution coefficients of a single component lanthanide chloride-DEHPA system. The model was based on lanthanide and hydrogen activity coefficients, the concentration of the reacting species, and terms for thermodynamic stability constants for the chloride complexes in solution. The main drawback of the model is that it made a broad assumption that the ratio of the activity coefficients in the organic phase was constant, which is not true for all the concentrations of the metal extracted.

Given the wide range of models that differ from both their approach and ultimate results, the models are categorized and summarized in and Table 2.4

Table 2.3 Summary of the predictive models for distribution coefficients: system and approach.

Name	**Year Reported**	**System**	**Approach**
Alstad [110]	1974	REE-DEHPA	Empirical
Sharp and Smutz [108]	1965	REE-TBP	Empirical
Goto [111]	1971	REE-DEHPA	Empirical
Ioannou[118]	1972	REE-DEHPA	Empirical
Lloyd and Ortel[112]	1963	Uranium-Amine Extractant	Semi-empirical

Ioannou [97]	1970	REE-DEHPA	Semi-empirical
O’ Brien [96, 113]	1974	REE-DEHPA, REE-TBP	Thermodynamic
Nevarez and Bautista [114]	1976	REE-DEHPA	Thermodynamic
Hoh and Bautista [115]	1978	Cu-LIX	Thermodynamic
Han and Tozawa [119]	1988	REE-DEHPA	Thermodynamic
Giles [116]	1996	REE-DEHPA	Artificial Neural Network (thermodynamic)

Table 2.4 Summary of the predictive models for distribution coefficients: thermodynamic parameters considered in the model.

Name	Complexation	Activity of species	Estimation using initial condition
Alstad [110]	Not considered	No	Yes
Sharp and Smutz [108]	Not considered	No	Yes
Goto [111]	Not considered	No	Yes
Ioannou[118]	Not considered	No	Yes
Lloyd and Ortel[112]	Not considered	No	No
Ioannou [97]	Not considered	No	No
O' Brien [96, 113]	Extraction Method	Vapor pressure measurement	No
Nevarez and Bautista [114]	Extraction Method	Ion-electrode measurement	No
Hoh and Bautista [115]	Extraction Method	Ion-electrode measurement	No
Han and Tozawa [117]	Not considered	Activity Coefficient estimation	Yes
Giles [116]	Least-squares	ANN estimation	No

Even though there are a large number of predictive models discussed in the literature, they are either empirical in nature, or require quantities at equilibrium as input or do not consider the non-idealities in the aqueous and organic phase. Therefore, there is a necessity of a chemical reaction based model which can predict the distribution coefficient using the initial conditions of the system, so that it can be meaningfully applied for design of a solvent extraction process. In this study, a predictive model, which takes the lanthanide complexation as well as the thermodynamic non-idealities in both organic and aqueous phase into consideration was developed.

3 MATERIALS AND METHODS

3.1 Materials

3.1.1 Coal samples

Coal samples were collected from three processing plants that process high-volatile bituminous coal produced by active mines in two different coal basins (i.e, Illinois Coal Basin and the Central Appalachian Coal Basin) and from three different seams (i.e., Illinois No. 6, West Kentucky No. 13 and Fire Clay) (Figure 3.1)

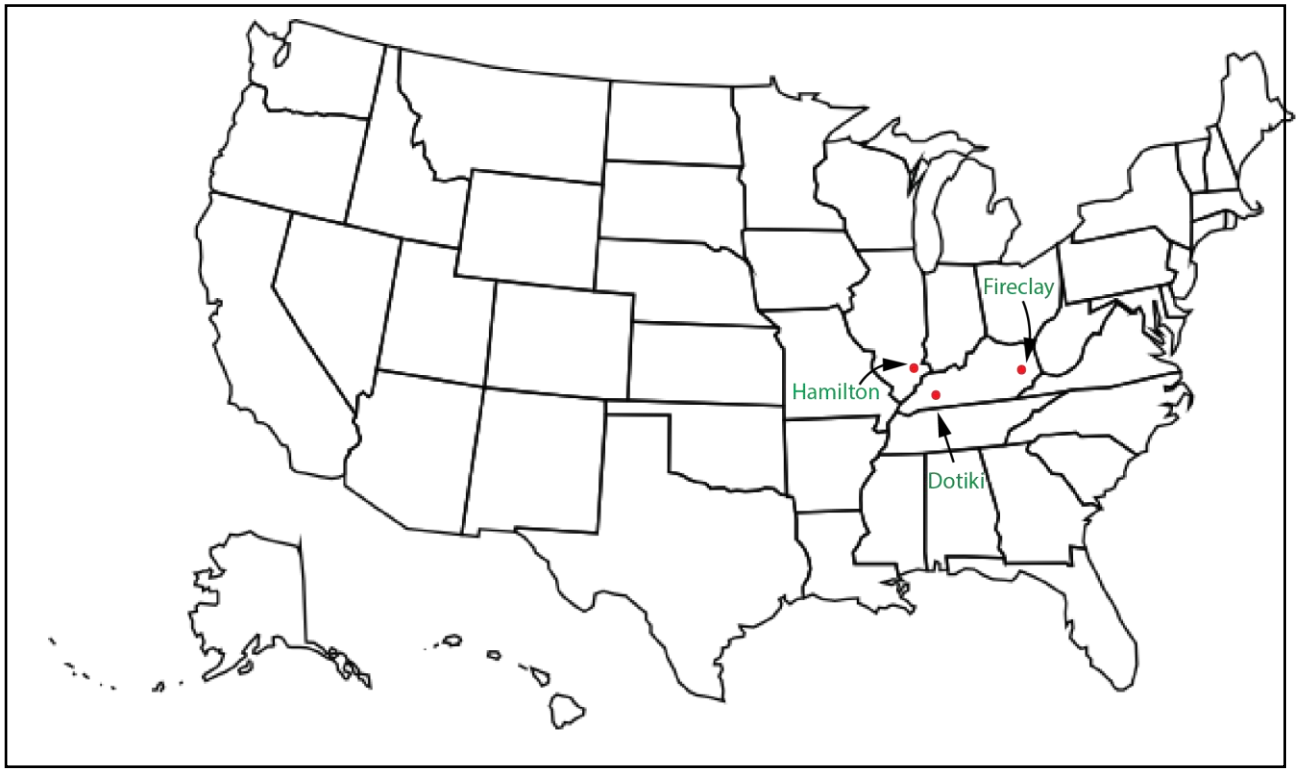

Figure 3.1 Summary of locations from where coal samples were collected for the test program.

Table 3.1 Description of the processing plants from where the samples were collected for testing.

Coal Seam	Location	County	Preparation Plant Capacity (tph)
Kentucky No. 13	Western Kentucky	Webster	1800
Fire Clay	Eastern Kentucky	Perry	1400
Illinois No. 6	Southern Illinois	Hamilton	1800

The Fire Clay coal seam is a high-quality bituminous coal source that is commonly used as low sulfur fuel for coke ovens, stoker boiler units and pulverized coal combustion (PCC) units. The seam is internationally recognized for its enriched rare earth content which resulted from exposure to volcanic deposition during the coalification stage of the seam formation. The deposition created a parting layer known as 'tonstein' material, which is hard, compact sedimentary rock composed of mainly kaolinite. Over geologic time, the rare earth content leached out of the tonstein layer and distributed into various segments of the coal and surrounding rock material as shown in the graph and associated photograph of the seam cross-section in Figure 3.2. The roof material and coal sections below the tonstein layer of total REE contents well above 400 ppm on a dry whole mass basis. Ash-based REE content values in the coal segments range from 0.1% to 0.4%. The coal seam is relatively thin and thus requires removal of a significant amount of roof and floor material during extraction by continuous miners to make room for equipment. As such, a significant amount of the enriched REE rock material is removed during the upgrading that occurs in the coal preparation plant which reports primarily to a coarse refuse stream and transported by conveyor belt to permanent storage.

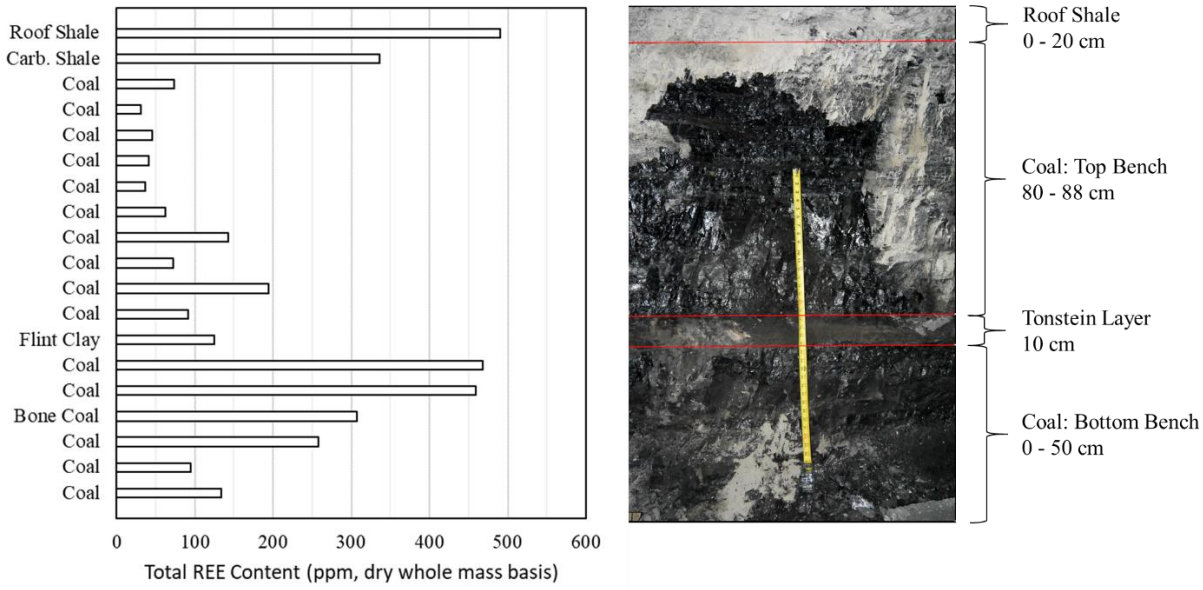

Figure 3.2. Cross-section of the Fire Clay coal seam.

The bituminous coal sources in the Illinois Coal Basin are primarily used as fuel to utilities for electric production. Relative to the Fire Clay coal, both the West Kentucky No. 13 and Illinois No. 6 coals have a higher inherent moisture content and lower heating values. An important characteristic of Illinois Basin coals is the relatively high pyritic sulfur content which creates acidic water discharge when oxidized. As such, the pyrite sources provide a natural acid solution that is useful for assisting in the leaching of the REEs from the coal. Mineral content analysis results of a representative sample of West Kentucky No. 13 coarse refuse using X-ray Diffraction (XRD) is shown in Figure 3.3. The peaks labeled as 'P' represent pyrite and the number and height of the peaks indicates a significant presence of pyrite in the coal source. Quartz and kaolinite are other major minerals present in the coarse refuse. Although not indicate, highly soluble acid consuming minerals such as calcite are also present in significant quantities based on analyses of the leachates produced from the leaching experiments performed on the coal and acid consumption values.

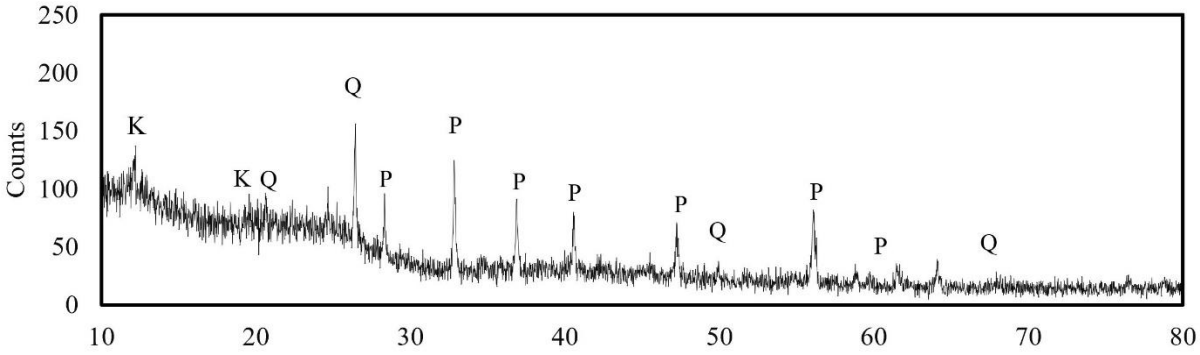

Figure 3.3. XRD analysis on 1.6 float fraction of Dotiki coarse reject. Peaks marked with 'P' refer to pyrite while peaks marked with 'Q' refer to quartz and 'K' kaolinite.

The West Kentucky No. 13 seam coal has been identified as being enriched with REEs relative to most other Illinois Basin coal sources[120]. The rock material associated with the seam occurs in the floor and roof as well as a series of partings. As shown in Table 3.2, very high concentrations of REEs occur in a few of the partings that are extracted as part of the mining process. Material collected from the parting second from the top was found to have around 5% fluorapatite which is a source of soluble REEs. The parting contained nearly 0.1% total REEs on a dry whole mass basis. The coal is extracted using room-and-pillar mining and continuous miners. The seam is relatively thick which limits the amount of roof and floor material that is removed during extraction to less than 15 cm. Thus, most of the rock material removed during the cleaning process originates from the parting material.

Table 3.2. Petrographic analysis including REE concentrations in each segment of the West Kentucky No. 13 coal seam obtained from a core sample.

Description	Lithology	REE (ppm, ash-basis)			REE (ppm, whole-basis)			HREE /LREE
		TREE	LREE	HREE	TREE	LREE	HREE	
Roof	Rock	259.5	218.2	41.3	239.1	201.0	38.1	0.19
Roof	Rock	277.6	237.1	40.5	256.5	219.0	37.4	0.17
Parting	Claystone	212.1	173.8	38.4	174.2	142.7	31.5	0.22
Parting	Claystone	1143.9	988.8	155.2	928.9	802.9	126.0	0.16
Parting	Claystone	362.7	317.5	45.2	322.1	282.0	40.1	0.14
Parting	Claystone	456.2	394.7	61.5	398.6	344.9	53.8	0.16
Parting	Claystone	334.5	287.5	47.1	265.0	227.7	37.3	0.16
Floor	Rock	389.8	286.2	103.6	334.7	245.8	89.0	0.36
Floor	Rock	161.2	135.9	25.2	143.3	120.9	22.4	0.19
	Total Rock	349.2	294.2	55.0	308.5	259.9	48.6	0.19

The Illinois No. 6 coal is the dominant source of utility fuel coal in the state of Illinois. The coal is extracted by longwall mining equipment at the location that the sample was collected. The naturally occurring pyrite creates a REE enriched liquid solution as a result of leaching from the organic matter and the associated mineral matter.

At all three preparation plants, samples were collected from the coarse refuse belts using in-line sweep belt samplers such as the unit pictured in Figure 3.4. The coarse refuse stream was comprised of the reject material generated from dense media cyclone circuit which treated the 75 x 1 mm fraction and spiral concentrator circuit which provided upgrading for the 1 x 0.15

mm fraction. A sample cut measuring about 10 kg was collected every 20 minutes for a period of about four operating hours. Each sample increment was placed into a 200 L barrel and transported to the research lab to be processed for use in the research program.

Figure 3.4 Sweep-belt sampler used to collect representative samples from the coarse refuse process stream of a coal preparation plant.

A representative sample was collected from the bulk samples of both the Fire Clay and West Kentucky No. 13 coarse refuse materials. Duplicate analyses were performed on the two samples and the results provided in Table 3.3 and Table 3.4. The results indicate that the standard error resulting from sample preparation and REE analysis using inductively coupled plasma optical emission spectrometry (ICP-OES) was relatively small. The total REE content

values averaged 324 ppm and 312 ppm on a dry whole mass basis for the Fire Clay and West Kentucky No. 13 samples, respectively.

Table 3.3. Rare earth analysis of the Fire Clay coarse refuse sample.

Source	Ash%	TREE (ppm)	
		Ash Basis	Whole Mass Basis
Leatherwood Coarse Refuse 121416 -1	87.75	364.6	320
Leatherwood Coarse Refuse 121416 -2	88.07	365.5	321.9
Leatherwood Coarse Refuse 121416 -3	87.40	375.1	327.9
Leatherwood Coarse Refuse 121416 -4	87.60	369.4	323.6
Leatherwood Coarse Refuse 121416 -5	87.65	372.8	326.8
Leatherwood Coarse Refuse 121416 -6	88.13	368.7	324.9
Average	87.77	369.4	324.2

Table 3.4 Rare earth analysis of the West Kentucky No. 13 coarse refuse sample.

Sample	Duplication	Ash%	TREE (ppm)	
			Ash Basis	Whole Mass Basis
Coarse Reject	1	84.68	364	308
	2		376	318
	3		360	305
	4		374	316
Average			369	312

As shown in Figure 3.5, the bulk samples obtained from all three sources were split into two density fractions, i.e., 1.8-2.2 s.g. fraction and 2.2 s.g. sink fraction by density fractionation using magnetite as the media (Figure 3.5). Magnetite was chosen as the medium to avoid the effect of potential chemical reactions if salt-based mediums were utilized. The solids in each density fractions were crushed using a laboratory jaw crusher followed by a hammer mill and

subsequently pulverized in a smaller hammer mill to achieve a top particle size of 177 microns (80-mesh). The pulverized feed was used as the feed for the leaching tests.

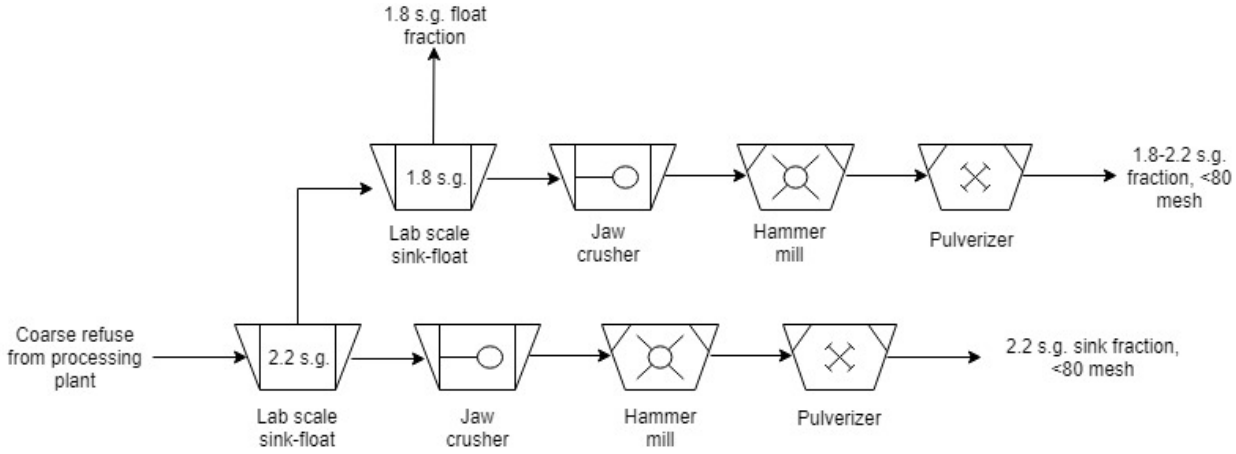

Figure 3.5 Schematic for sample preparation process conducted on the coarse refuse from the processing plant.

3.1.2 Heap leachate

The continuous solvent extraction process developed as the part of the study was tested on a pregnant leach solution (PLS) generated using a small heap leach developed with uncrushed coarse refuse from the West Kentucky No. 13 seam material as shown in Figure 3.6. A pump was placed in the trench that surrounds the coarse reject heap and a pipe run for the pump and up through the middle of the pile. The pump was used to circulate the PLS water generated from pyrite oxidation and natural rainwater from the trench through the spray that distributed the PLS across the entire heap. The system was operated for a period of approximately eight months. At the time of the test, a pump was placed in the trench which transported PLS from the trench to a tanker truck as shown in Figure 3.6(b).

An elemental analysis by ICP-OES of a representative sample found that the total REE content in the PLS was 14.45 ppm as shown in Table 3.5. Yttrium, gadolinium and cerium represented the largest portion of the REEs while the presence of neodymium, dysprosium and scandium were noteworthy. However, concentrations of problematic contaminant ions like iron and aluminum were more than two orders of magnitude greater. On the other hand, the

concentration of thorium was extremely low which was a clear advantage over other sources of PLS.

Figure 3.6 The site for generation of heap leachate from the coal coarse refuse of Dotiki coal preparation plant.

Table 3.5. Elemental analysis of the PLS collected from the heap leach pad constructed from West Kentucky No. 13 coarse refuse material.

Element	PPM
Sc	0.78
Y	3.9
La	0.31
Ce	2.25
Pr	0.88
Nd	1.09
Sm	0.62
Eu	0.19
Gd	2.65
Tb	0.29
Dy	0.95
Ho	<0.003
Er	0.01
Tm	0.09
Yb	0.31
Lu	0.14

Element	PPM
Th	<0.003
U	1.53
Fe	5453
Al	1467
Ca	459
Mg	572
Mn	77.6

3.1.3 Chemicals

In the present study, di-(2ethylhexyl) phosphoric acid (DEHPA) was used as the extractant for solvent extraction tests. DEHPA is a cation exchange extractant extensively used for the separation and concentration of REEs. Tributyl phosphate (TBP), which is a solvation type extractant, was used as a phase modifier to improve the phase disengagement behavior of the phases (Figure 3.7). Reagent grade odorless kerosene was used as the diluent for the extractant to improve the mixing characteristics of the organic and aqueous phase by reducing the viscosity of the organic phase. A similar aliphatic diluent, SX Orfom manufactured by Chevron Chemicals was used for the continuous testing of the process.

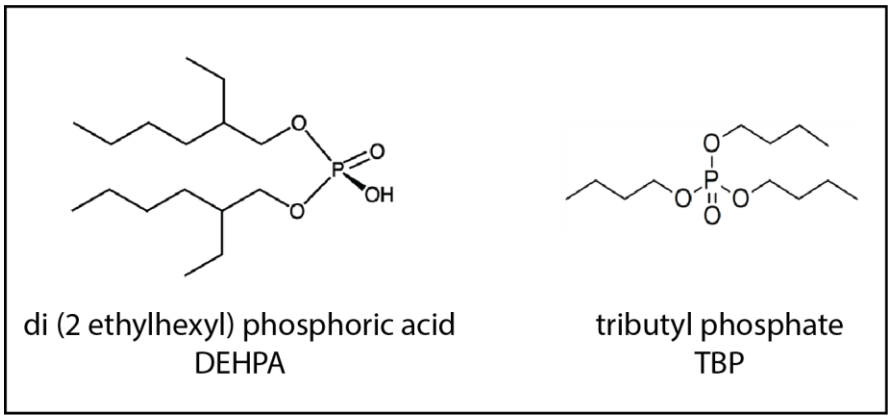

Figure 3.7 Molecular structure of di(2 ethylhexyl) phosphoric acid(DEHPA) and tributyl phosphate (TBP) used in the study as extractant and phase modifier, respectively.

Tracemetal™ grade sulfuric acid solution in de-ionized (DI) water was used as a lixiviant for leaching tests. Appropriate concentrations of sulfuric acid, hydrochloric acid, and sodium hydroxide were used as pH modifiers for the aqueous solutions. Hydrochloric acid was also used in different concentrations as scrubbing and stripping agents for the organic phase in the extraction tests. An aqueous solution of ascorbic acid in DI water served as a reducing agent for ferric ions present in the leachates. An aqueous solution of oxalic acid was utilized as a chelating agent for selective precipitation of the REEs. Reagent grade salts of lanthanum, neodymium, gadolinium, dysprosium, and yttrium were used to prepare the stock solution for the extraction tests of REEs while aluminum, iron and calcium salts were added as the contaminant species. The addition of sodium perchlorate solution maintained the appropriate ionic strength in the equilibrium studies for the determination of thermodynamic stability constants. The details of the chemicals utilized in the study are provided in Table 3.6.

Table 3.6 Details of the chemicals used in the current study.

Name	Formula	Molecular Weight (g/mol)	Purity Grade	Source
DEHPA	$(C_8H_{17}O)_2PO_2H$	322.43	95%	Alfa Aesar
TBP	$C_{12}H_{27}O_4P$	266.318	99%	Fisher Sci
Kerosene	N/A	~170	Reagent	Fisher Sci
SX Orfom	N/A	~170	Reagent	Chevron Chemicals
Sulfuric acid	H_2SO_4	98.079	> 99.99%	Fisher Sci
Hydrochloric acid	HCl	36.46	> 99.99%	Fisher Sci
Nitric acid	HNO_3	63.01	> 99.99%	Fisher Sci
Sodium hydroxide	NaOH	39.997	> 99.99%	Fisher Sci
Ascorbic acid	$C_6H_8O_6$	176.12	> 99.99%	VWR
Oxalic acid	$C_2H_2O_4$	90.03	99.6%	VWR

3.2 Methods

3.2.1 Experimental Setup

3.2.1.1 Leaching Test Apparatus and Procedure

Feed preparation for the solvent extraction experiments involved leaching coal samples using an acid solution to extract the REEs from the coal to the aqueous phase. The leaching process was performed in triple necked round bottom flasks submersed in a heated water bath as shown in Figure 3.8. The agitation in the reactor was provided using a magnetic stirrer while the solution temperature was maintained at the 75°C using an immersion water heater. A water jacket cooled reflux condenser was used on the middle neck to contain the evaporated liquid within the reactor. Solution pH and temperature was monitored, and sampling achieved using the side necks. The lixiviant was a 1.2 M solution of sulfuric acid in deionized (DI) water, which resulted in solution pH value of 0.0. The mass of solid sample (100g) needed to achieve a 10% solid concentration by weight was added to one liter of lixiviant in the reactor. The

solids were leached in the acid for two hours after which time the solids were separated from the acid leachate using a vacuum filtration setup that included a Buchner funnel.

Figure 3.8 Experimental setup used for leaching tests in the study.

The solution pH was periodically monitored, and additional acid was added to maintain the solution pH at 0.0. An Orion Versa STAR Pro pH meter with an Orion SureFlow glass probe provided by Thermo Fisher was used for measuring and monitoring the pH of the solution. The setup was capable of accurately measuring the pH from -2.00 to 20.00 and temperatures from 5ºC to 105ºC. The pH probe had a response time of 30 seconds at which the pH value measured by it was stabilized within 0.01 pH units. Both the temperature and the pH of the PLS were within the accuracy range of the pH probe. A 3-point calibration was performed on the pH probe using 1.68, 4.01 and 6.98 pH buffer solutions before each set of experiments to ensure accuracy.

3.2.1.2 Solvent Extraction Apparatus and Procedure

The solvent extraction tests were performed by mixing equal volumes of aqueous solution and organic solution (1:1 organic-to-aqueous ratio) in an Erlenmeyer flask on a VWR orbital shaker. The orbital shaker had the capability to shake the flasks at a range of speeds from 15 RPM to 500 RPM. The speed of the shaker was maintained at 400 RPM throughout the test program to ensure sufficient mixing without formation of stable emulsions which prohibited

phase separation. The solution was allowed to stand in a separatory funnel for 10 minutes to allow for the complete disengagement of the phases, which resulted in the heavier aqueous phase to settle at the bottom of the funnel with the lighter organic phase floating on top. The aqueous and the organic phases were separated by first extracting the aqueous phase through the bottom export valve, and representative samples of the aqueous solution were analyzed using ICP-OES (Figure 3.9). The pH of the initial aqueous solution and the aqueous solution at equilibrium were measured using the Orion Sureflow glass bulb probe described previously in the leaching section.

Although the reaction kinetics of the equilibrium reaction of solvent extraction is relatively fast as indicated by a period of only 600 seconds to achieve a constant value as shown by Wang et al. [121] and Parhi et al. [23], the shaking time was 15 minutes to ensure that complete equilibrium was reached between the organic and aqueous phases. The metal concentration in the organic phase at equilibrium was calculated by the mass balance of the initial metal concentration and the concentration of metal at equilibrium in the aqueous phase.

The aqueous solutions used for the testing of contaminant rejection from the leachates were prepared using reagent grade salts of iron, aluminum, and calcium representing the contaminants present in the acid leachate based on typical concentration in PLS generated from coal-based materials while lanthanum salt was used to represent the REE in the leachate. Lanthanum being the lightest REE and having the lowest extraction efficiency of all the REEs [91] was used as the REE to represent the group of 17 total rare earth elements (TREE). Contaminant rejection was tested on real leachates from six coal sources from three different coal seams to produce an REO concentrate from each of the sources.

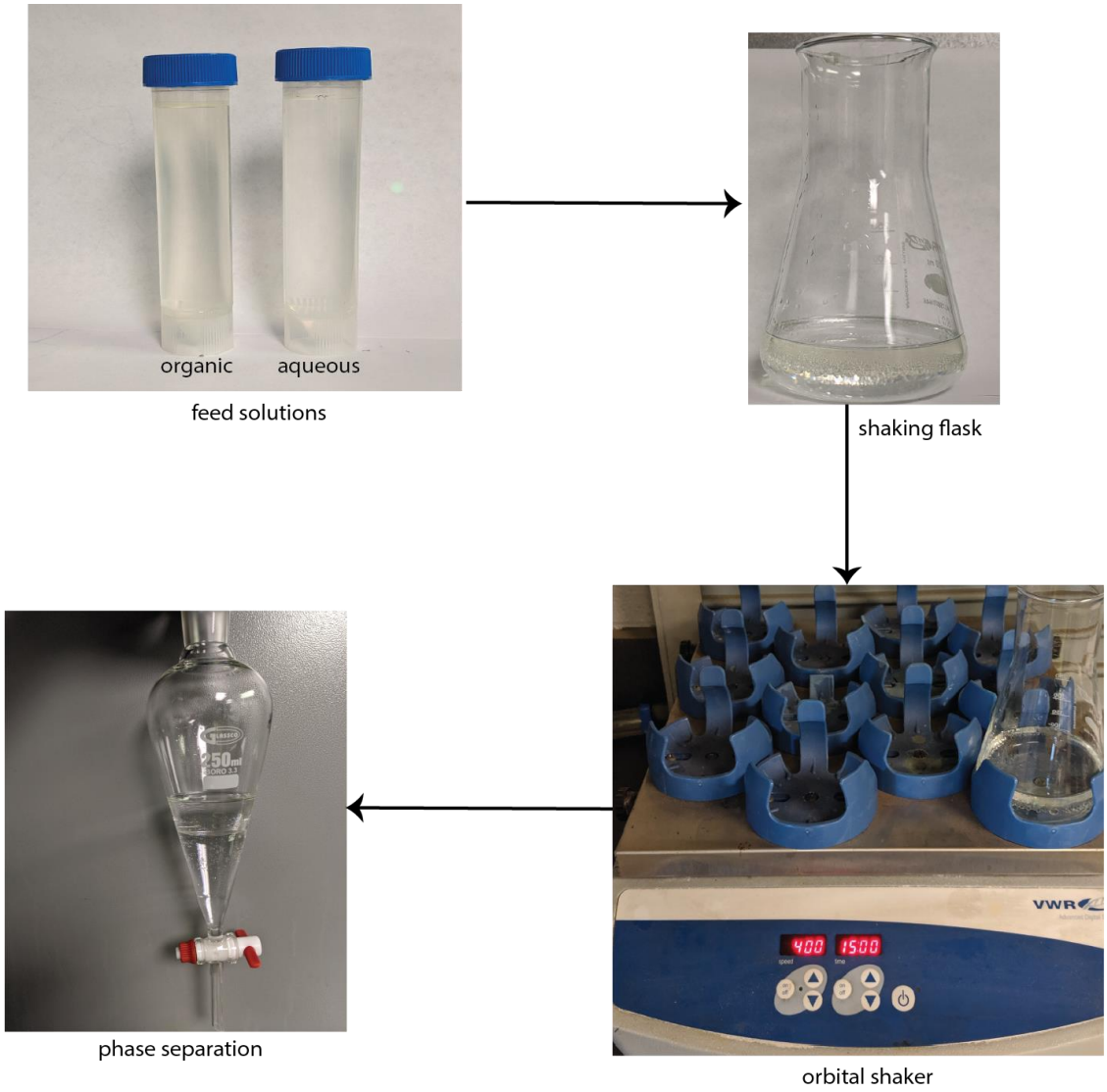

Figure 3.9 Bench-top solvent extraction test procedure.

The activity of the hydrogen ion (pH) and the chloride ion for the calculation of the thermodynamic stability constants were measured by pH probe and chloride ion-selective electrode (ISE), respectively. The ISE probe was calibrated using 3-point calibration by standard solutions of sodium chloride solutions of 1 M, 0.5 M, and 0.25 M solutions.

3.2.1.3 Continuous Solvent Extraction Testing

The continuous testing of the solvent extraction process developed from the research was performed on pilot-scale equipment, which had a capacity to process 4 L/min of PLS. The pilot-scale equipment was provided by SX Kinetics.

The typical mixer-settler consists of two chambers. The first chamber is referred to as the mixer chamber that contains an impeller providing the agitation to mix the immiscible phases as well as the pumping action to draw the liquids from the previous stages. The dispersed phase mixture then flows into the second chamber commonly called the settler chamber where the immiscible phases are allowed to disengage and separate. The aqueous phase, which is heavier than the organic phase, naturally flows out through the bottom of the settler chamber and advances to the next stage while the lighter organic phase floats and discharges from the top of the chamber through the organic outlet. The interface between the organic and the aqueous phase is controlled by the level of the adjustable weir, which also determines the height of the aqueous outlet (Figure 3.10).

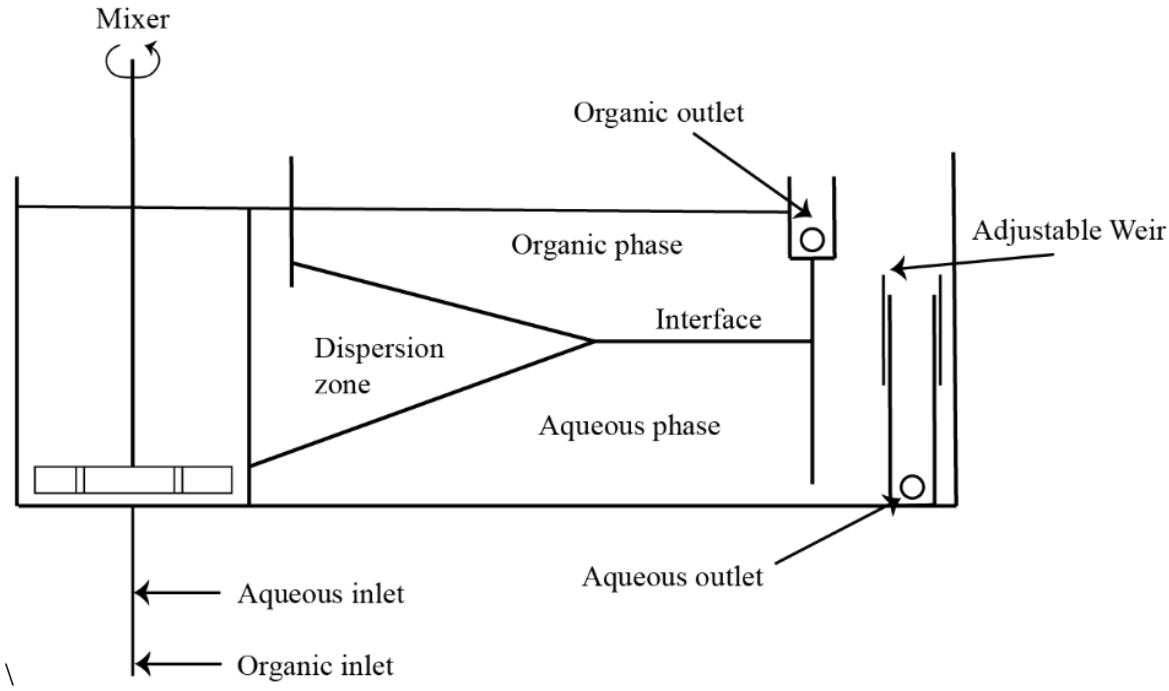

Figure 3.10 Schematic of a typical conventional mixer-settler used in a solvent extraction process.

The equipment used for the rougher cycle of the process was comprised of 10 conventional mixer-settlers (Figure 3.11) having a volume of 10 liters each. Similar to the cleaner cycle setup, a bleed stream from the either organic or aqueous stream was recycled from settler to the mixer chamber. The interface in the conventional mixer settler was controlled by the underflow weir, the height of which was adjustable by a jackleg sleeve.

Figure 3.11 Conventional mixer-settler setup used in the pilot-scale continuous scale solvent extraction testing.

The quality of the initial rougher solvent extraction product was not sufficient to meet typical market requirements. As such, the first stage stripped product was re-treated in a second stage solvent extraction unit often referred to as a cleaner stage. The equipment used for the cleaner cycle was comprised of glass mixer-settlers in which the organic-aqueous interface was controlled by an adjustable overflow weir in the form of a sleeve (Figure 3.12). The mixer chamber in the bench-scale setup had an effective volume of 500 ml, while the settler had an effective volume of 2000 ml. The mixer-settler was configurable to recycle a bleed stream of either the organic or aqueous phase from the settler back to the mixer as required by the process. The setup used in the study was comprised of a train of six glass mixer settlers, which were customized to run any number of loading, scrubbing and stripping stages (Figure 3.13). The unit was also capable of operating over a range of flow rates and aqueous-to-organic phase ratios in different stages.

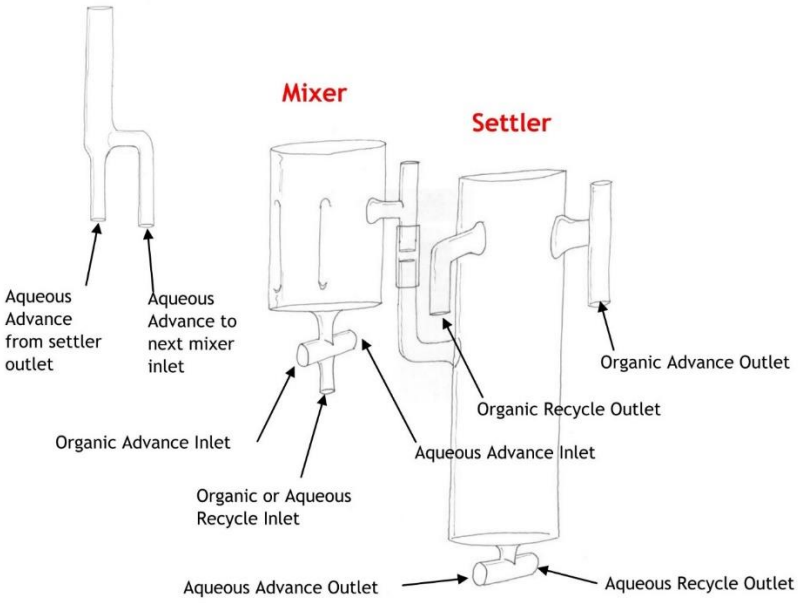

Figure 3.12 Schematic representation of the inlet and outlet ports of the glass mixer-settlers along with the overflow weir used in the continuous testing of the solvent extraction process in this study[122].

Figure 3.13 Laboratory scale setup of the solvent extraction equipment comprised of six glass mixer settlers used for continuous testing of the solvent extraction circuit.

3.3 Analytical Tools

3.3.1 Elemental analysis

Inductively coupled plasma-optical emission spectroscopy (ICP-OES) was used to analyze the elemental compositions of the aqueous solutions for all test samples. The Spectro Arcos unit shown in Figure 3.14 was utilized along with a multi-element calibration standard VHG-SM68-1-100 manufactured by the LGC group for calibration. The standard contained 47 elements that included all 17 REEs and major contaminant elements (aluminum, calcium, iron, magnesium, etc.) typically present in the PLS generated from coal-based materials. The calibration regression for the ICP was performed using 0.05 ppm, 0.5 ppm, 1 ppm, 5 ppm, and 10 ppm dilutions of the calibration standards. The aqueous samples that contained metal concentrations higher than the calibration range were diluted using 5% HNO_3 solution by appropriate factor to bring the concentration of the metals within the regression range. The elemental analysis for each batch of samples was verified by continuing calibrating verification(CCV) where a 1 ppm dilution of the standard was run and continuing calibration blank(CCB) where 5% HNO_3 was run every 10^{th} sample to ensure that there was no inherent variability in the calibration curve. For the purpose of replication. There were three measurements made for each sample. The standard deviation associated with each element of interest was less than 0.05 ppm as shown in Table 3.7

Table 3.7 Standard deviation for the measurement of rare earth elements and the contaminants using ICP-OES.

Element	Standard Deviation (PPM)	Element	Standard Deviation (PPM)
Sc	0.0164	Fe	0.0325
Y	0.0130	Al	0.0115
La	0.0208	Ca	0.0185
Ce	0.0117		
Pr	0.0193		
Nd	0.0191		
Sm	0.017		
Eu	0.051		
Gd	0.01765		
Tb	0.0135		
Dy	0.0108		
Ho	0.0240		
Er	0.0126		
Tm	0.0237		
Yb	0.0174		

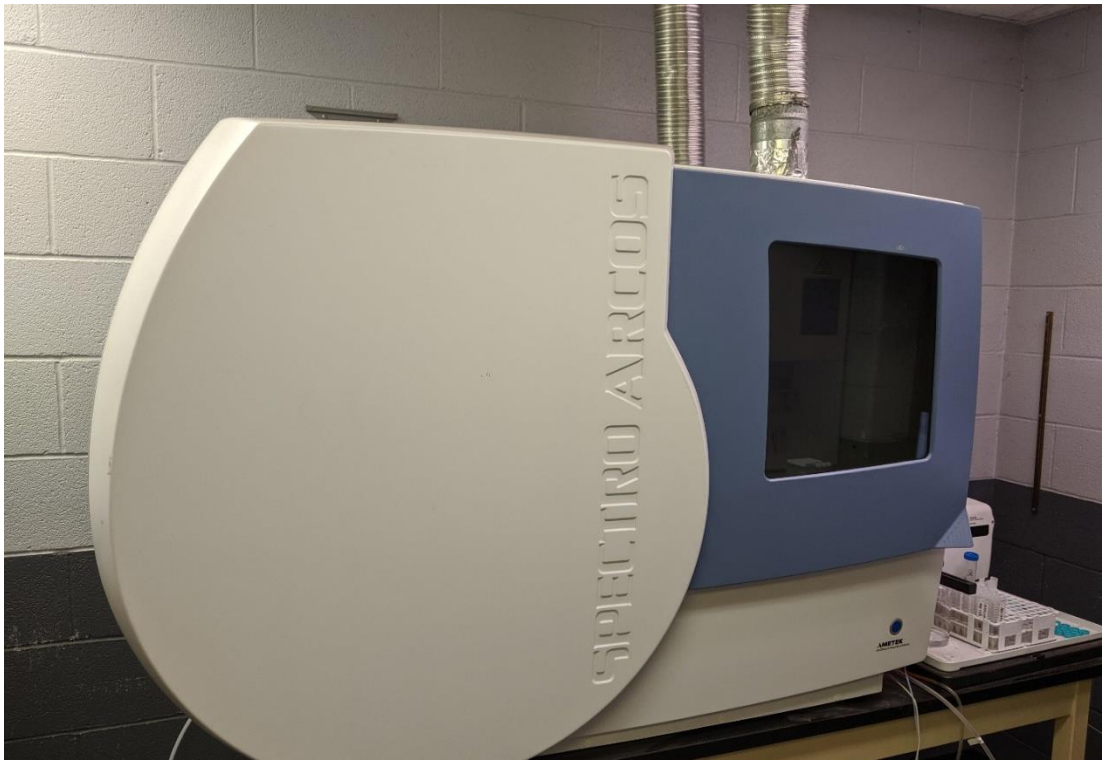

Figure 3.14 Inductively coupled plasma - optical emission spectroscopy (ICP-OES) apparatus at the University of Kentucky used for elemental characterization of the aqueous phase.

3.3.2 Ion activity measurement

For the development of the model used to predict the distribution coefficients for each element, the activity of the anionic species in the aqueous system was required to calculate the thermodynamic stability constants. To achieve this task, a chloride half-cell electrode was used for the measurement of the chloride ion activity. The electrode measures the potential difference between itself and a reference electrode as shown in Figure 3.15. The measured electrode potential value is related to the activity of the chloride ion by the Nernst equation using the following expression:

$$E = E_0 + \frac{RT}{nF}\log[Cl^-] \tag{3.32}$$

The term RT/nF is called the slope factor and the value is 59.16 m for the chloride ion. This value implies that every tenfold increase in the activity of the chloride ion would result in an increase of 59.16 mV of electrode potential. The primary advantage of using an ISE as opposed to other analytical techniques like ion chromatography is that the activity of the chloride ion in the solution can be calculated whereas other techniques calculate the total concentration of the chloride ion.

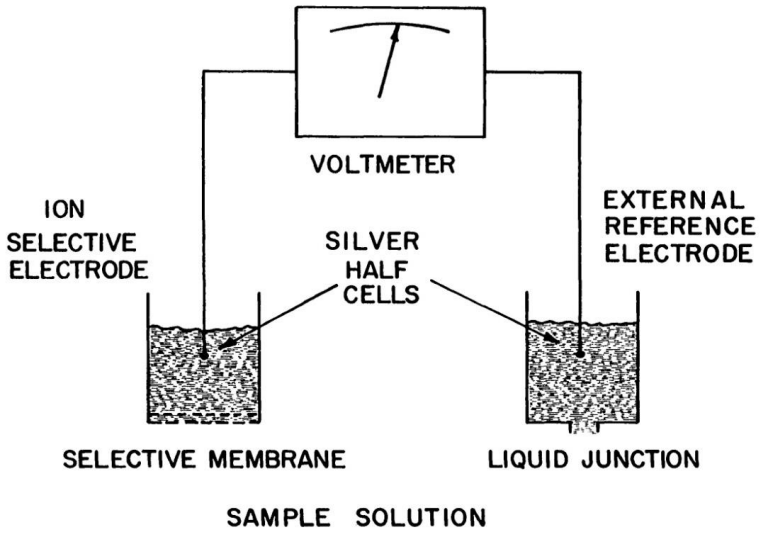

Figure 3.15 Schematic showing the general ion-selective electrode system for measuring the activity of an ion in a system[113].

3.3.3 Fourier-Transform Infrared Spectroscopy (FTIR) Analyses

Fourier transform infrared spectroscopy (FTIR) is a technique used to obtain an infrared spectrum of absorption and emission of a solid, liquid or gas sample. The main advantage of using an FTIR spectrometer of a dispersive spectrometer is that it collects high-spectral-resolution data over a wide spectral range as opposed to the narrow range by a dispersive spectrometer. The term Fourier transform arises from the fact that the Fourier transform is required to process the raw data into the actual spectrum. The resulting spectrum is a representation of the molecular absorption. Each functional group has its unique adsorption peaks. For example, the characteristic peaks of the DEHPA molecule are 1282 (P=O

stretching), 1225 cm^{-1} (P-O-C vibration), 1030 cm^{-1} (P-O-H vibration), and 1650 cm^{-1} (O-H, vibration).

For this study, FTIR characterization was performed to study the mechanism of interaction of the DEHPA molecule with the TBP molecule and the resulting change in metal complexation mechanism. The FTIR spectra of pure TBP and pure DEHPA and different blends of TBP and DEHPA were investigated as a part of the study. Additionally, the spectra of organic phases for different blends of TBP and DEHPA were evaluated when loaded with lanthanum. The formation of new bonds in the organic phase between DEHPA and TBP molecules was also explored. The FTIR analyses were conducted by a Varian 7000e spectrometer using the attenuated total reflection (ATR) method. The analyses were conducted from 4000 cm^{-1} to 700 cm^{-1} using 32 scans with a resolution of 4 cm^{-1}. The data from the FTIR equipment was processed using the peak fitting tools of the software associated with the equipment.

4 CONTAMINATION REJECTION FROM DILUTE PLS

4.1 Determination of solvent extraction process parameters

The focus of this chapter is the design, testing and optimization of an solvent extraction process for the concentration of REEs from a pregnant leach solution (PLS) containing a high concentration of contaminant ions and a low concentration of REEs using Di-(2-ethylhexyl)phosphoric acid (DEHPA) as the extractant. A model test solution was prepared using laboratory-grade sulfate salts of aluminum, iron, calcium, and lanthanum for conducting the series of tests to determine the optimum parameters. The concentrations of the metals in the test solution were chosen to represent typical PLS generated from coal-based sources (Table 4.1)

Table 4.1 Elemental composition of the test solution used for the determination of process parameters.

Element	Concentration (mg/L)
Lanthanum	10
Iron	5000
Aluminum	1000
Calcium	1000

4.1.1 Pretreatment of Feed Solution

The distribution coefficient of ferric ion (Fe^{3+}) is an order of magnitude higher than ferrous ion (Fe^{2+}) in DEHPA and other related cation exchange extractants[123, 124]. This is due to the trivalent nature of the ferric species and the higher affinity of the cation exchange extractant for the trivalent species. Since iron was one of the major contaminants present in the leachate and the majority was present in Fe^{3+} form, the valence state of iron in the solvent extraction feed was an important factor for the separation of REEs of contaminants.

For efficient separation of REE, the iron present in the solution was reduced using a reducing agent to its ferrous state. The oxidation-reduction potential (ORP) of the solution can be used

as a quantity to measure the relative concentrations of Fe^{3+} and Fe^{2+}. The ORP of the aqueous solution containing both Fe^{3+} and Fe^{2+} species is given by the following equation [125]:

$$E = \frac{2.303\ RT}{nF} \log_{10} \frac{[Fe^{3+}]}{[Fe^{2+}]} + \text{constant} \tag{4.1}$$

in which $[Fe^{2+}]$ and $[Fe^{3+}]$ are the elemental molar concentrations, *R* is the universal gas constant (8.31 J/mol K), *T* is the absolute temperature in Kelvin, *F* is the Faraday constant (9.6485 × 104 C/mol). For this study, ascorbic acid ($C_6H_8O_6$) was used as the reducing agent since it requires a low volumetric dosage which prevents significant dilution of the elemental concentrations. The mechanism by which ascorbic acid reduces ferric ion can be described by the following reaction:

$$2Fe^{3+} + C_6H_8O_6 = 2Fe^{2+} + C_6H_6O_6 + 2H^+ \tag{4.2}$$

With the reduction of the ORP of the model test solution, a color change of the solution was observed which was an indicator of the reduction from Fe^{3+} (deep red) state to Fe^{2+} (pale green) state (Figure 4.1).

Figure 4.1 Visual change in the color of the test solution with incremental additions of 200g/L (1.136 M) solution of ascorbic acid.

The extraction efficiency of iron reduced from 58% to less than 10% as the ORP was reduced from 460 mV to 300 mV (Figure 4.2). As an increasing amount of iron is reduced to its ferrous state, the extraction efficiency reduces. This is explained by the difference in the distribution coefficient of ferrous and ferric ions[124]. It was also noteworthy that the extraction efficiency of REE and other contaminants is not affected by ORP manipulation. All the subsequent tests for parametric tests were carried out on the test solution after adjusting the ORP of the solution to the optimum value of 400 mV.

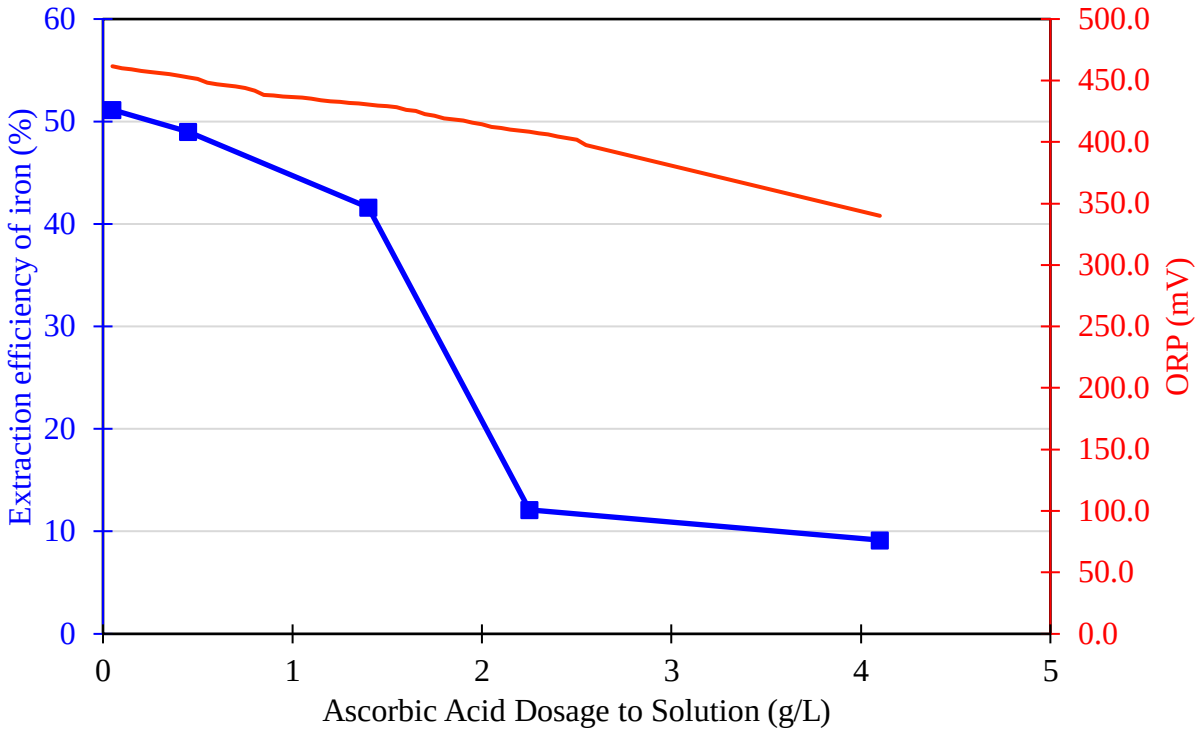

Figure 4.2 Impact of ascorbic acid on ORP of the solution and extraction efficiency of iron by 5% DEHPA at pH 2.0. (The ORP measurement was done for a large number of data points and therefore the symbols in the plot are not shown).

4.1.2 Extraction Tests

The extraction efficiency of metals (both REE and contaminants) in a solvent extraction process is dependent on the H^+ concentration (i.e., solution pH) and the concentration of extractant in the organic phase. The optimal pH and extractant concentration for the highest selectivity between the REEs and contaminants were investigated in this section of the study.

The separation of two species is typically evaluated based on the ratio of distribution coefficients of the species which is commonly known as the selectivity factor [5]. However, due to very high relative concentrations of the contaminants with respect to the REEs in the solutions studied in the present work, the selectivity of the process in this study was evaluated based on decontamination factor, defined as the ratio of the relative concentrations of contaminants to the REEs in feed and product, i.e.:

$$\text{Decontamination Factor} = \frac{([\text{Contaminants}]_{\text{feed}})/([\text{REE}]_{\text{feed}})}{([\text{Contaminants}]_{\text{product}})/([\text{REE}]_{\text{product}})} \tag{4.3}$$

Four different organic solutions were prepared with 5%, 10%, 15% and 20% v/v concentration of DEHPA in kerosene. The extraction efficiency of lanthanum as a function of the initial pH value of the model solution is shown in Figure 4.3 for the different concentrations of DEHPA studied. Tests were not conducted at pH values higher than 2.2 due to very slow phase disengagement. The extraction efficiency increased with an elevation in the initial pH for each organic test solution. The extraction efficiency also exhibited an increase with DEHPA concentration. The maximum extraction of lanthanum measured in the study was 78% at pH 2.2 using 20% DEHPA in the organic phase.

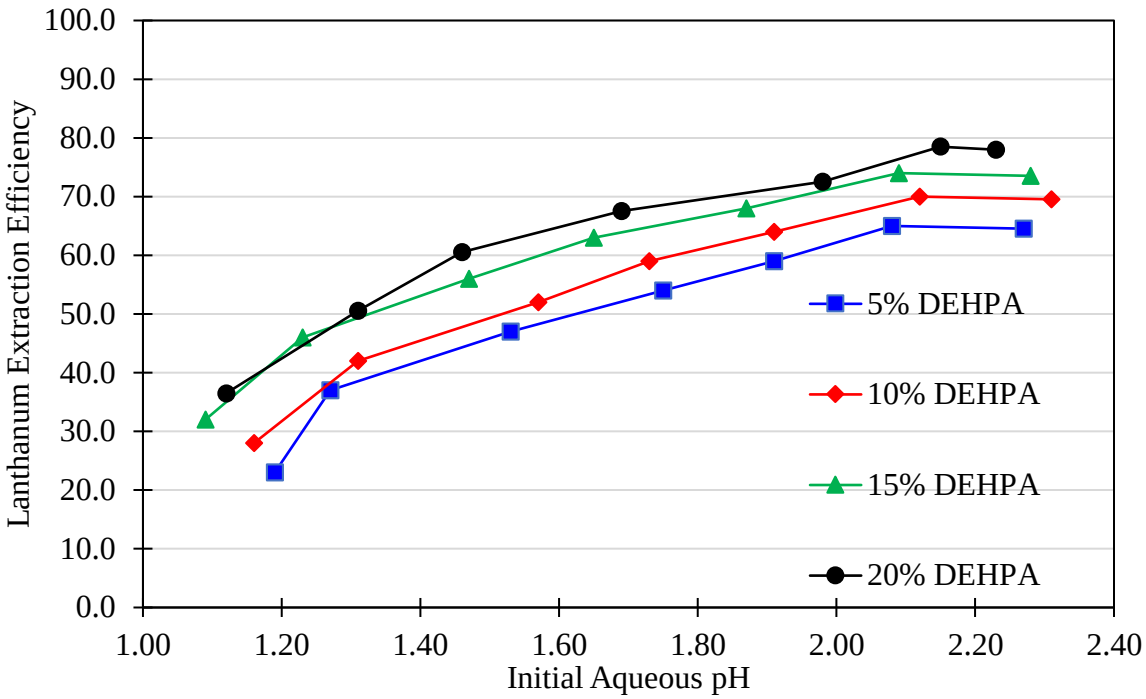

Figure 4.3 Extraction curves of lanthanum from model test solution at different initial pH values for different concentrations of DEHPA in kerosene (5%, 10%, 15%, 20%); A:O ratio = 1:1.

The impacts of DEHPA concentration and aqueous pH on the extraction efficiency of the contaminant elements was similar to the lanthanum results (Figure 4.3, Figure 4.4, Figure 4.5, and Figure 4.6). The extraction efficiency of iron increased from 10.1% to 16.8% when the pH was elevated from 1.1 to 2.2 when using a 5% DEHPA solution, while for aluminum, the increase was from 6.7% to 11.8% under the same conditions. Interestingly, the extraction efficiency of calcium was observed to be largely independent of the initial pH. However, calcium extraction exhibited a dependence on the extractant concentration with an increase 4.5% to 8.0% when the DEHPA concentration was increased from 5% to 20%. The extraction of iron increased from 16.8% to 20.4%, and that of aluminum increased from 11.8% to 15.7% for the same increase in DEHPA concentration.

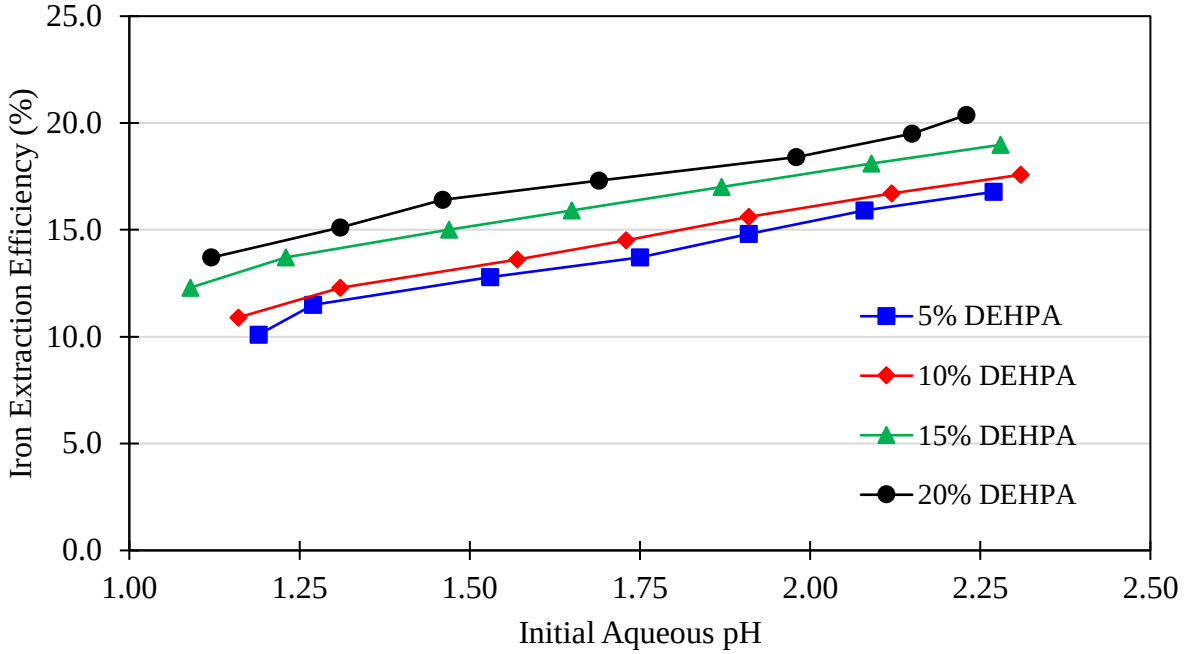

Figure 4.4 Extraction efficiency of iron for different concentrations of DEHPA in the organic phase over a range of aqueous pH values ; A:O ratio = 1:1.

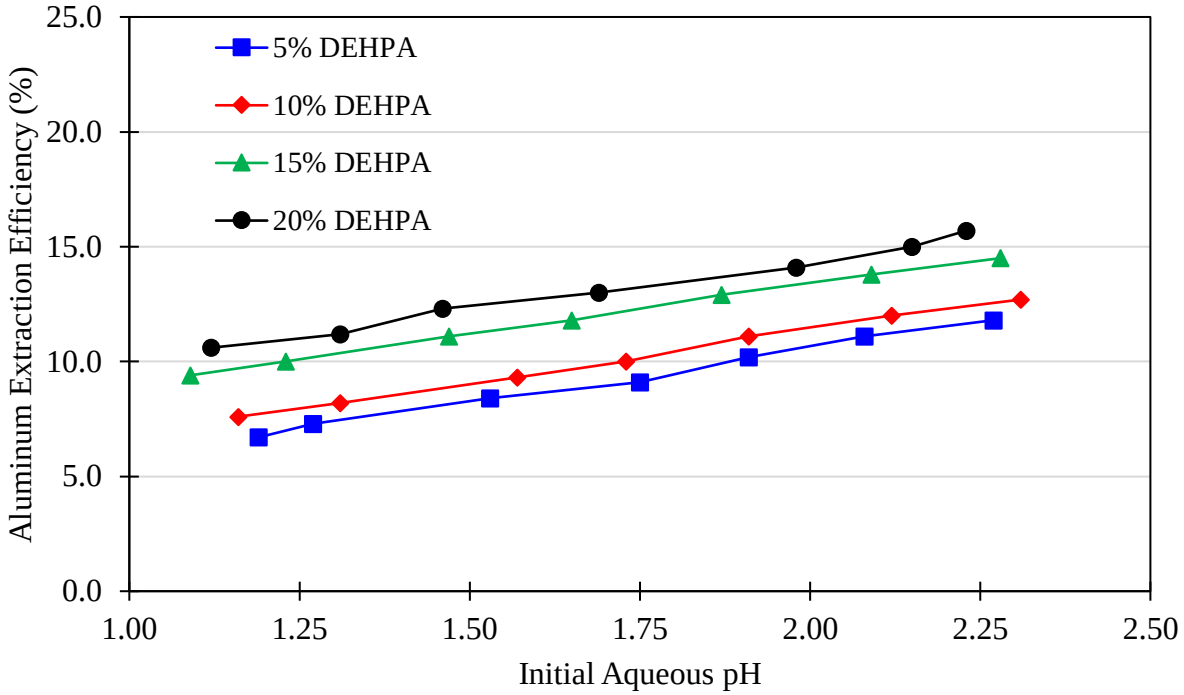

Figure 4.5 Extraction efficiency of aluminum for different concentrations of DEHPA in the organic phase over a range of aqueous pH values; A:O ratio = 1:1.

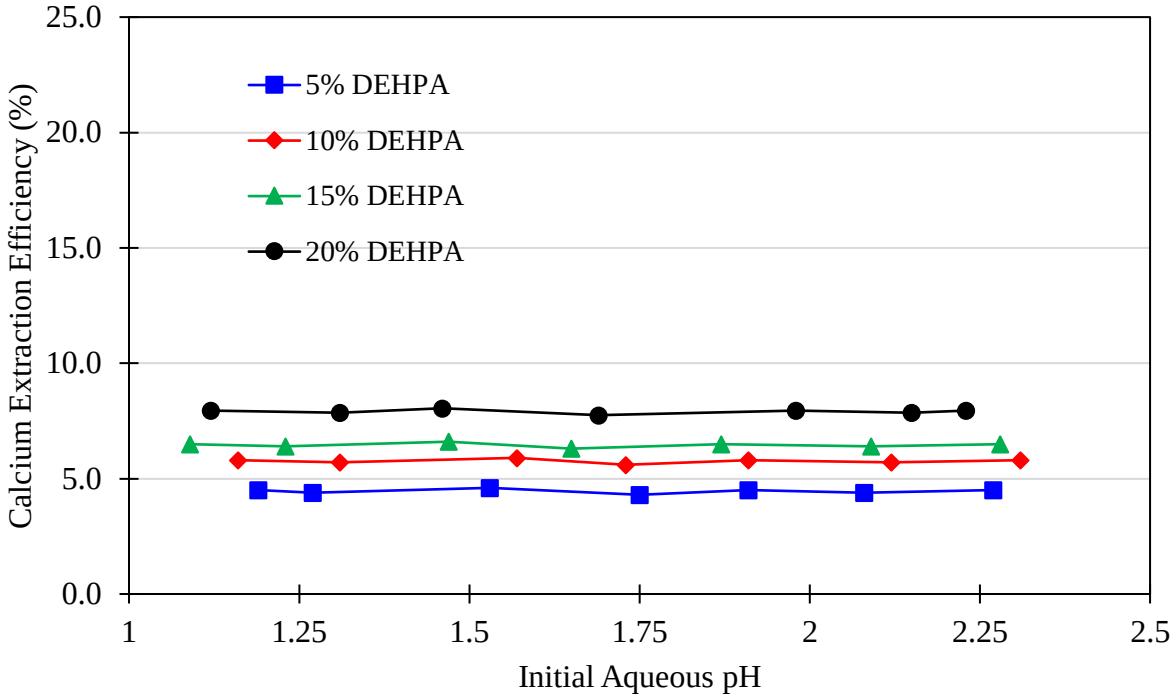

Figure 4.6. The extraction efficiency of calcium from the model test solution over a range of aqueous pH values using 5%, 10%, 15%, and 20% DEHPA solutions in kerosene; A:O = 1.

The selectivity of the solvent extraction process, which was quantified using the decontamination factor, was shown to be largely independent of extractant concentration over the range of values tested (Figure 4.7). This finding was reflective of the nearly equal impact that extractant concentration had on the extraction efficiency of lanthanum and the contaminant ions.

The selectivity of the process was, however, shown to be dependent on the initial pH of the test solution. The decontamination factor showed an increase from 2.93 to 4.91 when the pH of the solution was increased from 1.1 to 2.0 and dropped slightly to 4.63 at pH 2.2. Therefore, it was concluded that the initial pH of 2.0 was optimum for the selective extraction of REEs

from the contaminant ions. An organic solution containing 5% DEHPA was identified as optimum due to lower costs and better phase disengagement properties as compared to higher concentrations.

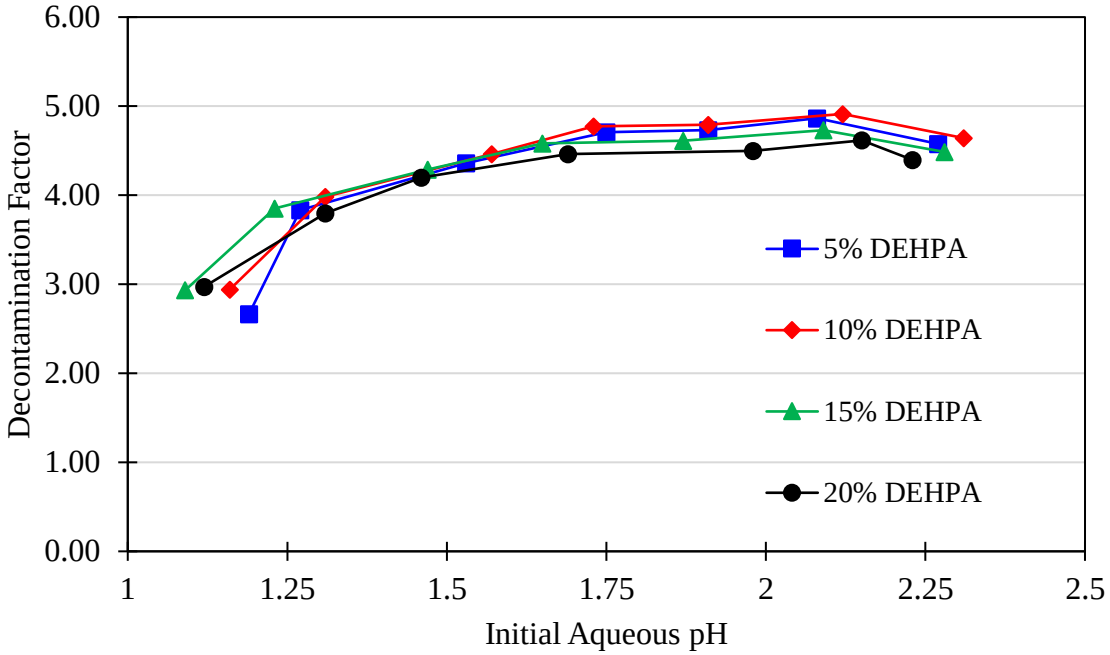

Figure 4.7. Decontamination ratio for the test solutions over a range of aqueous pH values using 5%, 10%, 15% and 20% DEHPA solution in kerosene.

The optimum concentration of the DEHPA in the organic phase, and the pH of the solution were identified to be 5% and 2.0, respectively. However, the extraction efficiency of lanthanum under these conditions was approximately 61%. To maximize the recovery of lanthanum from the test solution, extraction of lanthanum at different aqueous-to-organic (A:O) phase ratios was investigated. Extraction tests were conducted using an aqueous pH value of 2.0 and a 5% DEHPA concentration over A:O phase ratios of 1:1 to 1:10 (Figure 4.8). The recovery of the lanthanum increased from 67.3% at 1:1 to around 94.0% at an A:O ratio of 1:6. Further enhancements in lanthanum extraction was not obtained using higher A:O phase ratios.

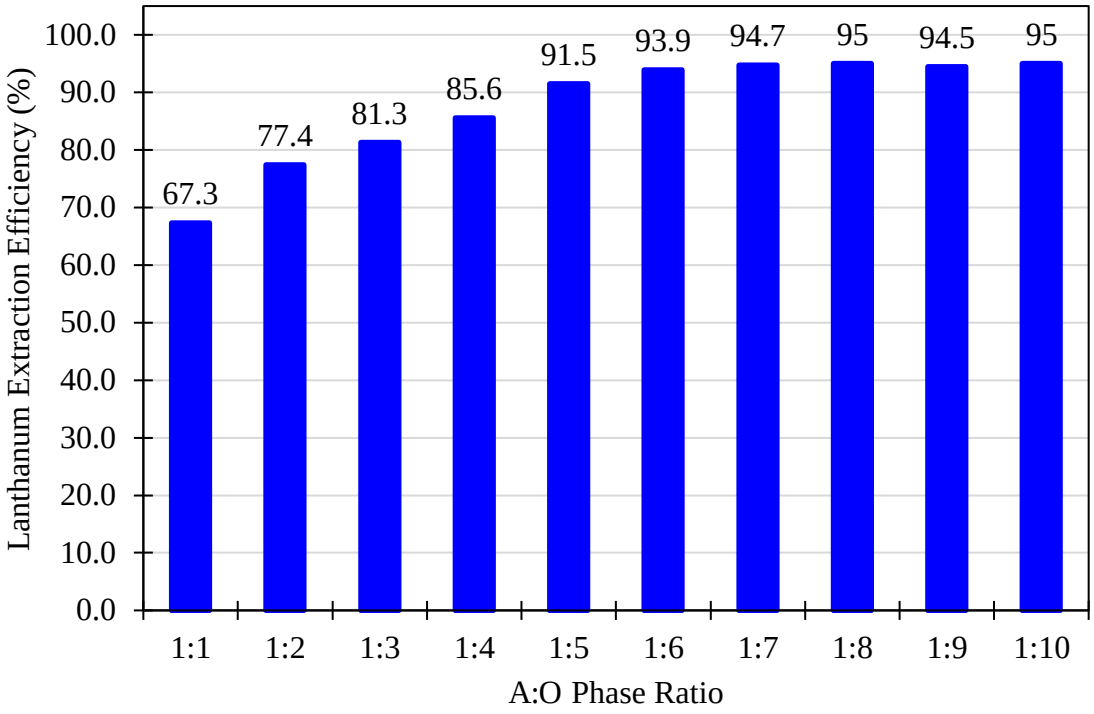

Figure 4.8. The extraction efficiency of lanthanum from the test solution over a range of A:O ratios; Loading conditions: pH 2.0, organic phase 5% v/v DEHPA solution in kerosene.

4.1.3 Scrubbing Tests

As seen from the extraction test results, a substantial amount of contaminants was co-extracted in the organic phase due to their high relative concentration in the original model solution. A 50 mL volume of loaded organic was contacted with 50 mL HCl solutions over a range of molar concentrations from 0.1 M to 0.5 M to evaluate the effect on the removal of co-extracted contaminants. The scrubbing efficiency for the process was calculated using the equation:

$$\text{Scrubbing Efficiency} = \frac{[\text{M}]_{\text{scrubbing solution}}}{[\text{M}]_{\text{Feed organic solution}}} \tag{4.33}$$

It follows that it is desirable to have a high scrubbing efficiency for the contaminants while having a low scrubbing efficiency of the lanthanum. It was observed that, in general, the scrubbing efficiency of the metals increased with the increase in the acid concentration in the

scrubbing solution (Figure 4.9). Scrubbing was most effective for selective removal of calcium, and for given conditions, around 90% calcium was scrubbed from the loaded organic phase.

The scrubbing efficiency of calcium increases from 70% to 89% when the scrubbing acid concentration was increased from 0.1 M to 0.5 M. A similar trend was also observed for the scrubbing efficiency of the iron for which the scrubbing efficiency increased from 9% to 21% and for aluminum for which the scrubbing efficiency increased from 8% to 35% when the scrubbing solution concentration was increased from 0.1 M to 0.5 M. However, the scrubbing efficiency of lanthanum also increased for the same increase in concentration. Therefore, even though higher contaminant rejection was achieved at higher concentration, using a high concentration scrub solution would result in substantial loss of recovery.

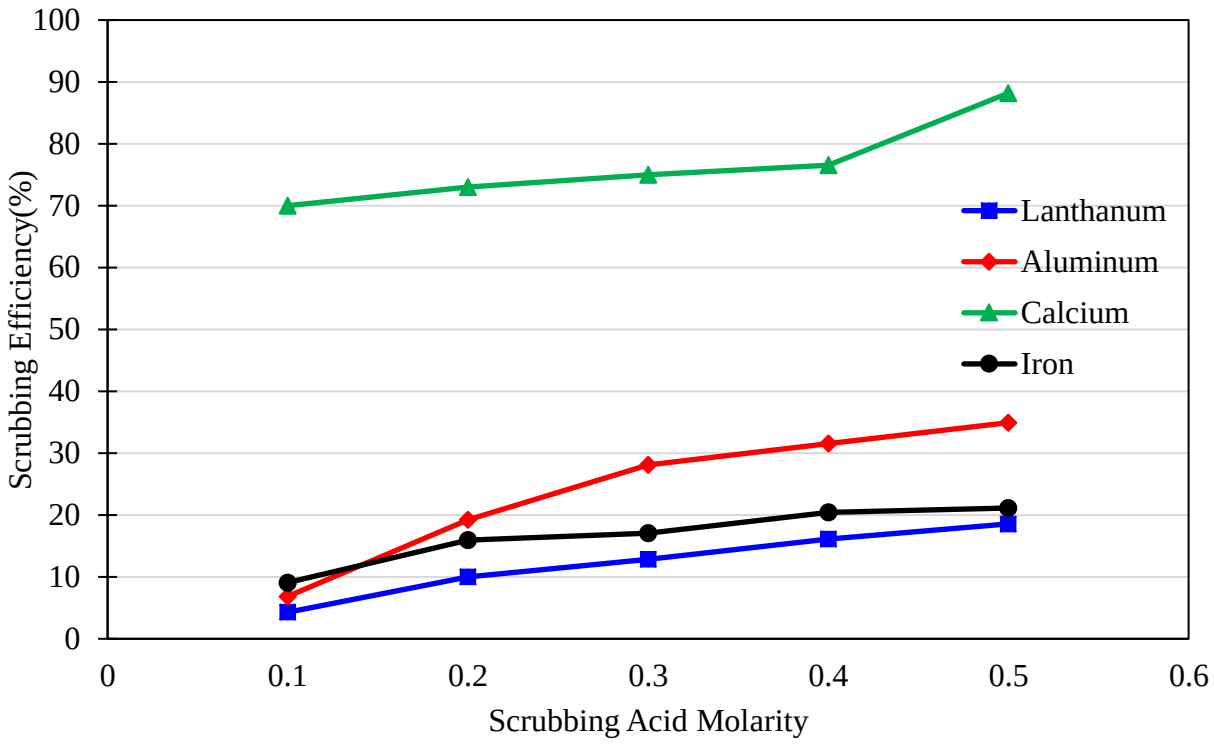

Figure 4.9 Scrubbing efficiencies of lanthanum, iron, calcium, and aluminum for solutions of different HCl concentrations.

Similar to the extraction tests, the selectivity of the scrubbing process was determined by the decontamination factor of the contaminants. The decontamination ratio was highest (1.1) for 0.1 M HCl, and the ratio reduced for solutions with higher acid concentration (Figure 4.10).

Interestingly, the decontamination factor converges to 1 at higher concentrations of acid, implying that there is little to no selectivity between contaminants and REEs at higher acid concentrations. This is an important learning as it is the reason that stripping of the metals, which is carried out by very high concentrations of acid (6M HCl), cannot be used to create a separation between the contaminants and REEs. The separation was achieved solely in the loading and to some extent, in the scrubbing stage.

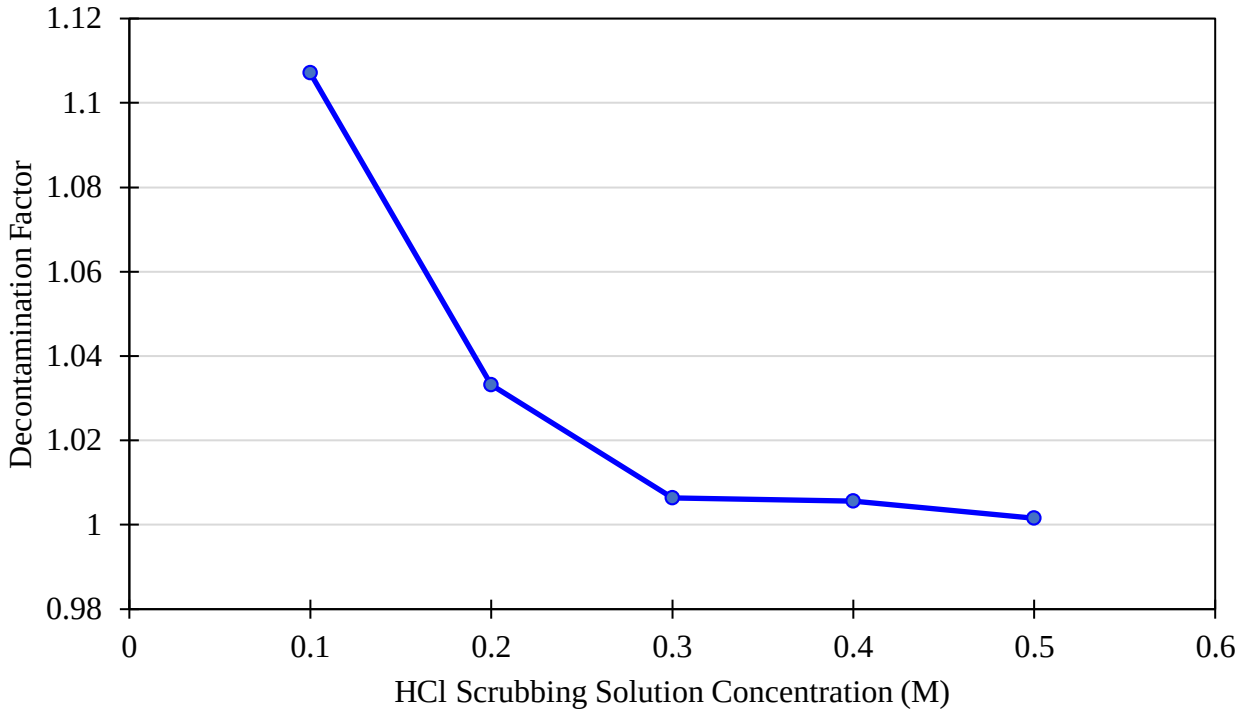

Figure 4.10 Decontamination factor as a function of the molar HCl concentration in the scrub solution.

4.1.4 Stripping Tests

The metals loaded in the organic phase were stripped into the aqueous phase by mixing with a strong acid solution of 6 M HCl. The concentration of the acid was selected as it is the industrial standard to use 6M HCl acid solution for stripping[4, 126]. Due to the relatively low concentrations of REE in the PLS, the stripping solution could be contacted at a higher aqueous to organic (A:O) phase ratio to increase the concentration of REE in the stripped solution as well as reduce the acid cost of the process without compromising the stripping efficiency. The

optimization test was carried out by contacting 6 M HCl solution with 100 ml of the organic phase loaded solution in incremental A:O phase ratios. The stripping efficiency of the process was calculated for each test condition by the expression:

$$\text{Stripping Efficiency} = \frac{[\text{M}]_{\text{stripped solution}}}{[\text{M}]_{\text{Feed organic solution}}} \tag{4.34}$$

The stripping efficiency of lanthanum was reduced from almost 100% (99.7%) for A:O phase ratio 1:1 to 88.0% for A:O phase ratio of 1:100 (Figure 4.11). The concentration of lanthanum in the aqueous solution was higher in the case of a higher A:O ratio. As a result, a higher A:O ratio corresponds to a higher equilibrium concentration of lanthanum in the organic phase, which in turn means lower stripping efficiency of the metal. The stripping efficiency was 95.9% for the A:O ratio of 1:25. As the A:O phase ratio was increased, stripping efficiency further decreased. The minimum volumetric ratio of stripping solution , that could effectively strip 95% of lanthanum in the loaded organic solution was determined to be 1:25. It was noted that different concentrations of acids were not tested in this study as stripping is not the selective step in this process and lower concentrations of acid would result in incomplete stripping of metals resulting in the build-up of metals in the organic stream resulting in poisoning of the organic phase.

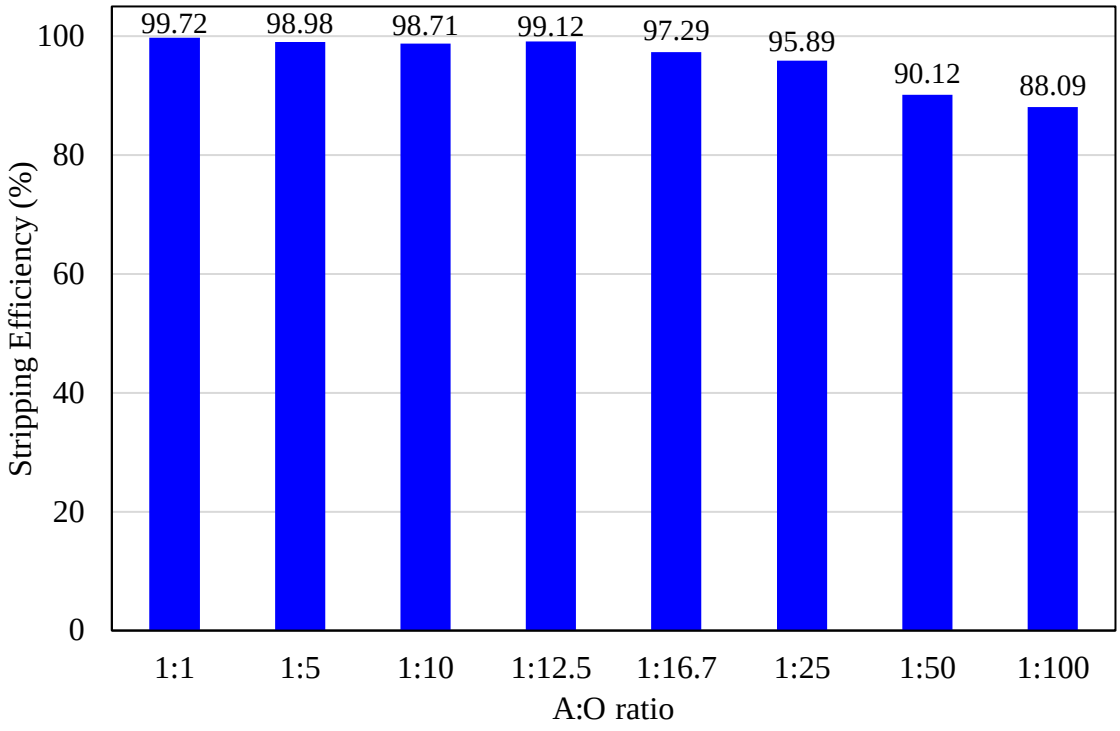

Figure 4.11. Stripping recovery of lanthanum from loaded organic solution using 6 M HCl solution over a range of A:O phase ratios; Test conditions: 5% v/v DEHPA solution, model PLS, initial pH = 2.0 and A:O ratio = 1:6 in the initial loading stage).

Based on the extraction, scrubbing and stripping test results, the elemental composition of the aqueous and organic phase was calculated at the beginning and end of each step of the process. The elemental composition of the organic phase was calculated by the mass balance (Table 4.2). The extraction step rejected the majority of the contaminants in the exit stream. The scrubbing step was significant for contaminant removal as the calcium content in the organic phase was reduced by 70.0% from 46.7 to 14.0 ppm. It is also interesting that the organic after stripping stage was not completely barren and small quantities of metal were left as residue which indicates that the organic phase would experience problems with elemental build up when the process ran continuously. To avoid this problem, a portion of the stripping acid stream has to be bled from the circuit continuously so as to avoid the build-up in the organic phase. As ascertained from the lab tests, if the volumetric flow rate of the strip solution is maintained at 1:25 of the volumetric flowrate of the feed, the residual concentration in the organic phase will remain consistent at the levels calculated.

Table 4.2 Elemental composition in the aqueous and organic phase in each step of the SX process.

		Aqueous Phase (ppm)				Organic Phase (ppm)			
		La	**Al**	**Ca**	**Fe**	**La**	**Al**	**Ca**	**Fe**
Extraction	Feed	12.0	916.0	1037.0	4340.0	0.0	0.0	0.0	0.0
	Exit	3.9	783.2	990.3	4047.9	8.1	132.8	46.7	292.1
Scrubbing	Feed	0.0	0.0	0.0	0.0	8.1	132.8	46.7	292.1
	Exit	0.3	9.1	32.7	26.6	7.7	123.7	14.0	265.5
Stripping	Feed	0.0	0.0	0.0	0.0	7.7	123.7	14.0	265.5
	Exit	7.6	121.4	13.9	262.1	0.1	2.3	0.1	3.4

4.2 **Rare Earth Oxides from Coal Based Sources.**

The process conditions determined in the study with the model test solutions were implemented in a continuous SX circuit treating six pregnant leach solutions (PLS) from six different sources (as described in the materials section) to produce high purity REO concentrates. The PLS sources were produced by leaching the coal density fractions (pulverized to 80 mesh) in a 1.2 M H_2SO_4 solution at 75^oC for 2 hours at 10% solids concentration by weight. The leachate was filtered and re-contacted with fresh solids. The process was repeated for a total of 5 times to build up the concentration of the REEs in solution. Due to differences in the modes of occurrence of the REEs, the concentration of the TREEs, as well as the element distribution of individual REEs, varied significantly between sources (Table 4.3). The leachates generated from West Kentucky No. 13 coal sources had a significantly higher H/L ratio with yttrium being the biggest contributor to the composition. The leachates from Fireclay coal sources contained a relatively high concentration of cerium and neodymium, whereas the leachates from Illinois No. 6 coal sources contained a high concentration of both yttrium and neodymium.

Table 4.3 REE distribution of the leachates generated from the heavy density fractions of six different coal sources in ppm (where WK13= West Kentucky No. 13; FC=Fireclay; IlL6 = Illinois No. 6

Source	TREE	HREE	LREE	H/L	Sc	Y	La	Ce	Pr	Nd
WK13 (1.8-2.2 sg)	20.84	10.52	10.32	1.02	1.64	5.17	0.65	3.47	0.85	2.4
WK13 (2.2 sg sink)	17.96	8.92	9.04	0.99	0.54	4.05	0.65	3.76	0.78	2.42
FC (1.8-2.2 sg)	50.75	10.54	40.21	0.26	0.69	3.7	6.15	19.5	2.61	9.16
FC (2.2 sg sink)	13.9	2.99	10.91	0.27	0.36	1.47	2.22	1.90	1.07	3.84
ILL6 (1.8-2.2 sg)	15.22	5.71	9.51	0.60	0.85	2.8	1.14	3.56	0.72	2.42
ILL6 (2.2 sg sink)	26.9	9.99	16.91	0.59	1.79	4.7	1.97	6.16	1.4	4.19

Source	Sm	Eu	Gd	Tb	Dy	Ho	Er	Tm	Yb	Lu
WK13 (1.8-2.2 sg)	1.31	0.36	2.6	0.32	1.15	0.18	0.18	0.16	0.35	0.05
WK13 (2.2 sg sink)	0.89	0.23	2.68	0.35	0.95	0.08	0.12	0.1	0.29	0.07
FC (1.8-2.2 sg)	2.1	0.21	4.17	0.46	1.13	0.06	0.12	0.15	0.37	0.17
FC (2.2 sg sink)	1.51	0.09	0.77	0.07	0.15	0.10	0.11	0.03	0.18	0.24
ILL6 (1.8-2.2 sg)	0.82	0.16	1.68	0.17	0.62	0.03	0.04	0.02	0.17	0.02
ILL6 (2.2 sg sink)	1.4	0.31	2.95	0.33	1.1	0.08	0.06	0.05	0.32	0.09

An important factor that influences the efficiency and cost of the solvent extraction process is the ratio of contaminants to total REE concentrations. Higher ratios tend to negatively impact the purity of the final product and require higher amounts of acid to be used in the stripping stage. In this study, the primary contaminant ions included iron, aluminum and calcium. The ratio of the total concentrations of contaminant ions to REEs was referred to the 'Relative Concentration' (RC) which is defined by the following expression:

$$\text{Relative Concentration (RC)} = \frac{[\text{Contaminants}]}{[\text{TREE}]} \qquad (4.35)$$

The RC value for West Kentucky No. 13 sources was relatively low. For the 1.8-2.2 s.g fraction, the value was 242.0 and the value for the 2.2 sink fraction was somewhat higher at 363.3. The Fireclay 1.8-2.2 s.g. fraction had an RC of 256.0 while the 2.2 sink had a very high relative concentration of 1176.7. The Illinois No. 6 1.8-2.2 s.g. fraction had an RC of 321.5 while the 2.2 sink had an RC of 314.0 (Figure 4.12).

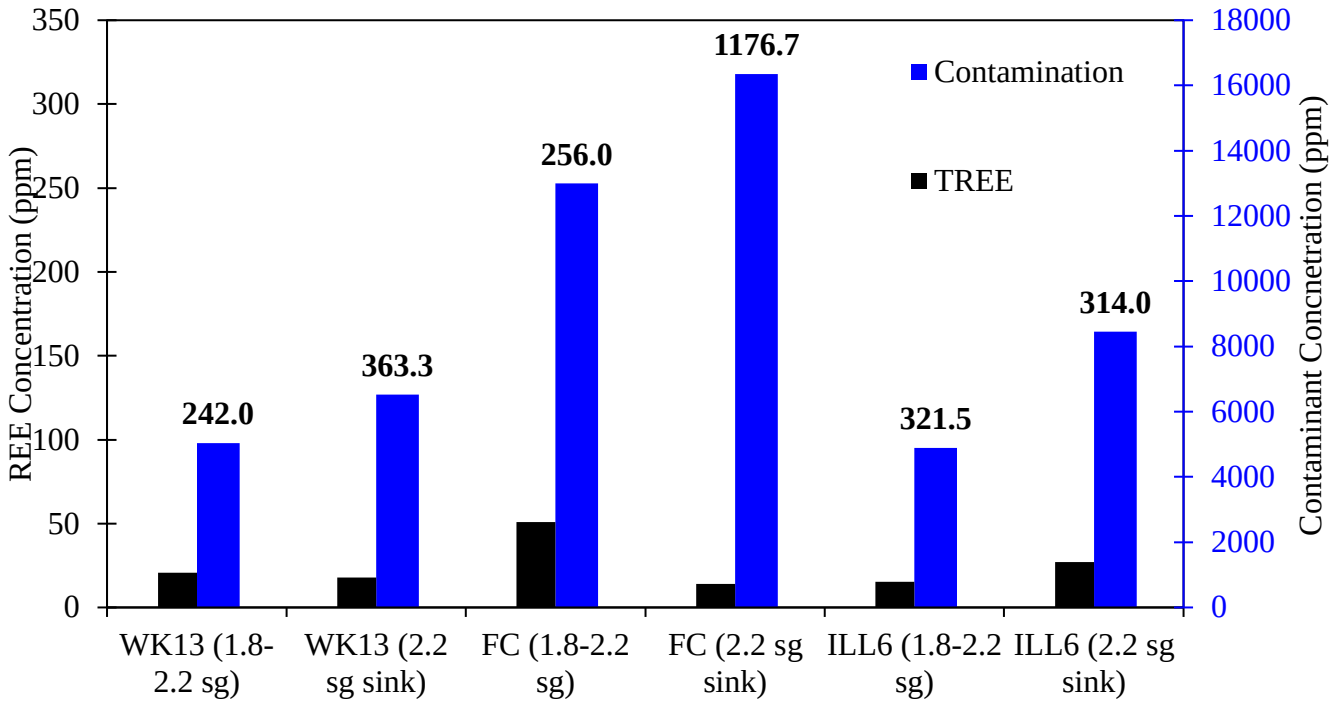

Figure 4.12 The concentration of the TREE (in black) and primary contaminants (in blue) in the PLS generated from different coal sources. The numbers in bold represent the relative concentration (RC) of the contaminants to the TREEs in the solution.

The REO concentrate in the process was produced by selective precipitation using oxalic acid as described by Zhang et al. [127] The relative concentration of contaminants in the final aqueous solution that feeds the oxalic acid precipitation step must be sufficiently low to provide the upgrading desired by the selective precipitation process and minimize the oxalic acid dosage and cost. . Due to the very high relative concentrations of contaminants in the

PLS, the SX system was required to include both a rougher circuit and a cleaner circuit to reduce the relative concentration of the contaminants sufficiently. A schematic of the process used to separate REEs from the contaminants and produce a high purity REO mix product is shown in Figure 4.13.

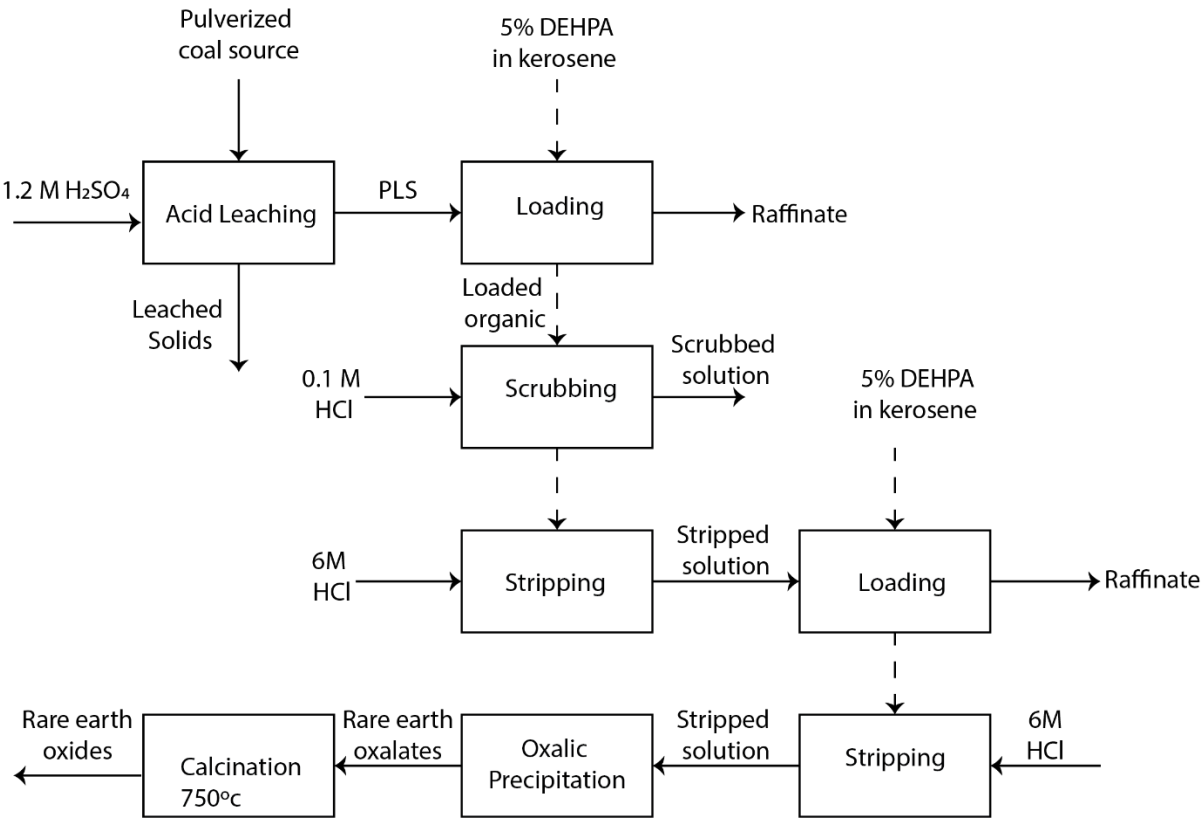

Figure 4.13 Schematic of the SX process procedure used to separate rare earth elements from the contaminant elements in the pregnant leach solutions from six coal sources.

The rougher stage rejected a significant amount of the contaminants as shown in Figure 4.14. The relative concentrations (RC) of contaminants dropped to 69.9 and 129.8 in the West Kentucky No.13 sources, 63.9 and 35.4 in the Fireclay sources and 100.4 and 58.8 in the West Kentucky No.11 sources in the stripped solutions of the respective solutions. The stripped solutions, which were highly acidic (6M HCl) were neutralized using 10M NaOH, and the pH of the solutions was adjusted to 2.0 before processing in the cleaner stage.

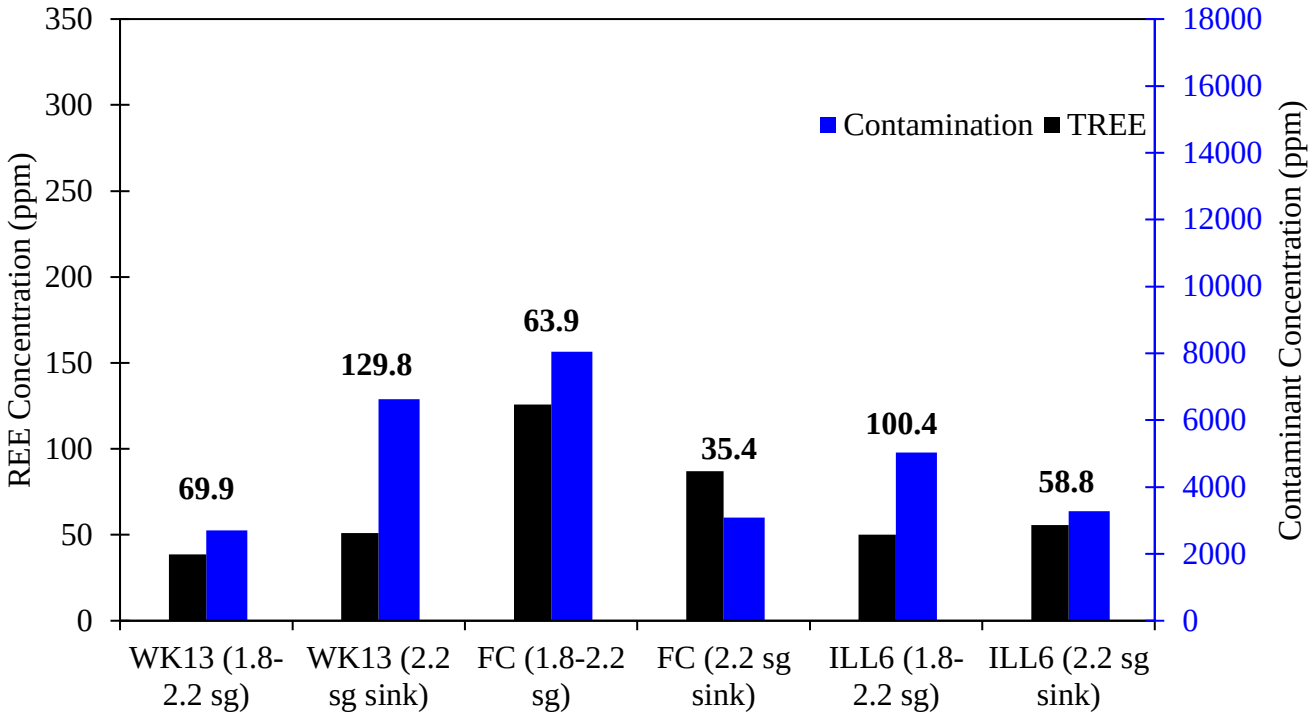

Figure 4.14 Concentration of the TREEs and contaminants (Fe, Al, Ca) in the stripped solution of the rougher cycle for different coal sources in PPM. The numbers in bold represent the relative concentration of the contaminants in the aqueous solution.

A significant reduction in contaminants was achieved by the cleaner stage as shown in Figure 4.15. The relative concentrations of the contaminants reduced to 11.9 and 20.1 in West Kentucky No. 13 sources, 7.8 and 9.8 in Fireclay sources, and 4.3 and 5.9 in Illinois No. 6

sources. The relative concentration of the contaminants was reduced sufficiently for the selective precipitation to be performed on the stripped solution from the cleaner circuit.

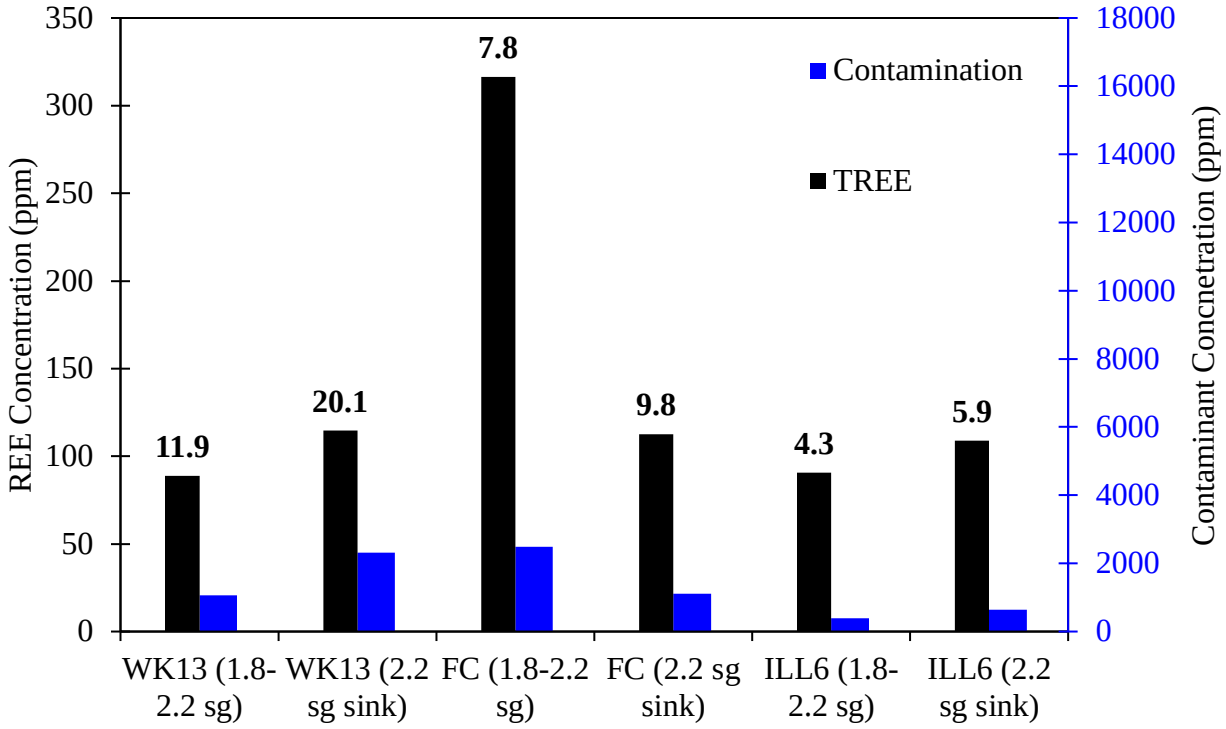

Figure 4.15 Concentration of TREEs (black) and primary contaminants(blue) in the stripped solution of cleaner cycle for different sources in ppm. The numbers in bold represent the relative concentration of the contaminant in the aqueous solution.

The ideal pH for oxalic acid precipitation is 1.2 as determined by previous studies[127]. Since the stripped solution is highly acidic, the solution pH was adjusted to 1.2 by the addition of 10M NaOH. A saturated solution of oxalic acid was prepared by dissolving 160 g of solid oxalic acid in 1 L of deionized water. For precipitation of rare earth oxalates, 1 mL of oxalic acid solution was added per 10 mL of stripped solution. After precipitation of the REEs, the precipitates were recovered from solution by filtration and washed with deionized water using three sequentially rinses through the filter cake to remove entrained sodium that was present from the addition of the NaOH solution. The washed oxalates were calcined in a muffle furnace at 750^{O}C to produce a REO mix concentrate.

The elemental compositions of the REO mix concentrates produced from the six source materials are summarized in Table 4.4 . Products containing greater than 97% rare earth oxide mix were generated from all sources. However, it is interesting to note the significant differences in the composition of individual REOs in each product. For example, the processing of the leachate generated from the 2.0 sink fraction in the Illinois No. 6 coal source produced a product containing 51.34% Y_2O_3, 12.52% Gd_2O_3 and 12.93% Dy_2O_3 with Dy_2O_3 being the most significant due to its value in permanent magnet manufacturing. The 1.8 x 2.2 sg fraction material was the source of the higher Dy_2O_3 values. Neodymium oxide was near the 20% content level for most samples which is also significant due to its use in permanent magnets. Significant concentrations of Sm_2O_3 were also achieved which is noteworthy due to its role in samarium-cobalt magnets, infrared adsorbing glass and solar applications.

Table 4.4 Rare earth oxide contents by element in the final products generated from solvent extraction process using rougher-cleaner steps followed by oxalic acid precipitation when treating the six coal sources expressed as % by weight (WK13= West Kentucky No. 13 FC=Fireclay ILL6 =Illinois No. 6);).

Source	TREO (%)	Sc_2O_3 (%)	Y_2O_3 (%)	La_2O_3 (%)	Ce_2O_3 (%)	Pr_2O_3 (%)	Nd_2O_3 (%)	Sm_2O_3 (%)
WK13 (1.8-2.2 sg)	98.16	0.03	19.14	4.93	21.98	3.91	18.44	8.38
WK13 (2.2 sg sink)	97.97	0.06	2.49	9.17	42.78	6.09	23.15	6.27
FC (1.8-2.2 sg)	97.49	0.04	19.47	6.08	23.25	3.96	17.80	7.36
FC (2.2 sg sink)	97.08	0.03	10.67	5.05	34.31	5.61	21.77	6.91
ILL6 (1.8-2.2 sg)	97.48	0.06	24.54	3.05	17.94	3.48	16.44	7.51
ILL6 (2.2 sg sink)	98.83	0.19	51.34	0.08	0.80	0.38	2.07	4.98

Source	Eu_2O_3 (%)	Gd_2O_3 (%)	Tb_2O_3 (%)	Dy_2O_3 (%)	Ho_2O_3 (%)	Er_2O_3 (%)	Tm_2O_3 (%)	Yb_2O_3 (%)	Lu_2O_3 (%)
WK13 (1.8-2.2 sg)	1.98	9.48	1.10	5.70	0.90	1.89	0.00	0.28	0.01
WK13 (2.2 sg sink)	0.65	5.06	0.24	1.50	0.16	0.34	0.00	0.01	0.00
FC (1.8-2.2 sg)	1.73	8.37	0.93	5.23	0.86	1.90	0.03	0.44	0.03
FC (2.2 sg sink)	0.76	5.72	0.56	3.45	0.55	1.25	0.02	0.38	0.03
ILL6 (1.8-2.2 sg)	1.97	10.13	1.32	7.08	1.13	2.33	0.01	0.45	0.02
ILL6 (2.2 sg sink)	2.02	12.52	2.29	12.93	2.12	4.80	0.29	1.85	0.16

4.3 Scandium Recovery

As shown in Table 4.4 the concentrations of scandium in the REO products are very low. This is attributed to very poor scandium stripping efficiency in the acid stripping step, as observed by other researchers [19, 128, 129]. As scandium is one of the most valuable REEs, efficient scandium recovery is desirable. There are two methods for recovering scandium that were explored in this study. The first method involves alkaline stripping or saponification of the

loaded organic phase, which replaces the metals in the organic phase with sodium ions. The second alternative is the recovery of scandium using a separate circuit to treat the original PLS solution first using an extractant that is selective toward scandium only. The raffinate from the scandium recovery loading step would then be treated in a separate SX circuit using DEPHA as the extractant to recovery the REEs. In this study, Cynex 272, which is a proprietary dialkyl phosphinic acid extractant manufactured by Solvay, was tested for the recovery of scandium from the original leachate solution.

4.3.1 Saponification

To evaluate the efficiency of saponification on scandium recovery from a loaded organic phase, an organic solution comprised of 5% DEHPA with 10% TBP as a phase modifier in kerosene was loaded with a 100 ppm solution of commercial-grade scandium at pH 2.0. Under these conditions nearly 100% of the scandium was loaded into the organic phase. The reason for the use of TBP as a phase modifier in the saponification testing was to avoid the formation of an insoluble 3rd phase, which would prohibit phase disengagement and separation (Figure 4.16).

5% DEHPA

5% DEHPA
with 10% TBP

Figure 4.16 Difference in the phase separation characteristics in 5% DEHPA and 5% DEHPA with 10% TBP as a phase modifier.

The stripping efficiency of scandium from the organic solution loaded with scandium was tested by contacting it with solutions of different concentrations (i.e.,1M to 5M) of NaOH. It was observed that 8.09% stripping efficiency of scandium was achieved by using 2M NaOH (Figure 4.17). The scandium recovery dropped at higher concentrations of NaOH. It followed that 2M NaOH was the optimal concentration for alkaline stripping of the loaded organic phase. Although the recovery of scandium was relatively low, the scandium recovery would be higher as the concentration of scandium builds up in the organic phase after prolonged continuous operation.

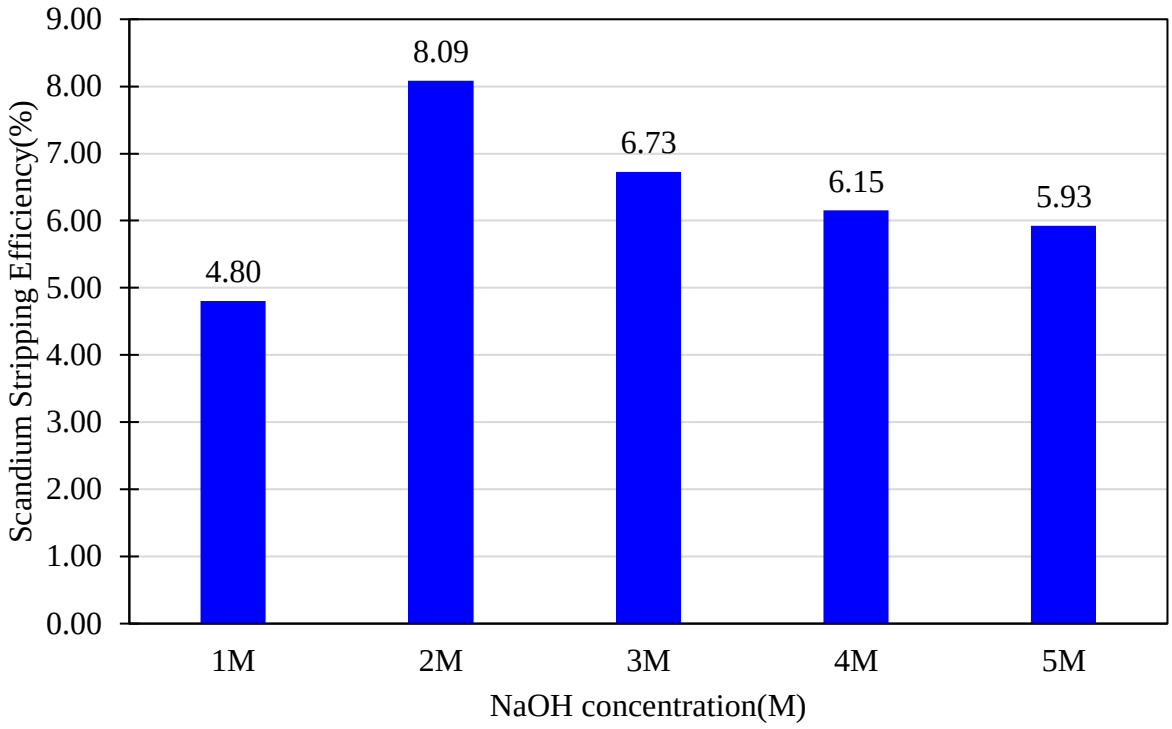

Figure 4.17 Stripping efficiency of scandium over a range of NaOH molar concentrations.

4.3.2 Cynex 272

An alternative methodology that was investigated for the recovery and separation of scandium from contaminant elements was to use Cynex 272, which is a dialkyl phosphinic acid-based proprietary extractant. The extractant is typically used for treating solutions containing cobalt, nickel, and copper. Extraction tests were performed using a 5% Cynex 272 solution in kerosene on the heap leachate produced from Dotiki coarse refuse material. The extractant solution exhibited high selectivity for scandium relative to TREEs and the major contaminant solutions. The extraction efficiency of scandium at pH 0.950 at an A:O ratio of 1:1 was 86.5%, whereas less than 0.5% of TREEs were co-extracted in the process. The co-extraction of primary contaminants was also very low, i.e., 2.26% aluminum, 2.44% calcium, and 2.66% iron (Figure 4.18).

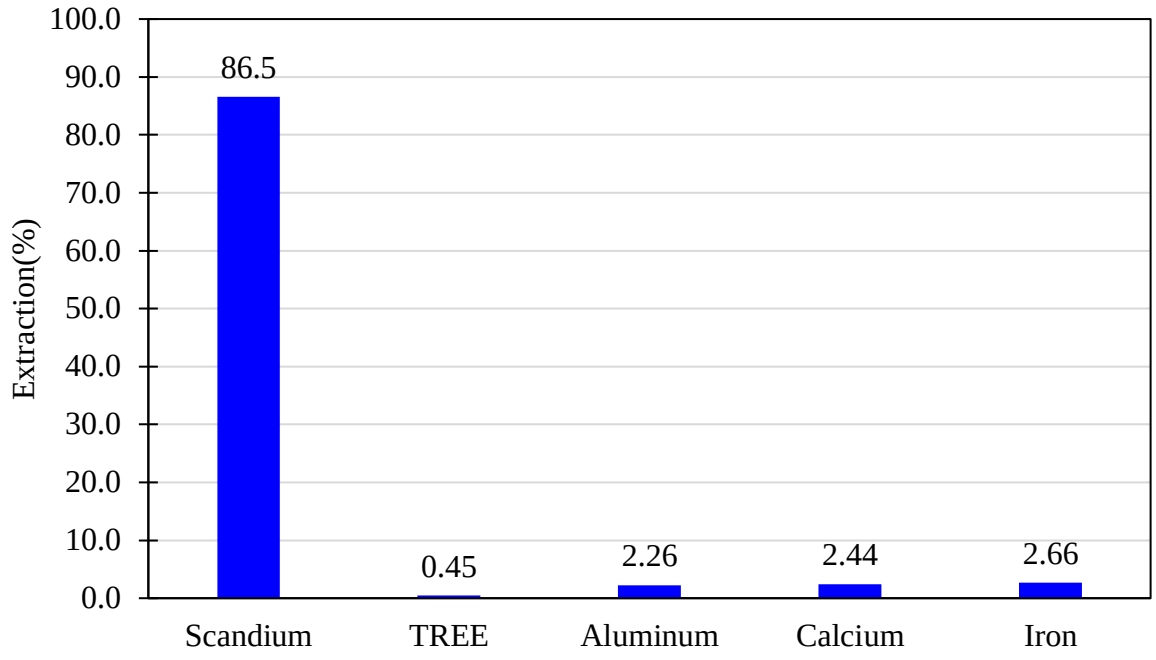

Figure 4.18 Extraction efficiency of scandium with a solution of 5% Cyanex in kerosene from the Dotiki coarse refuse heap leachate.

As reported in the literature [19, 128-131], unlike the low stripping efficiency associated with DEHPA, scandium can be recovered from a loaded Cyanex 272 solution using concentrated sulfuric acid solutions. In this study, the required sulfuric acid solution concentration needed to strip a loaded organic solution was evaluated over a range of 1M to 5M. Stripping recovery of 69.3% for scandium was achieved using 2M H_2SO_4 solution. Recovery reduced significantly at a higher acid concentrations with 4M sulfuric acid resulting in 36.4% stripping efficiency and 5M providing 10.5% stripping efficiency (Figure 4.19).

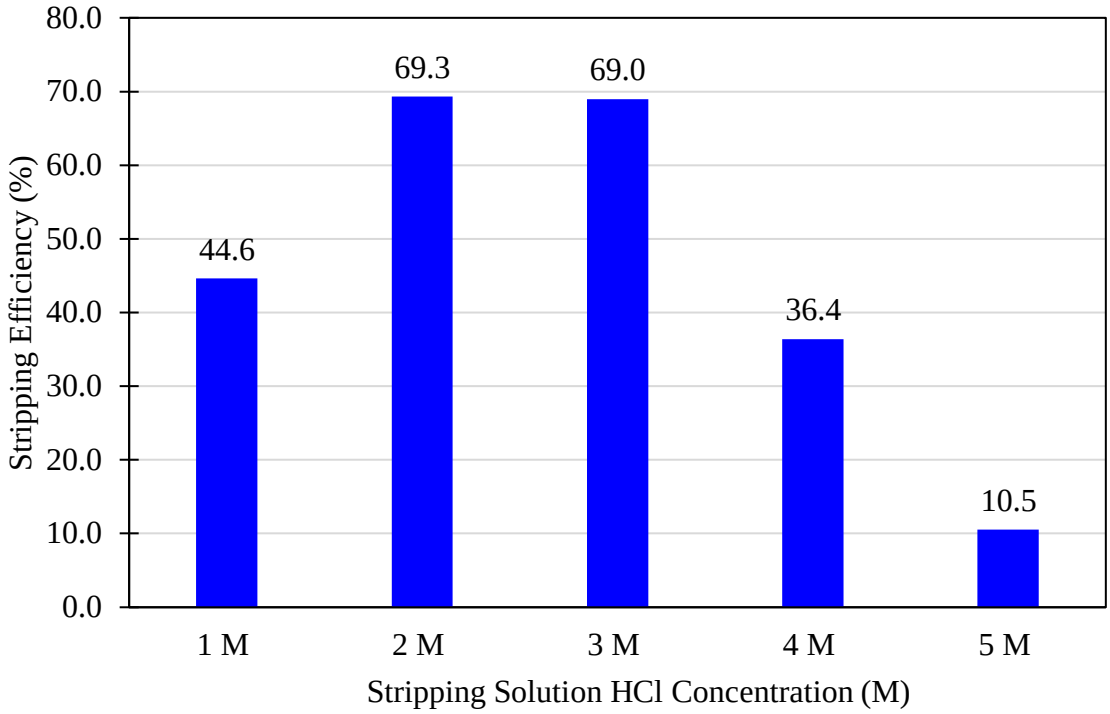

Figure 4.19 Stripping efficiency of scandium from loaded 5% Cynex 272 solution in kerosene using different concentrations of sulfuric acid solutions.

The stripped solution contained 2.0 ppm of scandium while having negligible concentrations of TREE. The primary contaminant levels were relatively low and included 3.8 ppm aluminum, 1.5 ppm calcium, and 20.7 ppm iron. The relative concentration of contaminants with respect to scandium decreased from 5465 in the feed to 13 in the stripped solution, which corresponds to a decontamination factor of 424.9 The performance reflects exceptional selectivity performance when using Cynex 272 to extract and concentrate scandium from a PLS source containing low concentrations of REEs and a much larger amount of contaminant ions. (Figure 4.20).

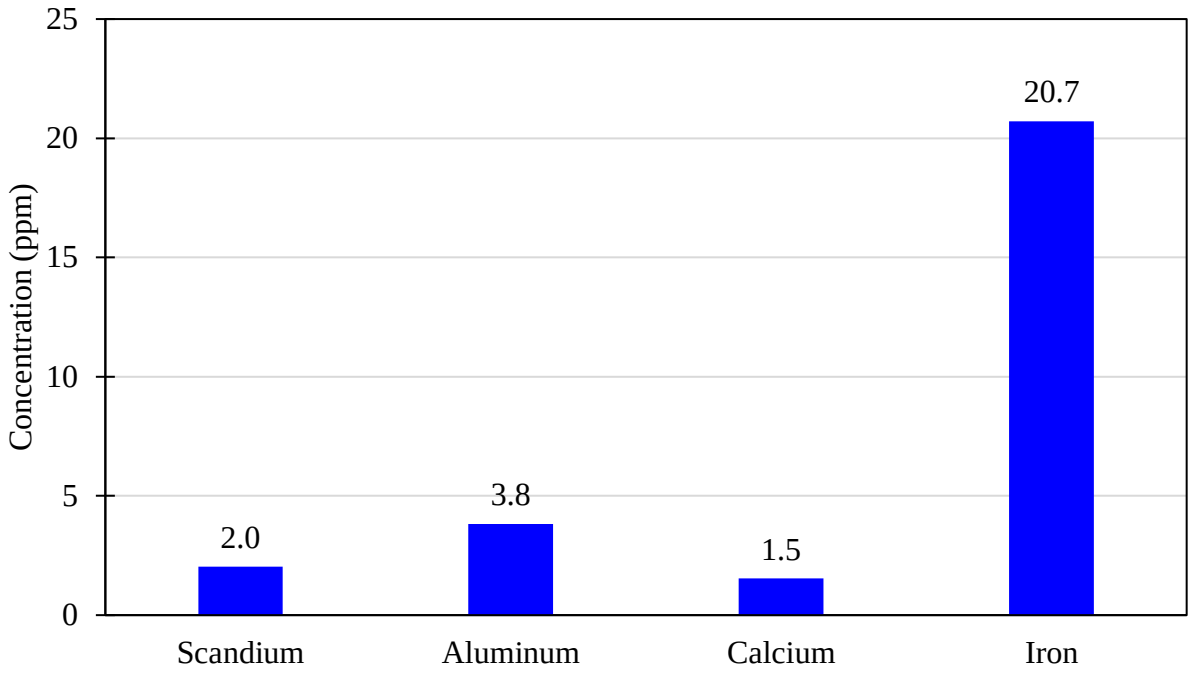

Figure 4.20 Elemental composition of the stripped solution from loaded Cynex 272 organic solution.

4.4 Pilot-Scale Evaluation of Solvent Extraction Process

4.4.1 Description of Setup

The SX process developed for the rejection of contaminant elements from coal-based PLS and concentrating the REEs was tested in a continuous counter-current solvent extraction circuit in a pilot-scale facility. The feedstock for testing of the process was the heap leachate generated by coarse refuse generated from the Dotiki coal processing plant. The acid leachate contained around 13.02 ppm of REE. The total concentration of the primary contaminants (iron, aluminum, and calcium) in the PLS was 4483 ppm (Table 4.5).

An aliphatic diluent (SX Orfom by Chevron Philips) containing 5% DEHPA and 10% TBP by volume was used as the organic solution for this study. The train of mixer-settlers was configured (Figure 4.21) to have two stages of loading, one stage of scrubbing with 0.1 M HCl solution and two stages of stripping with 6 M HCl solution. One stage of alkaline stripping or saponification with 2M NaOH was added in the circuit for scandium recovery. A reprotonation stage using 6 M HCl solution was also added in the circuit to replace the Na^+ ions in the

DEHPA complex with the H^+ ions as the organic stream is recycled back to the loading stage. As determined in the lab-scale study, due to the very low concentration of REEs in the feedstock, the A:O phase ratio should be kept high (1:25 in the lab-scale study) in the stripping step. Such high phase ratios are not feasible in a continuous circuit as it leads to inefficient mixing in the mixer tank. To implement high A:O phase ratios, internal recirculation was used in the mixer-settler setup. A stream of the stripped solution was recirculated from the bottom of the settler tank back to the mixer tank to allow for the concentration to build up. In the absence of any additional acid solution added to the stage, the interface remained static without any aqueous advancing. Once the concentration of the REE in the stripped solution was sufficiently built up, a small volumetric fraction of the stripped solution was bled out of the system and an equal amount of fresh acid was added to the system. The excess volume of the aqueous phase overflowed out of the top of the settler tank, which was collected and processed in the cleaner circuit. The flow volume of the fresh acid addition in the stripping step was adjusted based on the elemental analysis of the strip solution.

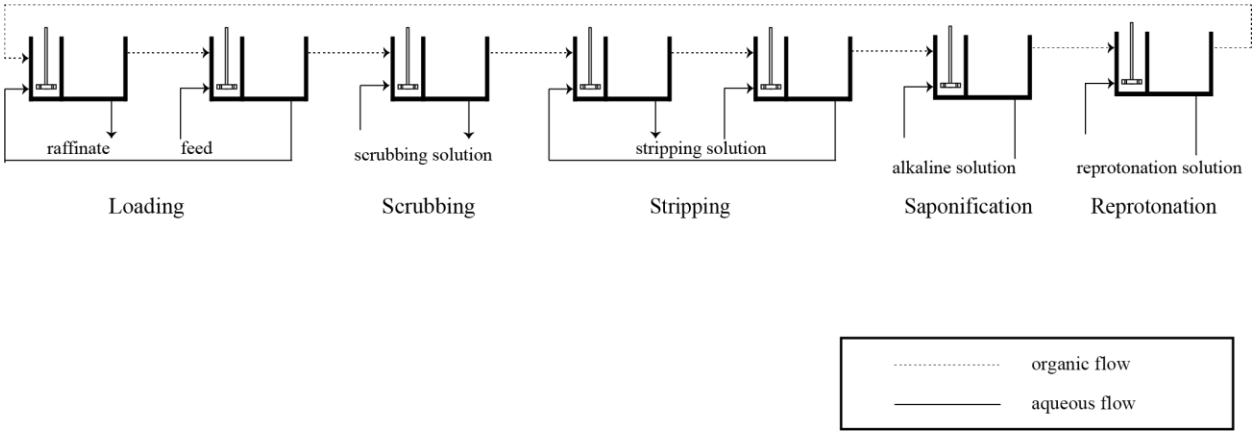

Figure 4.21 Schematic for the configuration of the rougher cycle for the continuous testing of the solvent extraction process.

The PLS was first treated with a solution of ascorbic acid to reduce the iron in the solution to its ferrous state and adjust the ORP to 400 mV followed by pH adjustment using 2 M NaOH solution to 2.0 as ascertained by the lab-scale tests. The ascorbic acid mixing tanks are shown in Figure 4.22. The pH and the ORP of the solution were controlled by a PID controller programmed using Allen Bradley PLCs (Figure 4.23).

Figure 4.22 Tanks used for mixing and dosing the ascorbic acid to the feed solution for the solvent extraction process.

Figure 4.23 (Left) Tanks used for pH and ORP adjustment of the solvent extraction feed;(Right) Interface for pH and pump control used for the automation control of the process.

The stripped solution from the rougher cycle was treated by the cleaner cycle of the process. The cleaner cycle SX utilized the glass mixer-settlers. The mixer-settlers were configured to run three stages of loading and three stages of stripping (Figure 4.24). Similar to the rougher cycle, the stripped solution was internally recirculated from the bottom of settler tank to mixer tank to build up the concentration of REEs, and a small fraction was bled once the concentration was sufficiently built and replaced by an equal amount of fresh 6M HCl stripping solution.

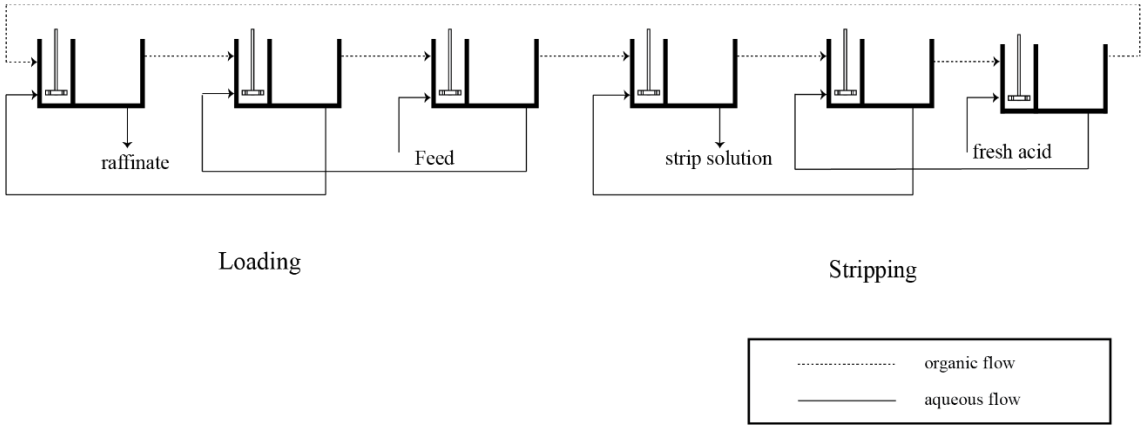

Figure 4.24 Schematic for the configuration of the cleaner cycle for the continuous testing of the solvent extraction process.

The stripped solution of the cleaner circuit was subjected to selective precipitation process using oxalic acid. The operating pH for the selective precipitation of REEs, as specified by Zhang et al. [127], was 1.2. Given that the strip solution from the cleaner cycle was highly acidic (~6 M HCl), the solution was neutralized by the addition of 10M NaOH, and the pH was adjusted before the addition of oxalic acid to precipitate the REEs as oxalates. The oxalic acid dosage was adjusted to 100mL per liter of cleaner stripped solution treated. The oxalate precipitates were recovered by filtration and calcined at 750^{o}C to produce the REO concentrate (Figure 4.25).

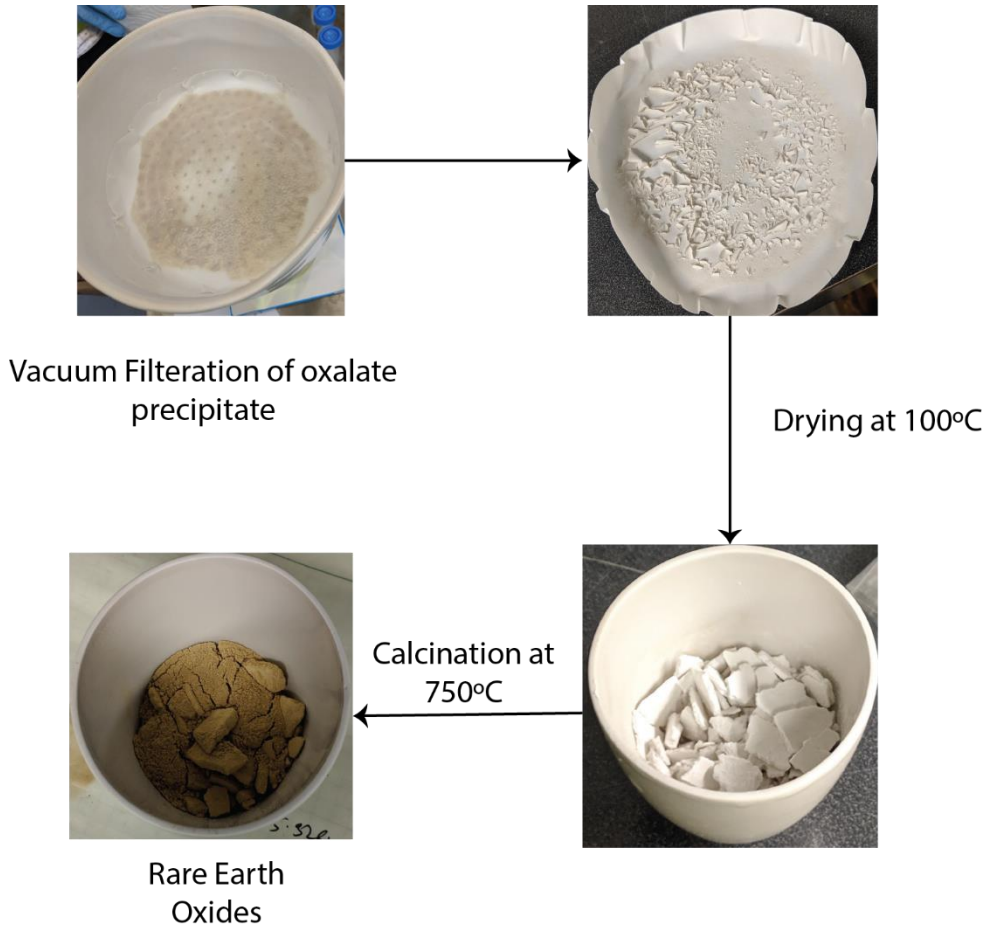

Figure 4.25 Production of rare earth oxide concentrates from oxalate precipitate produced from selective precipitation of stripped solution from cleaner cycle of SX process.

4.4.2 Results of Continuous Tests

The elemental compositions of the feed stripped solution from the rougher cycle and the stripped solution from the cleaner cycle after 100 hours of operation are shown in Table 4.5. It can be seen that the concentration of the REE was increased from 13.02 ppm in the feed PLS to 405.12 ppm in the stripped solution from the rougher circuit. The concentration of the major contaminants in the solution also increased from 4483.5 ppm in the feed PLS to 4909.80 ppm in the stripped solution from the rougher cycle due to high A:O ratio. The relative concentration of the contaminants decreased from 344.30 to 12.12, corresponding to a decontamination ratio of 16.20.

In the cleaner cycle, the concentration of the REEs increased from 405.12 in the feed of the cleaner to 1178.58 ppm in the stripped solution from the cleaner cycle. The contaminant concentration reduced from 4909.80 ppm to 1797.86 ppm. The resultant relative concentration reduced from 21.24 in the cleaner cycle feed to 1.34 in the stripped solution of the cleaner cycle, which equates to a decontamination ratio of 15.85.

Table 4.5 Elemental composition of the feed solution, stripped solution from the rougher cycle, and the cleaner cycle of the continuous solvent extraction process after 100 hours of operation.

Sample	TREE	Aluminum	Iron	Calcium	Contaminant	RC
Feed	13.02	219.74	3903.72	360.07	4483.54	344.30
Stripped solution	405.12	194.96	2127.19	2587.64	4909.80	12.12
Cleaner Stripped	1178.58	38.89	253.38	1505.59	1797.86	1.52

4.4.3 REE Recovery in Rougher Cycle

The recovery of the REE in the process was measured by the amount of REEs lost in the raffinate of the rougher cycle (equation 4.7) as REEs lost in the cleaner cycle were recycled back to the feed of the SX rougher circuit.

$$Recovery\ of\ REE = \frac{[REE]_{Feed} - [REE]_{Raffinate}}{[REE]_{Feed}} \tag{4.36}$$

As shown in Figure 4.26, REE recovery remained around 90% for the first 100 hours of operation after which recovery dropped to about 70%. The drop in the recovery was attributed to the saturation of the organic phase with REEs. Consequently, the volumetric flow rate of the strip bleed stream was incrementally increased, which had little effect on the recovery of the REEs, even though the concentration of REEs was dropping in the stripped solution. It was, therefore, concluded that the initial pH of the feed solution was required to be raised to obtain better recovery. The pH of the feed solution was raised to a value of 2.1 after 205 hours of operation, which resulted in better recovery (above 95%) for the rest of the continuous operation.

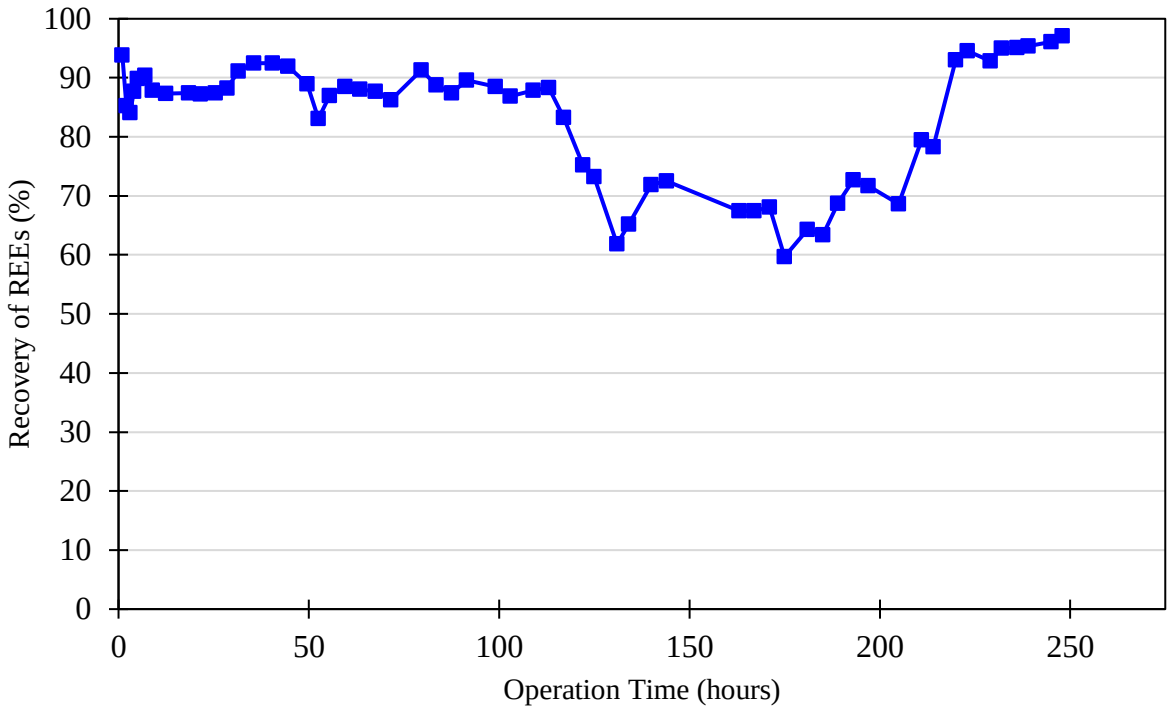

Figure 4.26 Recovery of rare earth elements in the rougher cycle of the solvent extraction process.

4.4.4 REE concentration in the strip solution stream

The bleed flowrate of the SX flowrate was adjusted based on the REE concentration in the stripped solution, i.e., the flow rate was increased when the concentration of REEs stopped increasing; decreased if the concentration decreased to find the steady-state flowrate for the feedstock.

It was interesting to note that even though the concentration of REEs and contaminants varied substantially in the stripped solution from the rougher cycle (Figure 4.27), the relative concentration of the contaminant stayed relatively consistent (around 14) for the majority of the continuous operation (Figure 4.28). This finding agrees with the lab-scale study that the selectivity between the REE and contaminants is not achieved in the stripping stage. It is also important to observe that though the concentration of the contaminants was higher than that in the feed stream, the relative concentration of the contaminants in the strip solution was much lower than the feed stream. The volumetric flow rate of the strip solution stream was much

smaller than the feed stream and the process results in a significant reduction in the amount of contaminants present in the stream.

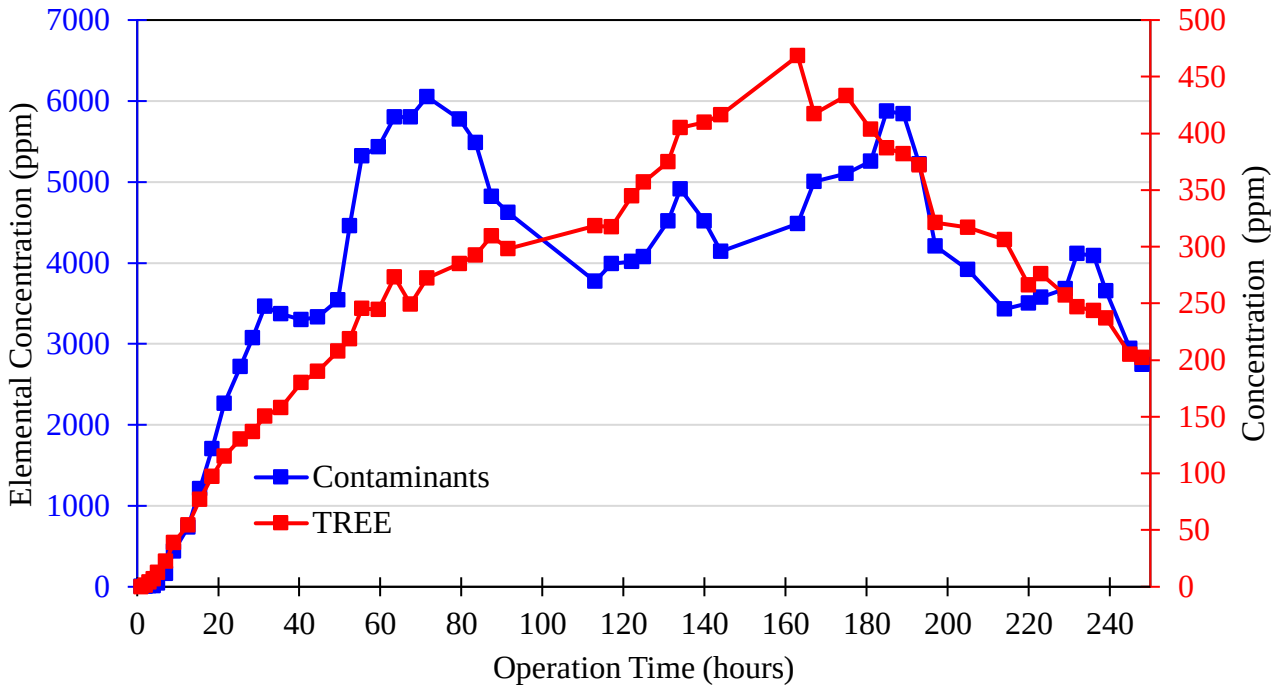

Figure 4.27 Concentration of primary contaminants (in blue) and REEs (in red) for the continuous testing of the solvent extraction process.

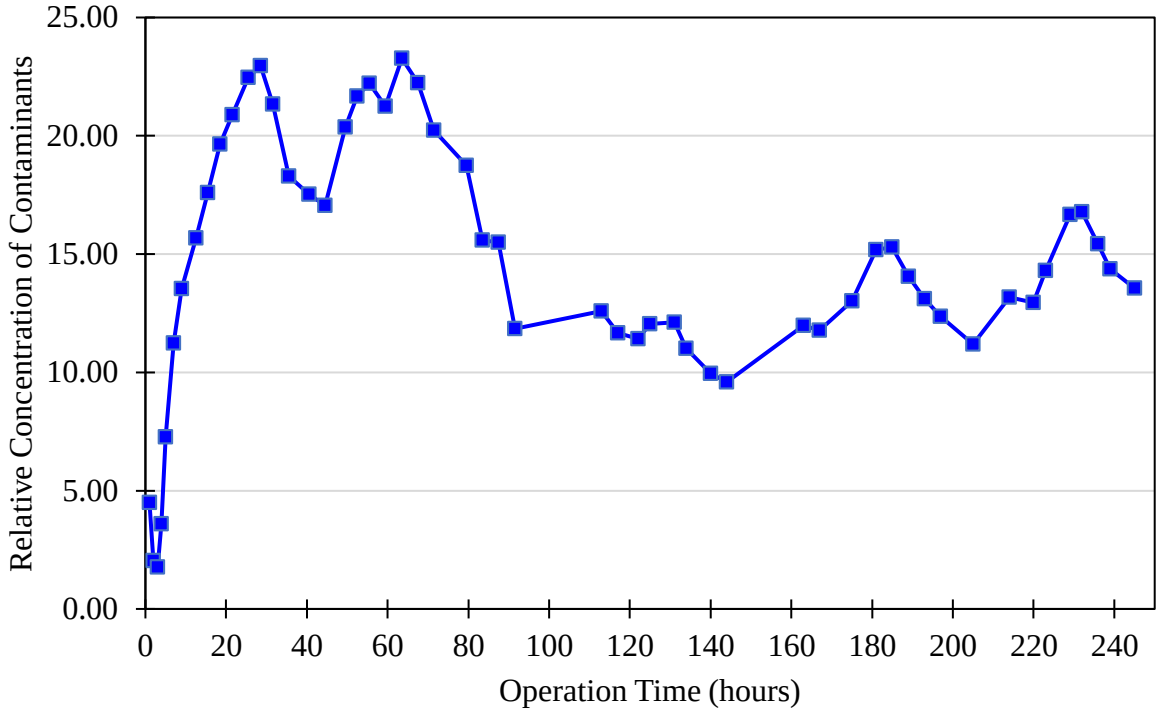

Figure 4.28 Relative concentration of the contaminants with respect to REEs for the continuous testing of the solvent extraction process.

4.4.5 Saponification Circuit

In the continuous operation, the saponification of the organic phase with 2 M NaOH resulted in phase disengagement problems despite the addition of TBP as the phase modifier. The alkaline stripping resulted in the formation of a stable emulsion in the settling tank which resulted in the loss of organic solution in the overflow. Due to this issue, the saponification circuit was turned off for the rest of the continuous operation. Continuing to operate the circuit without recovering scandium would result in scandium poisoning of the organic phase which would reduce the available organic and result in the deterioration of the circuit performance. For future studies, it is recommended to use a separate extractant such as Cynex 272 for scandium recovery.

4.4.6 REE concentration in the Cleaner Cycle

The cleaner cycle was made operational after a substantial quantity of the stripped solution from the rougher cycle was accumulated. The cleaner cycle was started after 187 hours of operation of the rougher cycle. The concentration of both the REEs as well as the primary

contaminants in the stripped solution was fairly constant throughout the operation of the cleaner cycle, and the variation in the concentrations was much lower than that in the rougher cycle (Figure 4.29).

Similar to the rougher cycle, the relative concentration of the contaminants in the stripped solution remained remarkably consistent throughout the operation and stayed within 1.5 to 2.0 (Figure 4.30). The relative concentration of the contaminants was low enough to be treated with oxalic acid to produce a high purity rare earth concentrate.

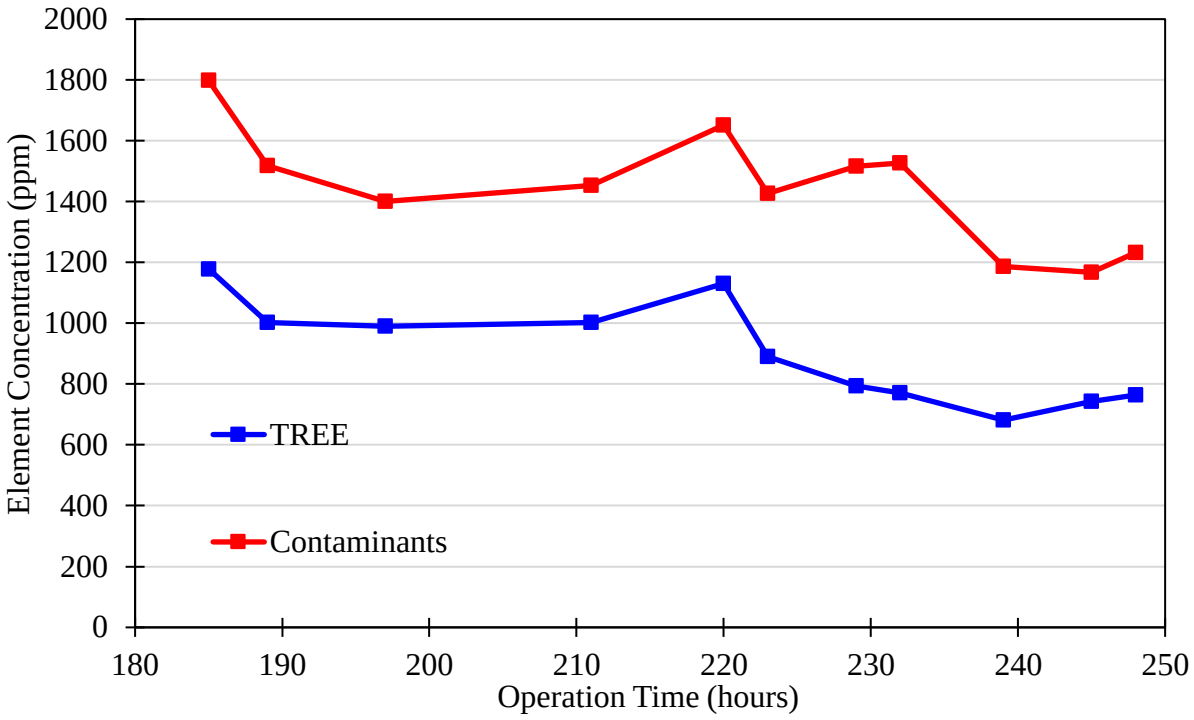

Figure 4.29 Concentration of the primary contaminants (blue) and total rare earth elements (red) in the stripped solution of cleaner cycle of the solvent extraction process.

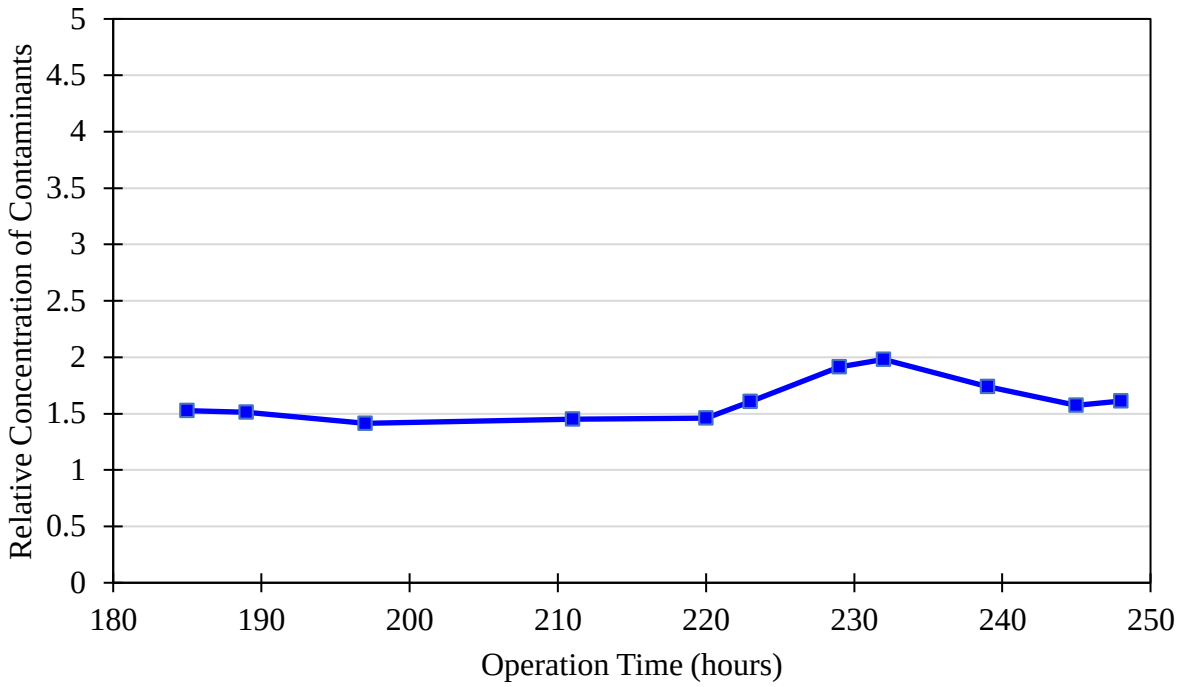

Figure 4.30 Relative concentration of the primary contaminants in the stripped solution from the cleaner cycle of the solvent extraction process.

4.4.7 REO concentrate

The REO concentrate generated by the calcination of the oxalate precipitate was analyzed for elemental composition, and it contained 94.5% REOs by weight. The elemental composition is shown in Figure 4.31.

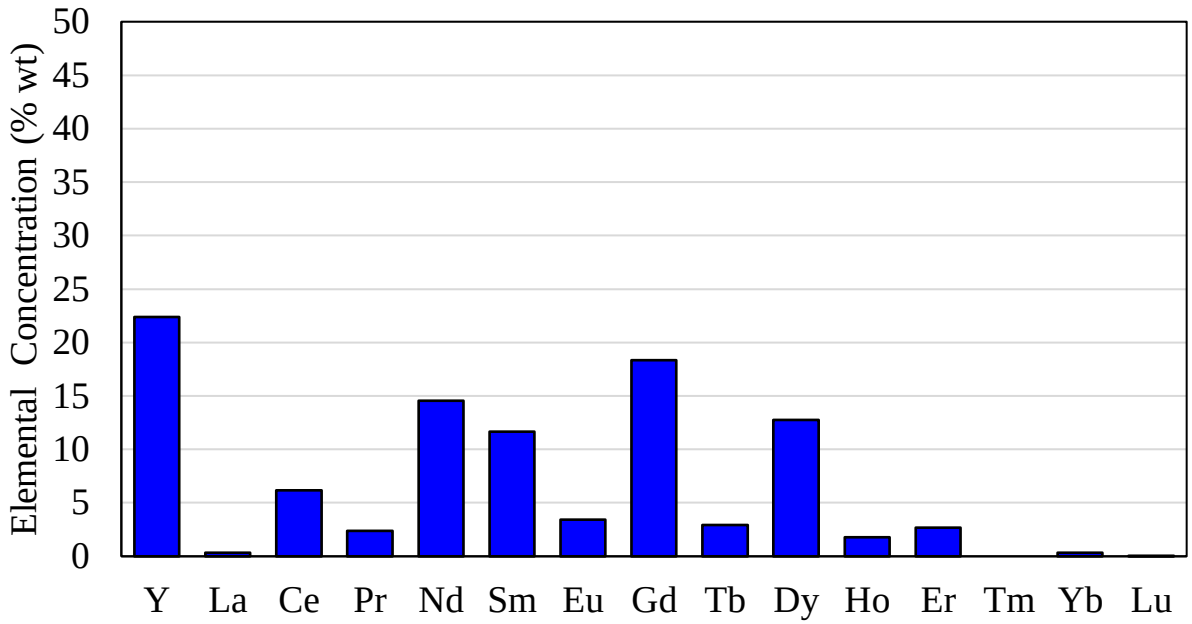

Figure 4.31 Elemental distribution of REO produced from the pilot-scale testing of the solvent extraction process.

4.5 Conclusions

In this chapter, the viability of using a solvent extraction process to reject the contaminants from PLS with very low concentrations of REE and a high concentration of contaminants with DEHPA as an extractant was studied. The different aspects of the process were first examined using a test solution prepared with the salts of the contaminant metals and lanthanum representing the REE. The process was then evaluated on a lab-scale study on PLS generated from six different coal sources. The process was also assessed on a continuous basis on a pilot-scale study performed on heap leachate generated from coal coarse refuse from the Dotiki coal preparation plant. The specific findings from the study include:

1. Iron in the PLS is predominantly present in the ferric form. As a result, the rejection of iron using SX requires the reduction of iron to its lower valence state using a reducing agent;
2. The selectivity of the SX process for rejection of contaminants, as quantified by the decontamination factor is independent of the DEHPA concentration in the organic phase. However, it is dependent on the initial pH of the feed solution (maximum for pH 2.0);
3. The contaminants co-extracted in the organic phase can be selectively scrubbed out using a dilute solution of hydrochloric acid. However, the selectivity diminishes at higher concentrations of acid. Therefore, there is little to no selectivity achieved in the stripping stage of the SX process;
4. Due to the very high relative concentration of contaminants in the PLS, the SX process was performed in two cycles, rougher and cleaner, to reduce the contaminant concentration sufficiently low for the selective precipitation to be viable;
5. Scandium recovery exhibits very poor stripping efficiency in the acid stripping of DEHPA, which results in low concentrations of scandium in the REO produced from PLS from coal sources. There are two alternative methods for recovery of scandium, alkaline stripping or saponification of the organic phase, which requires the addition of a phase modifier like TBP; or an alternate extractant like Cynex 272 for extraction of scandium prior to REE extraction by DEHPA; and
6. The SX process developed was evaluated on a pilot-scale continuous circuit. A 94.5 % by weight REO was produced by treated heap leachate generated from coarse refuse coal of Dotiki coal processing plant.

5 EFFECT OF TBP ON THE EXTRACTION OF RARE EARTH AND CONTAMINANT ELEMENTS

5.1 Introduction

In solvent extraction, phase modifiers are added to the organic phase for primarily three reasons, i.e.:[81, 85, 132]

1.) Improving the phase separation characteristics of the organic and aqueous phases;
2.) Prevention of insoluble compound formations in the organic phase (commonly known as ‘crud’); and
3.) Synergism, i.e., an increase in the extraction efficiency of the metal and/or selectivity of metal with respect to another metal.

A phase modifier, when added to the organic phase, assists in solubilizing the metal-organic species, which enhances the phase disengagement and reduces the third-phase emulsion formation. This is very pertinent for continuous solvent extraction processes where poor phase separation, as well as crud formation, can lead to extractant losses in the circuit [126, 132]. The third phase is suppressed by the addition of polar diluents such as long-chain alcohols, monoamides, and organic phosphates. These compounds have high dielectric constants and hence are capable of offering specific solvation to the metal-ligand complexes/acid-ligand salts either through dipole-dipole interaction or through hydrogen bonding, therefore preventing third-phase formation [133]. TBP is shown to be a relatively strong phase modifier as compared to long-chain alcohols due to its high dipole moment, which makes it better at secondary solvation of the complex [134].

The addition of TBP to the DEHPA solution also results in a significant change in the extraction behavior of metals, as noted by several researchers [81, 84, 85, 87, 135]. The addition has an anti-synergistic impact on the distribution coefficients of the metal, despite having a synergistic effect on the solubility of the metal-extractant complex. However, the impact differs from metal-to-metal, which in turn has the potential of enhancing or suppressing the separation characteristics of the metals. Previous studies [79, 81, 82, 84, 85] focused on the addition of a TBP as a synergistic agent for which TBP is added in relatively high concentrations (5%-20%). However, as a phase modifier, TBP is typically added in much

smaller quantities (1-2% by volume). There is a significant gap in the literature regarding the impact of the addition of TBP in small quantities to the organic phase on the extraction characteristics of the REEs which was addressed in this study

Additionally, solvent extraction was evaluated as a method to separate and produce individual REE concentrates as well as a method for the separation of REEs from major contaminant elements (aluminum, iron, and calcium). Previous studies related to this topic focused on TBP's impact on the separation characteristics of individual REEs, but there is a lack of a systematic study focused on the impact of addition into a DEHPA on the separation characteristics of REEs from contaminant metals.

5.2 **Methodology**

The extraction of six elements including three REEs (i.e., lanthanum, gadolinium and yttrium) and three contaminant metals aluminum, iron, and calcium) were studied in a system containing for 5% DEHPA in the organic diluent by volume with no TBP and with 1% and 2% addition of TBP by volume. The three REEs were strategically chosen to represent the light, middle, and heavy rare earth elements, respectively. Solutions of 100 ppm concentrations were prepared by dissolving chloride salts of the metals in DI water. Extraction curves were developed by performing tests at over a range of aqueous solution pH values. The pH of the solution was adjusted by adding 10M NaOH and 10M HCl to the solution as required.

The extraction characteristics of the metals were quantified by the $pH_{0.5}$ of the extraction curve. The $pH_{0.5}$ value of an extraction curve for a given metal is defined as the pH of the solution corresponding to 50% extraction of the metal into the organic phase[136]. The value of $pH_{0.5}$ for any metal can be calculated by a curve fitting method. Consider the fundamental reaction mechanism for tracer concentrations in a solvent extraction system proposed by Peppard et al. [91]:

$$M^{3+} + 3(HG)_2 \leftrightarrow M(HG_2)_3 + 3H^{\dagger} \tag{5.1}$$

$$K = \frac{[M(HG_2)_3][H^+]^3}{[M^{3+}][(HG)_2]^3} \tag{5.2}$$

where K is the equilibrium constant and the $[(HG)_2]$ the concentration of the extractant. Equation 5.2 can be expressed in the logarithmic form as:

$$\log D = \log K + 3 * \log[(HG)_2] + 3pH \quad (5.3)$$

in which D is the distribution coefficient of the metal ($=[M(HG_2)_3]/[M^{3+}]$). As K and $[(HG)_2]$ are constants, the log(D) has a linear relationship with the pH of the solution. As the concentration of the metal in the solution is higher than the tracer level,

$$\log D \rightleftharpoons P(pH) + Q \quad (5.4)$$

The constant parameters P and Q were calculated for each test condition by linear regression of the experimentally calculated log(D) corresponding to the measured pH. The 50% extraction corresponds to a distribution coefficient value of 1, where the concentration of the metal is equal in the organic and aqueous phase assuming the O:A phase ratio is maintained at a value of unity. As such, the value of the $pH_{0.5}$ is calculated by solving the regression equation for the pH value for which log D=0.

It is interesting to note that Eq. (5.4) provides the background behind the relationship between extractant dosage requirements and the solution pH. When high extractant dosages are required to treat solutions with elevated metal contents, low solution pH values are required. For dilute solutions, minimizing extractant dosage is desirable due to cost but the minimum value is limited by the pH value associated with the initiation of metal hydroxide precipitation.

5.3 Extraction Characteristics of REEs

Contrary to the effect when used for uranium enrichment, extraction tests found that the addition of TBP to the DEHPA organic solution had an anti-synergistic effect on the extraction behavior of the rare earth metals and contaminant elements which agrees with the findings reported by other researchers [90]. The addition of TBP to the organic phase resulted in an increase in the $pH_{0.5}$ of the metals. As shown in Figure 5.1 **,** the $pH_{0.5}$ value for lanthanum extraction using a 5% DEHPA solution was calculated to be 1.03. An increase of 28% and 30% in the $pH_{0.5}$ value was observed after the addition of 1% and 2% TBP to the organic phase, respectively. This finding means that the addition of TBP reduced the loading capacity of DEPHA solution.

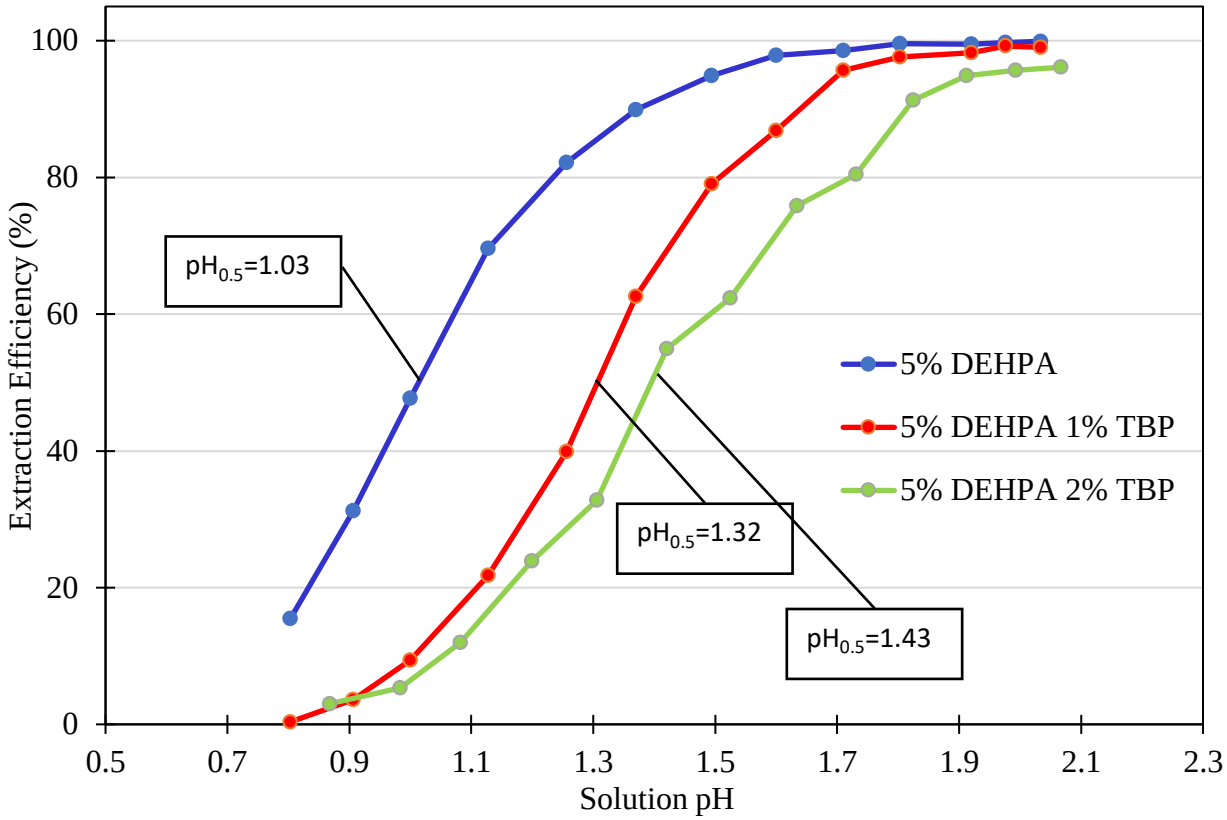

Figure 5.1 Extraction curves and corresponding pH0.5 of lanthanum by 5% DEHPA, and 5% DEHPA with 1% and 2% TBP added.

As shown in Figure 5.2, the $pH_{0.5}$ value for gadolinium changed from 0.709 for a 5% DEHPA solution to 0.736 and 0.847 for 1% and 2% TBP addition to the organic phase. The increase in $pH_{0.5}$ corresponds to a change of 2% and 10%, respectively. As such, the impact of TBP on the extraction of gadolinium was significantly less pronounced as compared to that lanthanum extraction.

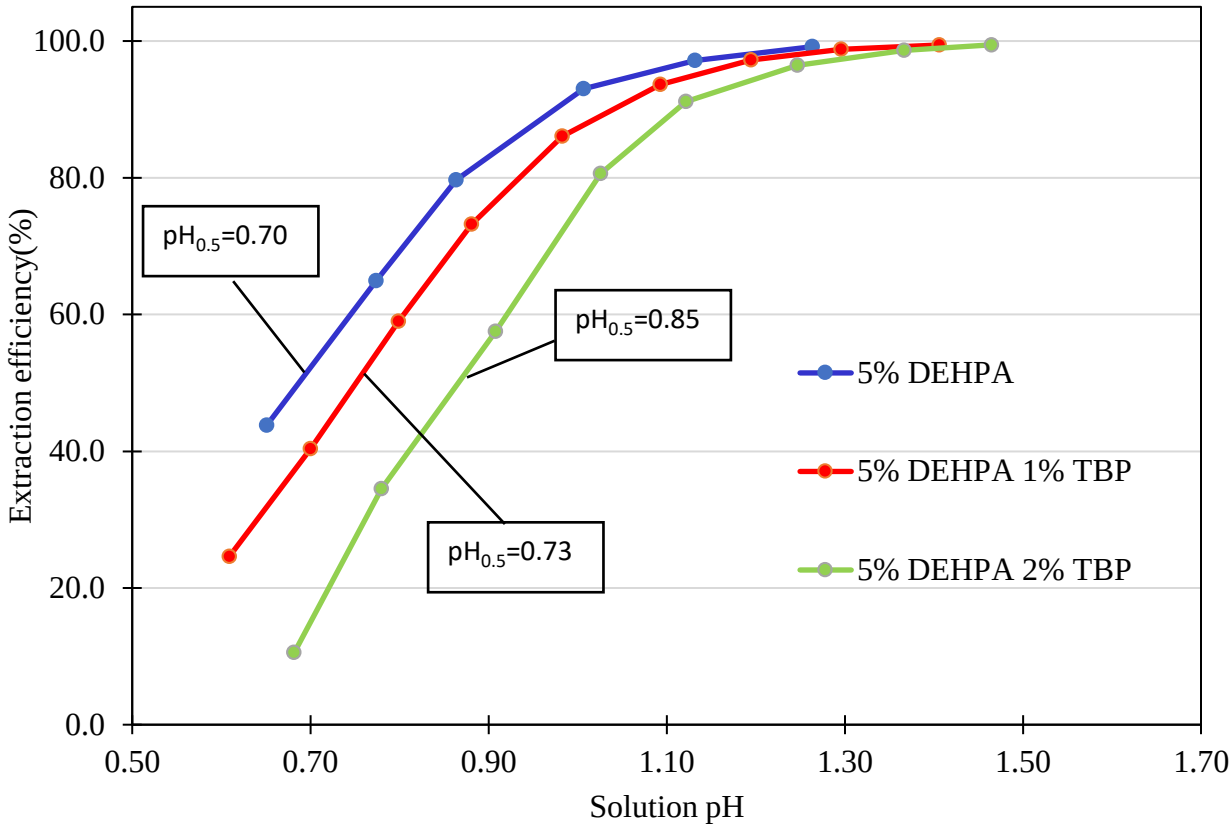

Figure 5.2 Extraction curves and corresponding pH0.5 of gadolinium by 5% DEHPA, and 5% DEHPA with 1% and 2% TBP added.

As shown in Figure 5.3, yttrium exhibited a pronounced change in the extraction curve when 1%TBP was added to the organic phase which resulted in a significant increase in the $pH_{0.5}$ value from 0.05 to 0.20. Though the absolute change in the $pH_{0.5}$ is 0.15, the value is 4 times the value for 5% DEHPA. Interestingly, the addition of 2% TBP had an almost identical effect on $pH_{0.5}$ as 1% TBP. The $pH_{0.5}$ was calculated to be 0.23. It can be seen in the figure that the extraction curves for 1% and 2% TBP in the organic phase are very close to each other, particularly at higher pH values of the aqueous solution.

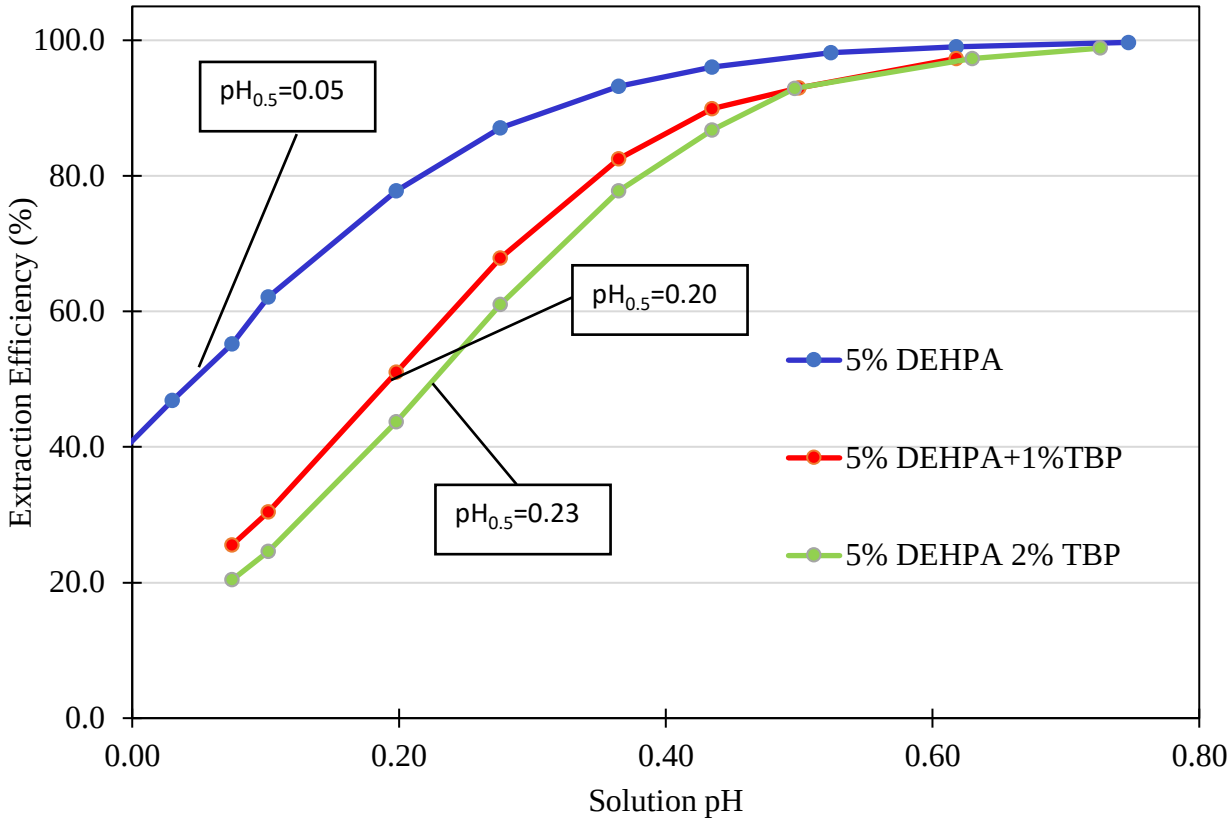

Figure 5.3 Extraction curves and corresponding pH0.5 of yttrium by 5% DEHPA, and 5% DEHPA with 1% and 2% TBP

5.4 Extraction Characteristics of Contaminants

As was the case with the REEs, the addition of TBP suppressed the extraction of contaminant metal to varying degrees resulting in different extraction characteristics and subsequently altered separation behavior as well. As shown in Figure 5.4, the impact on the extraction characteristics on iron followed the same pattern as that on the REEs. The $pH_{0.5}$ increased from 1.60 without TBP to 2.05 with the addition of 1% TBP (a change of 18%) and 2.21 with the addition of 2% TBP in the organic phase (a change of 32%).

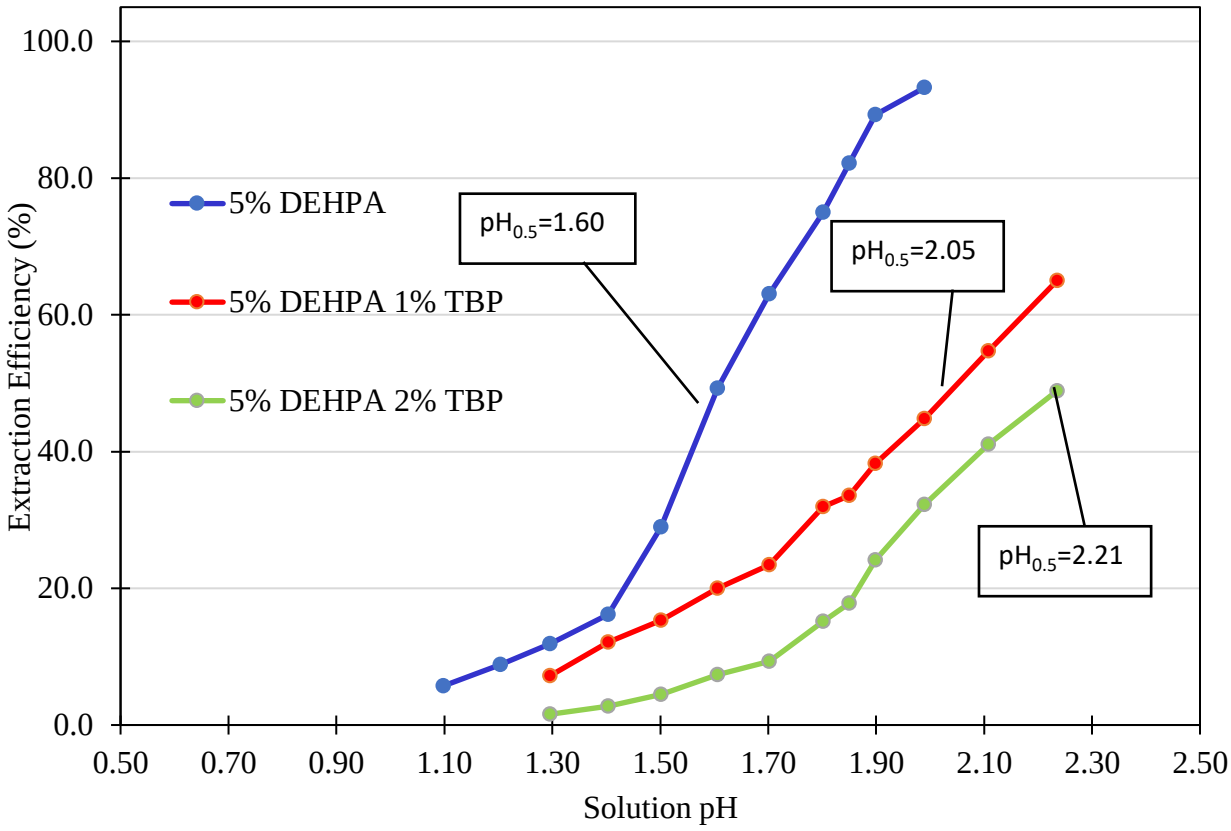

Figure 5.4 Extraction curves and corresponding $pH_{0.5}$ of iron by 5% DEHPA, and 5% DEHPA with 1% and 2% TBP

For aluminum, the $pH_{0.5}$ increased from 1.67 to 1.97 (an increase of 0.30 pH units) when 1% TBP was added to the organic phase. However, the effect was less prominent when TBP in the

organic phase was increased to 2% as the $pH_{0.5}$ increased 0.17 pH units from 1.97 to 2.14. (Figure 5.5)

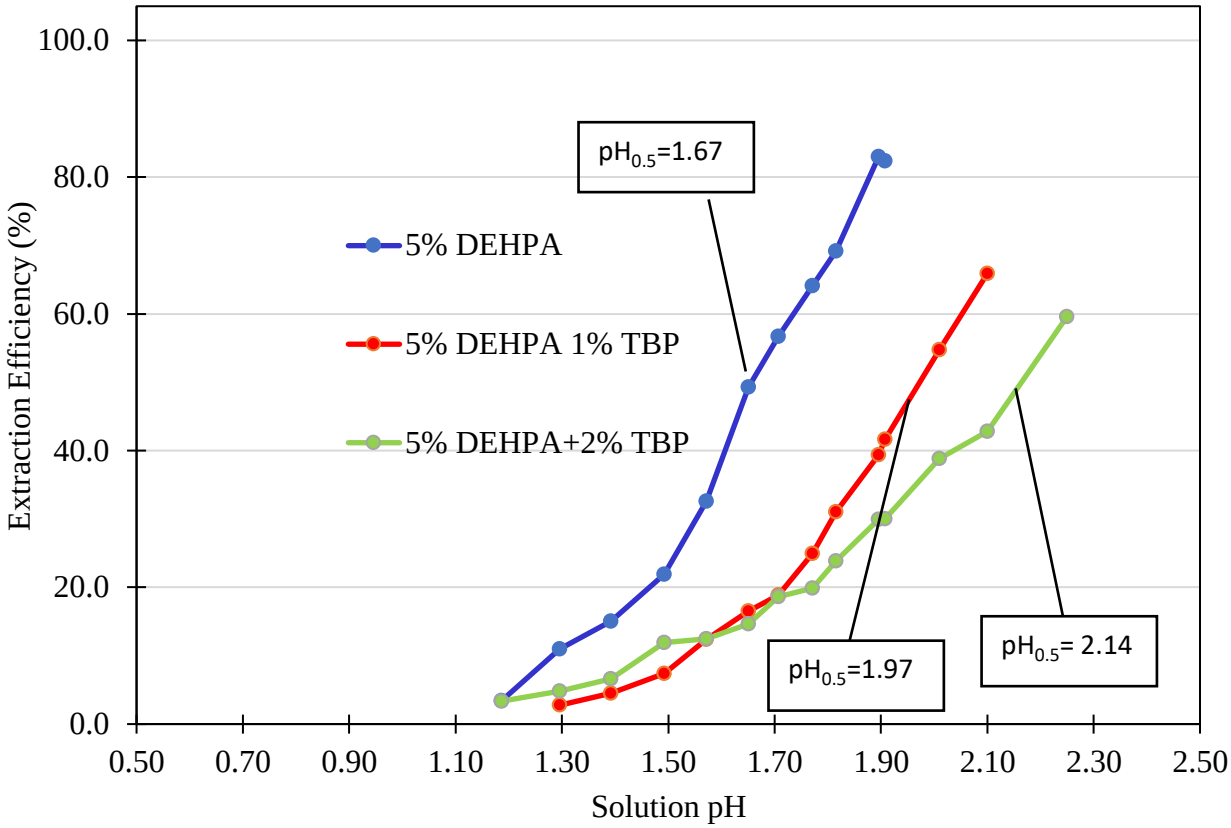

Figure 5.5 Extraction curves and corresponding pH0.5 of aluminum by 5% DEHPA, and 5% DEHPA with 1% and 2% TBP added.

As shown in Figure 5.6, the impact on calcium extraction characteristics was not significant as the $pH_{0.5}$ showed a nominal increase of 0.07 pH units (change of 3%) when 1% TBP was added to the system and 0.23 (change of 11%) when 2% TBP was added to the organic phase.

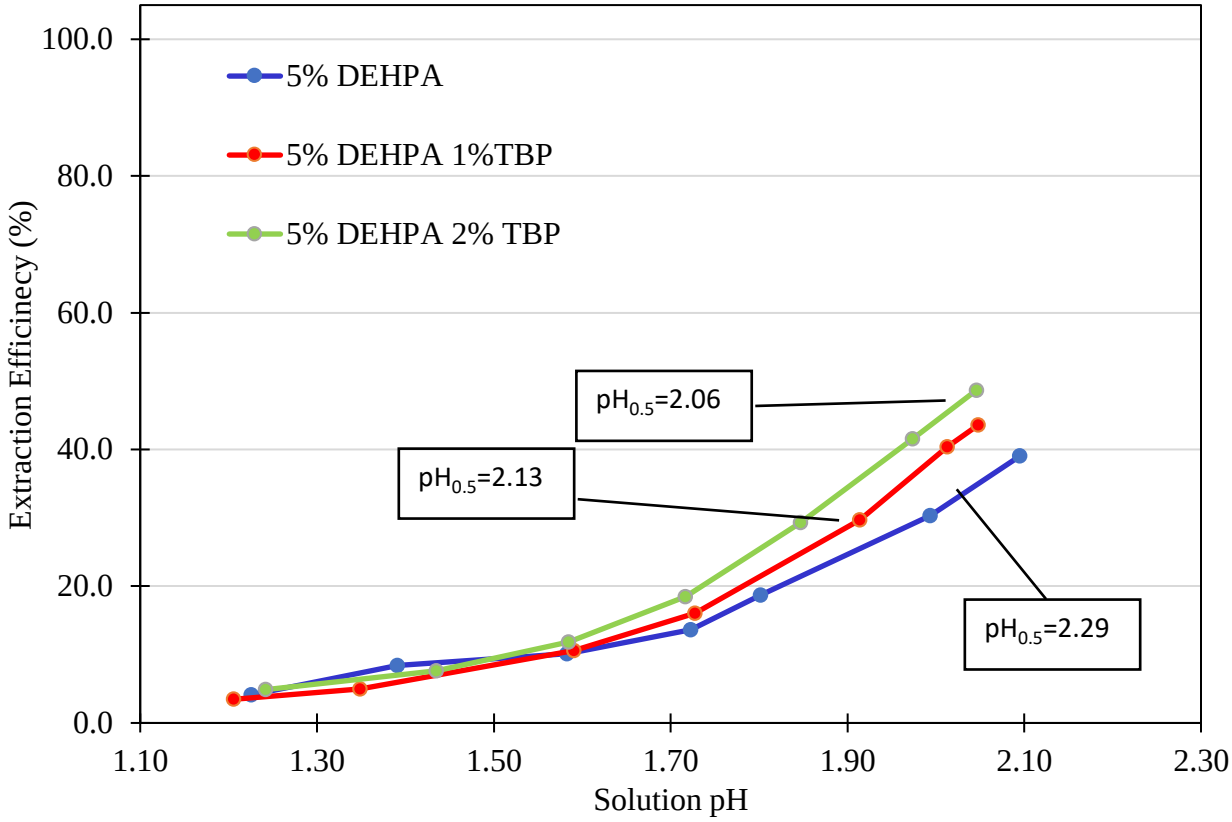

Figure 5.6 Extraction curves and corresponding pH0.5 of calcium by 5% DEHPA, and 5% DEHPA with 1% and 2% TBP.

5.5 Separation Characteristics

For the evaluation of the separation characteristics of the elements, the extraction curves were studied for each organic phase (Figure 5.7, Figure 5.8, Figure 5.9). It was observed that a greater differential in the extraction curves was achieved between the REEs and the contaminant elements when 1% and 2% TBP were added to the organic phase. The differentiation of the extraction curves can be attributed to the fact that the impact of TBP on extraction characteristics is not the same in magnitude from element-to-element. As such,

separation characteristics can be improved by the addition of TBP due to differential changes in $pH_{0.5}$ value for each metal.

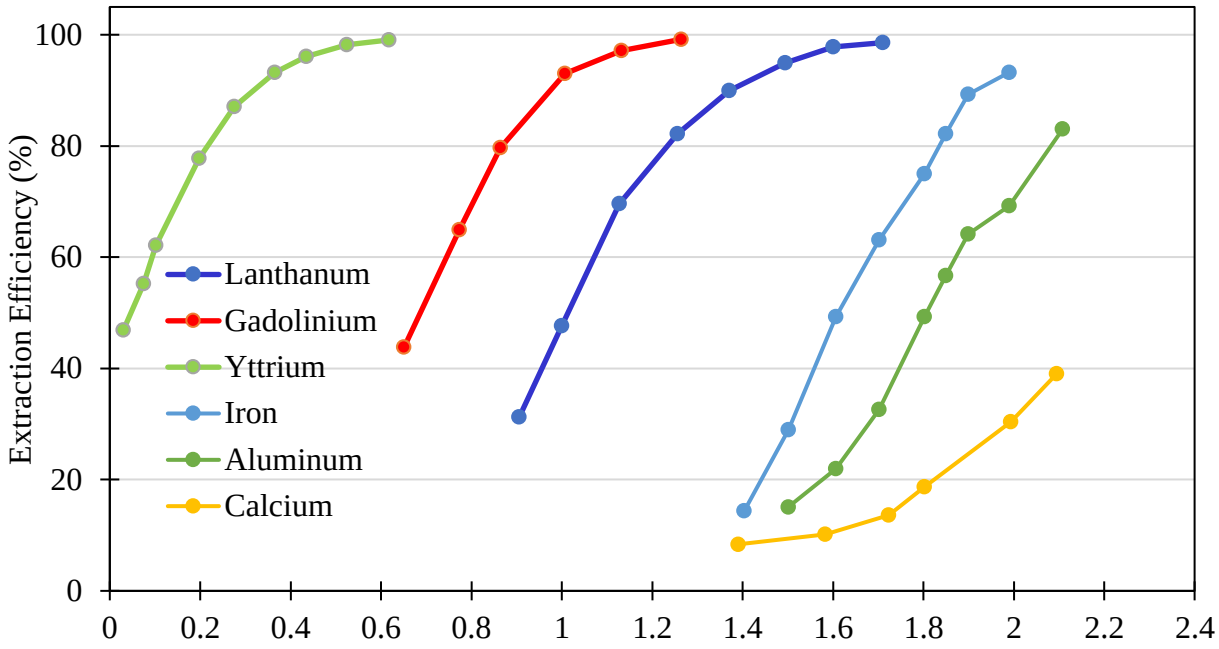

Figure 5.7 Extraction curves of the REEs and contaminants for 5% DEHPA.

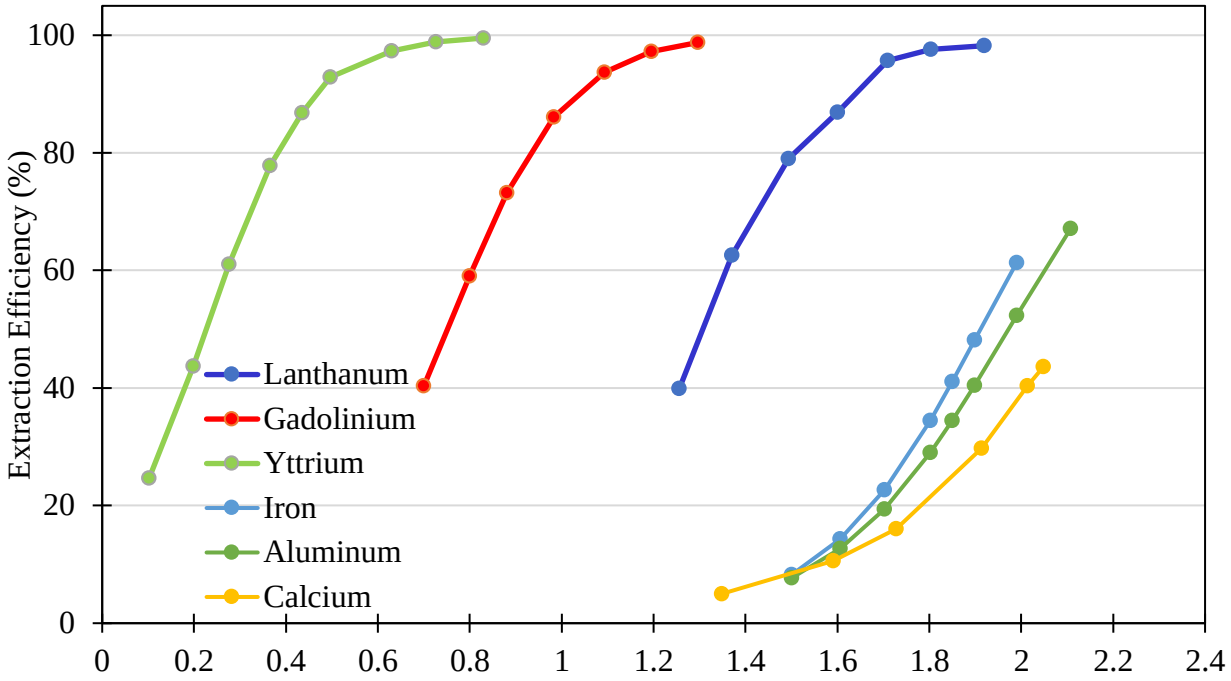

Figure 5.8 Extraction curves of the REEs and contaminants for 5% DEHPA with 1%TBP.

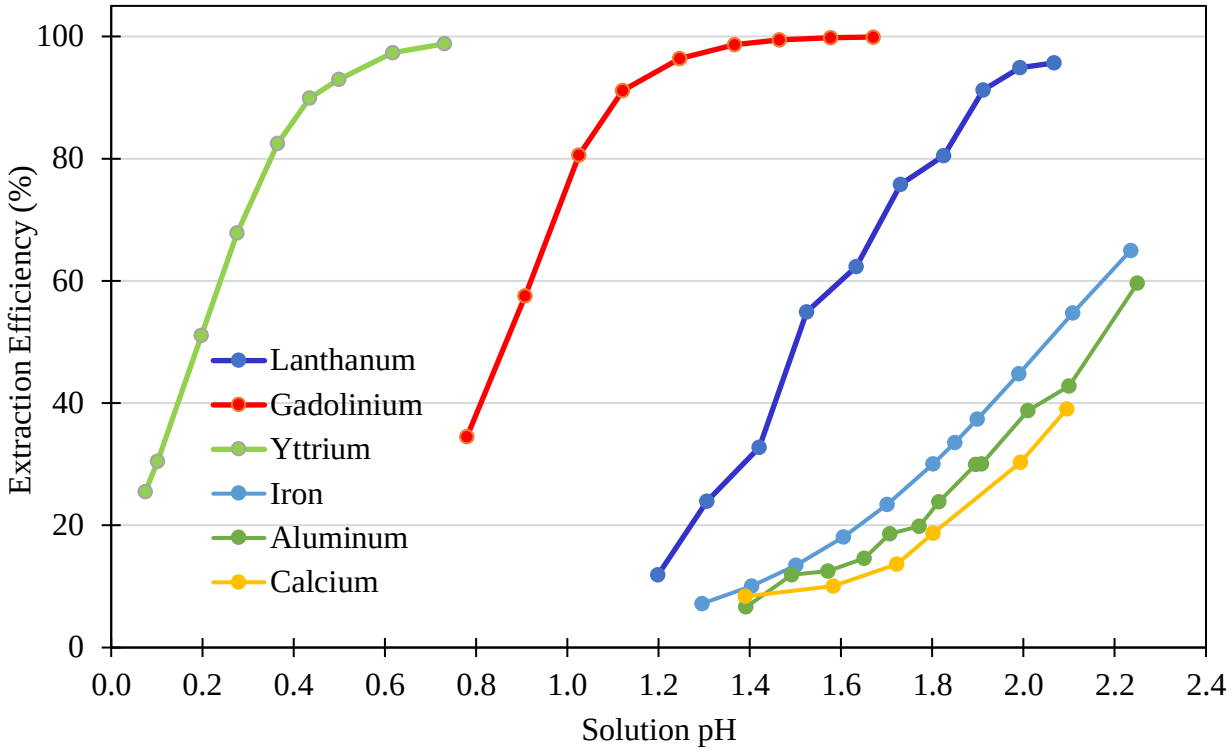

Figure 5.9 Extraction curves and REEs and contaminants for 5% DEHPA, with 2% TBP.

To allow a detailed assessment of the impact of the TBP addition on the selectivity of individual REE separation, the difference in the $pH_{0.5}$ ($\Delta pH_{0.5}$) values associated with the REEs was calculated for each of the organic solutions for each pair of REE (La-Gd, Gd-Y, and La-Y), i.e.:

$$(\Delta pH_{0.5})_{A-B} = (pH_{0.5})_A - (pH_{0.5})_B \quad (5.4)$$

As shown in Figure 5.10, it was observed that the La-Gd pair (representing the separation of light and medium REE) experience enhanced separation characteristics when 1% TBP was added to the organic phase ($\Delta pH_{0.5}$ increased from 0.32 to 0.59), while the addition of 2% TBP to the organic phase did not result in any additional benefit in the selectivity. Interestingly, the Gd-Y pair (representing the medium-heavy REE separation) experienced a diminished separation efficiency when 1% TBP was added, and there was no statistical difference in the separation efficiency of the Gd-Y pair for 2% TBP and without TBP addition. The reason for

the reduced separation efficiency was that the impact on the extraction of yttrium was more pronounced as compared to gadolinium, which resulted in the $pH_{0.5}$ values moving toward equality. Finally, for the La-Y pair (representing the light-heavy REE separation), the $\Delta pH_{0.5}$ increased from 0.99 without TBP addition to 1.12 in the case of a 1% addition of TBP and 1.21 in the case of 2% addition of TBP. The $\Delta pH_{0.5}$ increased even though the effect on the extraction curve of yttrium was more pronounced than that on the extraction curve of lanthanum. The shift in the $pH_{0.5}$ value for lanthanum was more in absolute terms (0.29 and 0.40) as compared to yttrium (0.15 and 0.18). It can be concluded that optimum separations were achieved under the following conditions:

1. lanthanum-gadolinium separation: 1% TBP with 5% DEHPA;
2. gadolinium-yttrium separation: 2% TBP with 5% DEHPA; and
3. lanthanum-yttrium separation: 5% DEHPA without TBP.

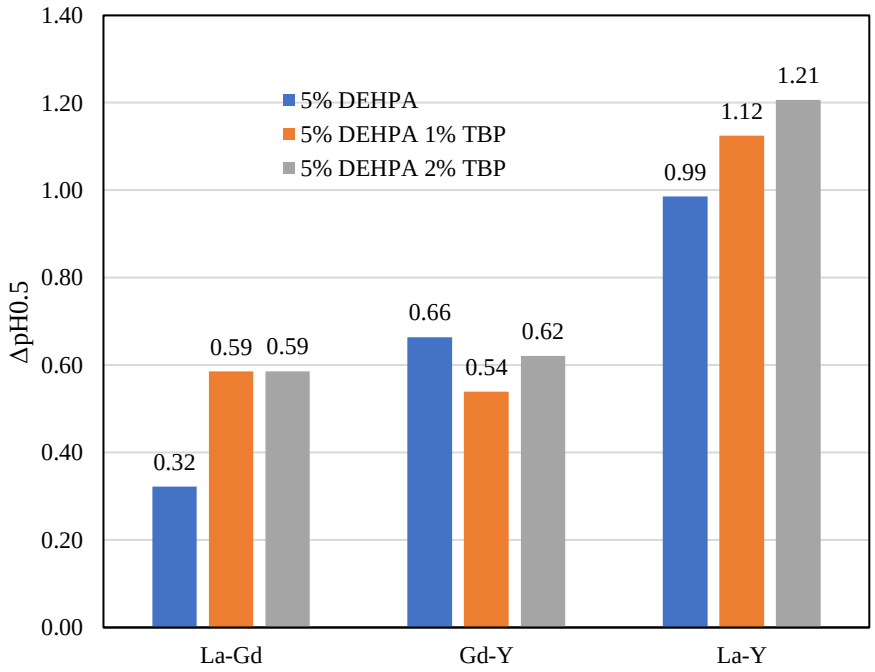

Figure 5.10 $\Delta pH_{0.5}$ values for different REE separation for 5% DEHPA, and 5% DEHPA with 1% and 2% TBP added.

Similarly, the difference in the $\Delta pH_{0.5}$ values associated with the impact on the selectivity between the REEs and the major contaminant elements were determined. Overall, 9 pairs of

$\Delta pH_{0.5}$ were evaluated (3 for each REE). It was observed that, for all Fe-REE pairs (representing the separation of iron with REE), separation characteristics were enhanced when 1% TBP was added to the organic phase, while the addition of 2% TBP to the organic phase did not result in any significant additional benefit in selectivity. While the La-Al pair did not exhibit any improved separation characteristics, there was a significant improvement in the separation in the case of Gd-Al and Y-Al pair. Lastly, calcium showed a significant reduction in the separation efficiency with lanthanum upon addition of TBP, while there was no significant impact in the $\Delta pH_{0.5}$ of calcium with respect to gadolinium and yttrium.

Therefore, it was concluded that 1% TBP addition to organic phase resulted in optimum selectivity for iron and aluminum rejection, whereas for calcium rejection, 5% DEHPA without any TBP yielded the best results. However, typical acid leachate generated from coal sources contains iron and aluminum in much higher quantities relative to calcium, and therefore, the addition of TBP can improve the overall contaminant rejection of the process.

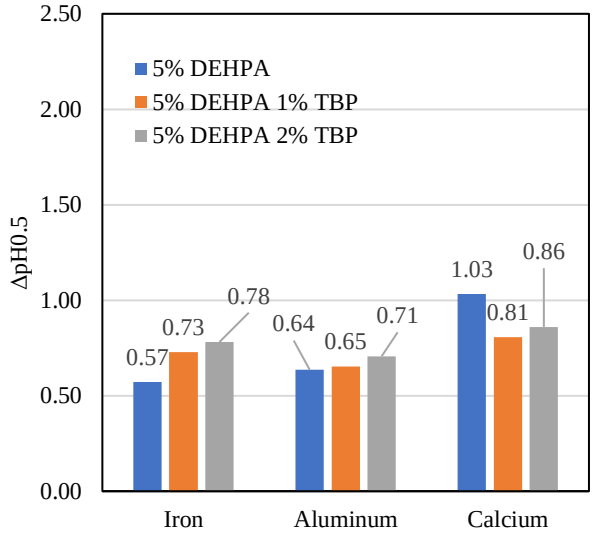
2.50
2.00
1.50
1.00
0.50
0.00
ΔpH0.5
5% DEHPA
5% DEHPA 1% TBP
5% DEHPA 2% TBP
0.57
0.73
0.78
0.64
0.65
0.71
1.03
0.81
0.86
Iron
Aluminum
Calcium

A

B

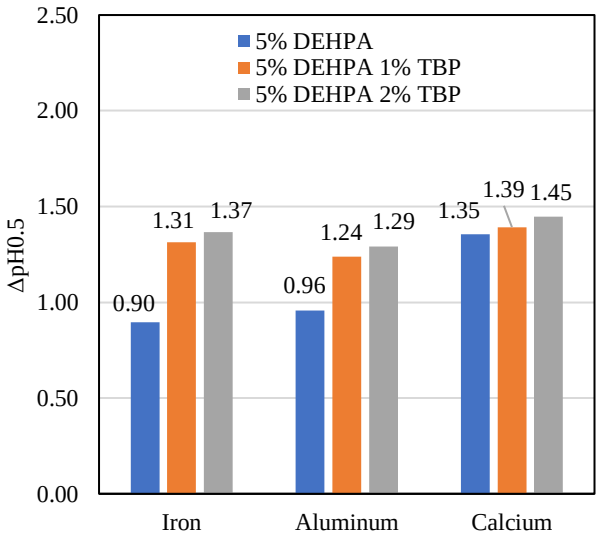
2.50
2.00
1.50
1.00
0.50
0.00
ΔpH0.5
5% DEHPA
5% DEHPA 1% TBP
5% DEHPA 2% TBP
0.90
1.31
1.37
0.96
1.24
1.29
1.35
1.39
1.45
Iron
Aluminum
Calcium

C

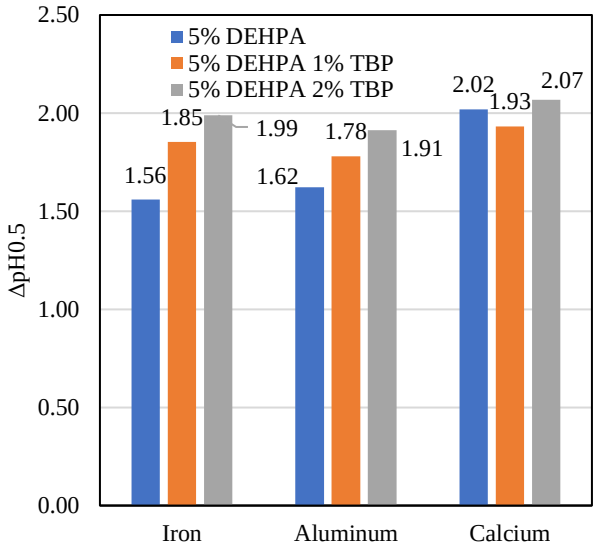

Figure 5.11 Differential $pH_{0.5}$ values for the REEs (**A**=lanthanum, **B**= gadolinium and **C**= yttrium) separation from the major contaminant elements when using 5% DEHPA only, and 5% DEHPA with 1% and 2% TBP.

5.6 FTIR studies on the mechanism of TBP addition on the DEHPA

FTIR analyses were used to assess the interaction of TBP with DEHPA and detect the change in the characteristic band structure of DEHPA due to the loading of metals during solvent extraction. The FT-IR spectrums of pure DEHPA and pure TBP are shown in Figure 5.12. Based on the literature review[81, 85], the peaks 1227 cm^{-1} and 1276 cm^{-1} were assigned to P=O stretching for DEHPA and TBP molecule, respectively. The peak for P-O-C stretching was identified to be the same for DEHPA and TBP at 1031 cm^{-1} (Table 5.1). The C=C stretching in both TBP and DEHPA was identified to be at 1460 cm^{-1}. There was an additional peak of O-H stretching at 1641 cm^{-1} for DEHPA, which was not present in the TBP spectra as the bond is not present in the TBP molecule.

Table 5.1 Fundamental wavenumber associated with vibration stretching of different bonds in DEHPA and TBP.

Characteristic vibration band	DEHPA	TBP

		(cm^{-1})
C=C ring stretching	1602	1602
P=O stretching	1227	1276
P-O-C stretching	1031	1031
O-H stretching	1641	N/A

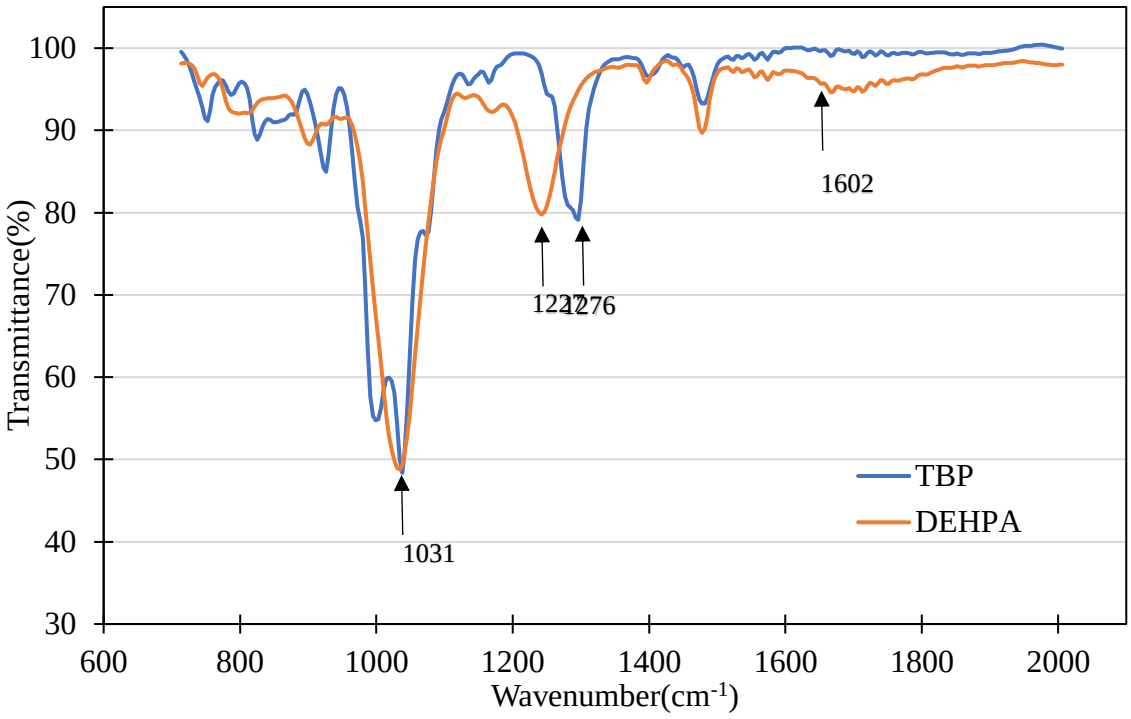

Figure 5.12 FTIR spectra of pure DEHPA and pure TBP.

DEHPA in non-polar diluents like kerosene exists as a dimer Figure 5.13 The addition of TBP is supposed to break the dimer structure of DEHPA to a certain degree and form an associated molecule (Figure 5.14) with DEHPA.

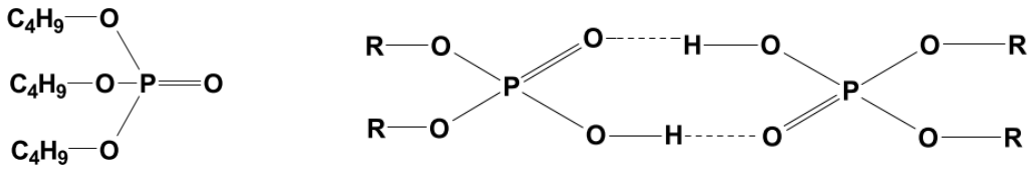

Figure 5.13 Structural formulae of TBP molecule and DEHPA molecule in dimer state.

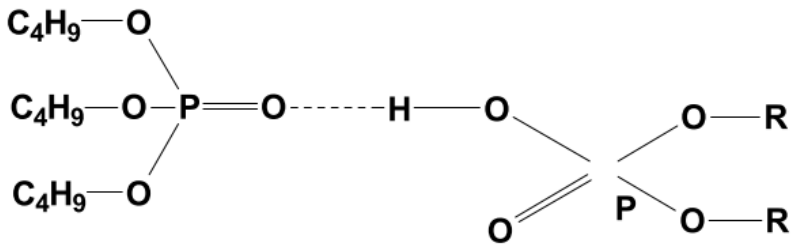

Figure 5.14 Structural formulae of associated molecule formed by hydrogen bonding of TBP and DEHPA molecules.

The FTIR analysis of the DEHPA-TBP mix (Figure 5.15) revealed that the P=O band associated with pure TBP vanished in the mix, and the intensity of the peaks associated with P=O, P-O-C, and O-H all decreased significantly. The finding was in agreement with observations reported from previous studies [79, 81, 85], which concluded that the increase in the transmittance can be attributed to the interaction of TBP with DEHPA.

Additionally, the decrease in the amount of DEHPA in the dimer form in the solution may cause the P-O bond to become shorter and subsequently result in the shift of the characteristic peak of P-O-C from 1033 cm^{-1} in pure DEHPA to 1049 cm^{-1} in the 5% DEHPA – 1 %TBP mixture. This serves as evidence of the formation of the associated molecule described in Figure 5.14. The formation of the associated molecule with TBP and reduction in the dimeric concentration of DEHPA can be used to explain the change in the extraction behavior of the metals when TBP is added to the organic phase.

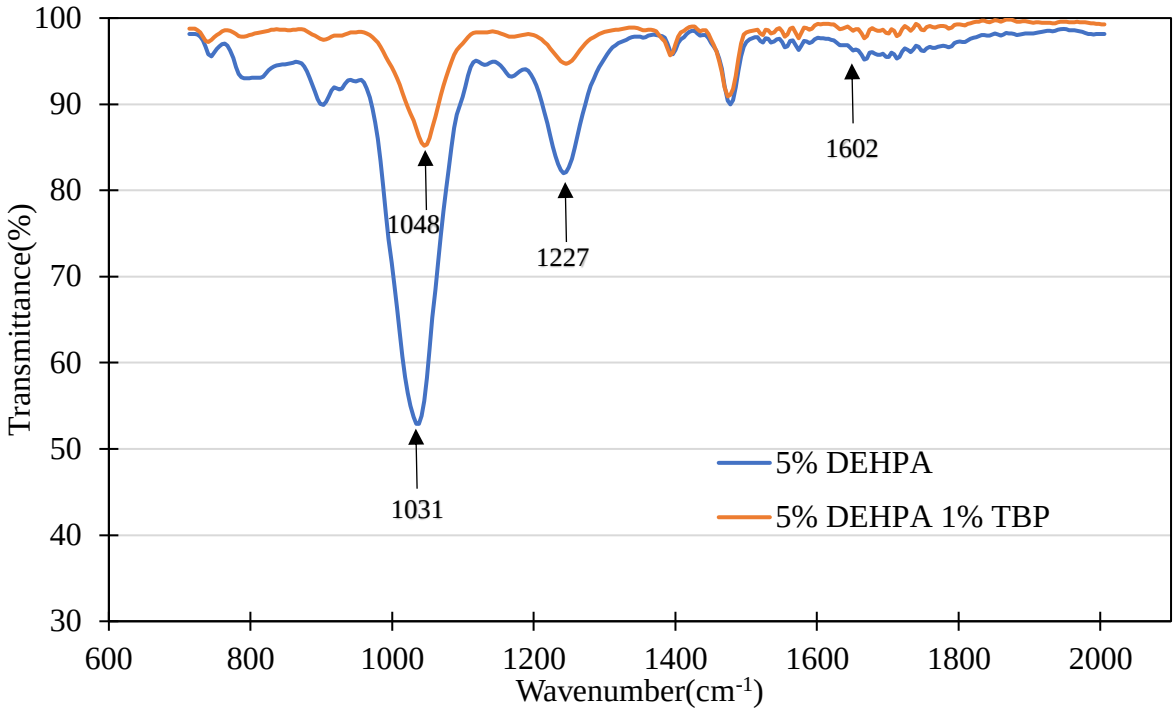

Figure 5.15 FTIR spectra of 5% DEHPA solution and 5% DEHPA solution with 1% TBP.

5.7 Conclusions

The use of TPB as an additive to DEPHA organic solutions in solvent extraction is common applied in industry for 1) synergistically improving the loading efficiency when treating metals like uranium, 2) enhancing phase separation characteristics and 3) reducing the formation of a third phase commonly referred to as 'crud'. However, the TBP application for enhancing the selectivity achieved on solutions having low concentrations of rare earth elements (i.e., <100 ppm) and high concentrations of contaminant elements is an original contribution as represented in this dissertation.

The findings of systematic solvent extraction studies aimed at quantifying the impact of TBP addition in a 5% by volume DEPHA organic solution on the extraction characteristics of representative REEs and contaminants were reported in this chapter. Extraction curves were developed for all elements for a system containing 5% DEHPA by volume in the organic phase with no TBP and two other systems that included 1% and 2% TBP as a phase modifier with

5% DEHPA by volume. The separation characteristics associated with the production of individual REE concentrates, as well as the production of a pure REE mix concentrate by the removal of the contaminant elements were studied. Additionally, the mechanism of TBP's effect on the extraction behavior of metals was investigated using FTIR analysis. The detailed findings of this chapter have been summarized as follows:

1) The addition of TBP had an anti-synergistic effect on the extraction characteristics of REEs, resulting in an increase in the $pH_{0.5}$ of the elements. In other words, the TBP addition reduced the loading capacity of the extractant, which is not typically desired when treating leach solutions having a relatively high REE content. However, in this study, the REE content in the feed leach solution is low while contaminant content is high. As such, extraction selectivity is a more significant issue. The $pH_{0.5}$ (= pH value corresponding to 50% metal extraction) of lanthanum increased from 1.03 to 1.32 upon addition of 1% TBP. For the same addition, the $pH_{0.5}$ increase for gadolinium was relatively small from 0.71 to 0.73 while $pH_{0.5}$ for yttrium increased from 0.05 to 0.20. In general, the incremental increase in the $pH_{0.5}$ resulting from the addition of 2% TBP was smaller than that observed after the addition of 1% TBP.
2) The addition of TBP resulted in a similar effect on the extraction curves of contaminant elements. The $pH_{0.5}$ of iron increased from 1.60 to 2.05 with the addition of 1% TBP, while the $pH_{0.5}$ value for aluminum was elevated from 1.67 to 1.97. The addition of TBP had a minimal impact on the extraction of calcium as indicated by an increase from 2.06 to 2.11. Similar to REEs, the increase in the $pH_{0.5}$ upon the addition of 1% TBP was more pronounced than that observed after the addition of 2% TBP. The formation of the DEHPA-TBP associated molecule after 1% TBP addition was more prominent, which was less pronounced for 2% due to reduced availability of free extractant concentration.
3) It was observed that an improved separation could be achieved between lanthanum and gadolinium as well as lanthanum and yttrium by adding at a 1% TBP by volume. The differential between the $pH_{0.5}$ values for the La-Gd separation increased from 0.32 to 0.59. Using the same conditions, the differential $pH_{0.5}$ value for the La-Y pair separation was enhanced from 0.99 to 1.12. The addition of 2% TBP did not result in

any additional benefit for the lanthanum-gadolinium separation. For the Gd-Y separation, separation characteristics was negative impacted by the TBP addition as indication by the $\Delta pH_{0.5}$ value reducing from 0.66-0.54. The separation characteristics between La and Y improved further as the $\Delta pH_{0.5}$ increased to 1.21. It was concluded that the addition of 1% TBP can improve the separation between lanthanum and gadolinium, and 2% TBP can improve the separation of lanthanum and yttrium, whereas the best separation efficiency for gadolinium-yttrium separation was achieved without TBP addition.

4) The addition of TBP resulted in improved separation of REEs from iron and aluminum. However, the separation between REEs and calcium was not improved upon the addition of TBP. However, typical acid leachate generated from coal sources contains significantly higher iron content relative to calcium. Thus, the addition of TBP can improve the overall contaminant rejection of the process.
5) FTIR studies revealed that the characteristic peak of the P-O bond shifted from 1033 to 1048 when TBP was added to the DEHPA solution. This finding may be due to the breaking of the DEHPA dimer, which caused shortening of the P-O bond. The shift in the peak due to the formation of DEHPA-TBP associated molecule results in reduced availability of DEHPA molecule in the organic phase, which can be used to explain the anti-synergistic effect of TBP on the extraction of metals with DEHPA.

6 PREDICTIVE THERMODYNAMIC MODEL FOR DISTRIBUTION COEFFICIENTS

6.1 Model Development

The mechanism of the solvent extraction reaction for any trivalent metal ion such as a Ln (lanthanide in this study) and a dimeric cation exchange extractant $(HG)_2$ (DEHPA in this study) can be described using the following expression [91]:

$$Ln^{3+} + 3(HG)_2 \leftrightarrow Ln(HG_2)_3 + 3H^+ \tag{6.37}$$

The corresponding equilibrium constant for this reaction can be written as

$$K_{ex} = \frac{|Ln(HG_2)_3||H^+|^3}{|Ln^{3+}||(HG)_2|^3} \tag{6.38}$$

The quantities in Eq. (6.2) within the | | are in the activities of the species. It is difficult to measure activities in a system directly. Therefore, to express the equilibrium constant in the form of concentrations, activity coefficients of the species involved must be included as shown in the following equation:

$$K_{ex} = \frac{[Ln(HG_2)_3][H^+]^3}{[Ln^{3+}] + [(HG)_2]^3} \times \frac{\gamma_{Ln(HG_2)_3}\gamma_{[H^+]}{}^3}{\gamma_{Ln^{3+}}\gamma_{[(HG)_2]}{}^3} \tag{6.39}$$

in which the quantities within [ ] represent the molar concentration, and γ represents the activity coefficient of the species. The reaction mechanism described above was determined by Peppard et al. [91] for tracer concentrations (<0.001M Ln concentration). At higher concentrations, mononuclear complexation of the lanthanide ions begins to dominate in the system[103, 115]. Due to complexation, lanthanides exist as Ln^{3+} species as well as LnX^{2+} and $LnX_2{}^+$ complexes. The formation of the lanthanide complexes with the anion X^- can be described as:

$$Ln^{3+} + X^- \leftrightarrow LnX^{2+} \tag{6.40}$$

$$Ln^{3+} + 2X^- \leftrightarrow LnX_2{}^+ \tag{6.41}$$

The thermodynamic stability constants for the complexes can be calculated as:

$$\beta_1 = \frac{|LnX^{2+}|}{|Ln^{3+}||X^-|} \tag{6.42}$$

$$\beta_2 = \frac{\left|LnX_2^{+}\right|}{|Ln^{3+}||X^{-}|^2} \tag{6.43}$$

As shown by Marcus[137], the LnX_2^+ starts to dominate in the aqueous phase only at ionic strength >8M, while LnX^{2+} occurs at even lower ionic strengths (i.e., 1M). Therefore, only β_1 will be considered for further calculations in this study and will be referred to as β.

The stability constant of LnX^{2+}can be expressed in terms of the concentration of the ionic species by including the activity coefficient as:

$$\beta = \frac{[LnX^{2+}]}{[Ln^{3+}][X^{-}]} * \Gamma \tag{6.44}$$

where Γ is the ratio of the activity coefficients of the ionic species and can be expressed as

$$\Gamma = \frac{\gamma_{Ln^{3+}}\gamma_{X^-}}{\gamma_{LnX^{2+}}}. \tag{6.45}$$

It follows that the concentration of the complex LnX^{2+} can be expressed in terms of the stability constant and the equilibrium concentration of the Ln^{3+} ion and Cl^- as follows

$$[LnX^{2+}] = \beta * [Ln^{3+}][X^{-}] \times \Gamma. \tag{6.46}$$

The distribution coefficient D of metal is defined as the ratio of total metal concentration in the organic phase to the total metal concentration in the aqueous phase, i.e.:

$$D = \frac{[Ln]_{org}}{[Ln]_{aq}}. \tag{6.47}$$

The total metal concentration in the aqueous phase is represented by $[Ln]_{aq}$, while the total metal concentration in the organic phase is represented by $[Ln]_{org}$. The assumption in the current model is that the total concentration of the lanthanide present in the aqueous phase is the sum of the concentrations of the Ln^{3+} and LnX^{2+} species, i.e., there are no other species of Ln present in the solution. Therefore, the distribution coefficient can be expressed as:

$$D = \frac{[Ln(HG_2)_3]}{[Ln^{3+}] + [LnX^{2+}]}. \tag{6.48}$$

By combining Eqs. (6.10) and (6.12), the distribution coefficient becomes:

$$D = \frac{[Ln(HG_2)_3]}{[Ln^{3+}]} * \frac{1}{(1 + \beta\Gamma[X^-])} \quad (6.49)$$

The term $\frac{1}{(1+\beta\Gamma[X^-])}$ is also known as the degree of formation (α) of the complex [113]. The degree of formation of a complex is a function of the stability constant, the ratio of the activity coefficients, and the concentration of the anionic species in the solution, i.e.:

$$\alpha = \frac{1}{(1 + \beta\Gamma[X^-])}. \quad (6.50)$$

The distribution coefficient, therefore, can be expressed in terms of the equilibrium constant, degree of freedom, concentrations and activity coefficients of the species as follows:

$$D = \frac{\alpha\,[(HG)_2]^3\,\gamma_{Ln^{3+}}\,{\gamma_{(HG)_2}}^3}{[H^+]^3{\gamma_{H^+}}^3\,\gamma_{(Ln(HG_2)_3)}} K\,. \quad (6.51)$$

The activity coefficients of the aqueous species can be estimated using different models. However, the activity coefficients in the organic species are difficult to calculate using existing models directly. Therefore, the activity coefficients of the organic species, i.e., the extractant and the metal-extractant complex, are combined with the thermodynamic equilibrium constant and expressed as:

$$K' = K\frac{{\gamma_{(HG)_2}}^3}{\gamma_{(Ln(HG_2)_3)}} \quad (6.52)$$

in which K' is the apparent equilibrium constant for the reaction. The simplified distribution coefficient becomes:

$$D = \frac{\alpha\,[(HG)_2]^3\,\gamma_{Ln^{3+}}}{[H^+]^3{\gamma_{H^+}}^3} K'. \quad (6.53)$$

In the previous attempts [95, 113, 117] to develop a predictive model, the ratio of activity coefficients in the organic phase $\gamma_{(HX)_2}$ and $\gamma_{(LnHX_2)}$ were assumed to be constant, which results in the apparent equilibrium constant to be constant as well per the following expression:

$$\log D = \log\alpha + 3\log[(HG)_2)] + \log\,\gamma_{Ln^{3+}} - (3\log[H^+] + 3\log\gamma_{H^+}) + \log K' \quad (6.54)$$

However, in the current study, experimental data (Figure 6.3) showed that the apparent equilibrium constant is not a constant and varies as a function of the free extractant concentration in the organic phase as indicated by the following expression:

$$\log K' = \log K + \lambda * [(HG)_2]. \quad (6.55)$$

Consequently, the model equation for the distribution coefficient in logarithm form can be expressed in terms of the apparent extraction coefficient as:

$$\log D = \log\alpha + 3\log[(HG)_2)] + \log \gamma_{Ln^{3+}} - (3\log[H^+] + 3\log\gamma_{H^+}) + \log K + \lambda * [(HG)_2] \quad (6.56)$$

As shown in Eq. (6.20), five different parameters are required for the estimation of the distribution coefficient including:

1. Degree of formation (α): The parameter is dependent on the thermodynamic stability constant of the complex and the anionic concentration in the aqueous phase;

2. The concentration of H^+: The concentration of the hydrogen ions is dependent on the initial concentration of acid and the amount of the metal that is extracted into the organic phase. Every molecule extracted releases 3 molecules in the aqueous phase;

3. The dimeric concentration of the extractant ($[(HG)_2]$): The parameter is a function of the initial extractant concentration and the amount of metal which is extracted in the organic phase;

4. Activity coefficients of the aqueous species: The aqueous species present in the solution (Ln^{3+}, $LnCl^{2+}$, Cl^-, and H^+) are required for the estimation of the distribution coefficient. As the solution which is being studied is non-ideal, therefore an activity model based on the Debye-Huckel equation (Bromley approximation) was used for estimation of the coefficients; and

5. Equilibrium constant: The equilibrium constant along with the constant λ is required for the calculation using experimental data. The quantities are constant for a given metal-extractant combination.

Of these parameters, the equilibrium constant and the constant λ must be calculated experimentally for each system. The stability constant for lanthanide systems has been calculated by several researchers and are in relatively good agreement. Therefore, the values in literature can be directly used in the model. The other parameters, i.e., the extractant concentration, aqueous concentrations, and activity coefficients, can be calculated using the initial conditions (i.e., the initial extractant concentration, initial acid concentration, and initial salt concentration) which the model uses as input data.

6.2 Parameters of the Predictive Model

6.2.1 Thermodynamic Stability Constants

Extensive studies have been conducted by multiple researchers [101-103, 138] for the calculations of the stability constants for lanthanide ions in chloride and nitrate media. The stability constants are calculated by measuring any property of the complex as a function of the ligand in the solution. The stability constants were calculated by Peppard et al.[103] using the extraction of the lanthanide ions in chloride and nitrate media. The distribution coefficient, as described in the previous section, can be expressed as

$$D = K\frac{[(HG)_2]^3}{[H^+]^3}\,\frac{1}{(1+\beta[X^-])} \tag{6.57}$$

For the hypothetical solution for which the X^- concentration is 0, the distribution coefficient can be described as:

$$D_o = K\frac{[(HG)_2]^3}{[H^+]^3}. \tag{6.58}$$

Rearranging Eq. (6.21) and substituting 6.22:

$$\frac{1}{D} = \frac{1}{D_o} + \frac{\beta}{D_o}[X^-] \tag{6.59}$$

The variation of 1/ D with the X^- ion concentration can be studied to yield the stability constant of the complex. The intercept of the plot equals $1/D_o$ and the slope β/D_o. Both the quantities can be used to calculate the stability constant of the complex (β).

In his study, Peppard et al. [103] calculated the stability constants of 7 lanthanides (lanthanum, cerium, praseodymium, europium, thulium, and ytterbium) using the method described above. The results from the study are shown in Table 6.1.

Table 6.1 Stability constants for nitrate and chloride complexes of selected lanthanides

Element	Stability constants	
	Chloride media	**Nitrate Media**
Lanthanum	0.9±0.3	1.3±0.3
Cerium	0.9±0.3	1.3±0.3
Praseodymium	0.9±0.3	1.7±0.3
Europium	0.9±0.3	2.0±0.3
Thulium	0.8±0.2	0.7±0.2
Ytterbium	0.6±0.2	0.6±0.2
Lutetium	0.4±0.3	1.8±0.3

6.2.2 Species Concentration and Activity Coefficients

The aqueous solutions in this study have high ionic strengths (typically >1M). As such, the deviations from the thermodynamic ideality must be considered for determining the thermodynamic direction of the reactions. The movement of ions along the phase boundary is an example. Hence, the activity coefficients (γ) of the species must be calculated. As shown in Eq. (6.20), the predictive model requires the estimation of activity coefficients of the aqueous species (Ln^{3+}, $LnCl^{2+}$, and H^+).

Many methods have been developed to estimate the activity coefficients of electrolyte solutions. Debye-Huckel, Bronsted-Guggenheim, Bromley, Davies, and Pitzer methods are the ones most commonly used depending on the system requirement. The ionic interactions in any aqueous solutions can be divided into two groups: i) Long-range interactions, the attractive electrostatic interactions between the ions of opposite charges, and ii) short-range interactions

that occur between ions and molecules or between two molecules. The long-range interactions dominate the non-ideality in dilute solution, whereas the short-range interactions should be taken into account at higher concentrations.

In this study, the Bromley model was used for estimation of the activity coefficients as it takes into account both short- and long-range interactions. The model is empirical in nature as opposed to the Pitzer model, which is based on statistical mechanical equations. As such, the model requires a large number of parameters that make the implementation in the predictive model cumbersome. The Bromley equation is accurate in ionic strengths of less than six molalities. As the solution strengths modeled in this study are typically less than 6 M, the Bromley approximation is accurate in the domain for which the model is developed. The equation is useful for the systems used in this study, as it contains only one interaction parameter and therefore is simple from the computational point of view. The model is based on molal concentrations and was converted to molar terms to be used in the predictive model. The model can be expressed as:

$$\log \gamma_i = \frac{AZ_i^2 I^{\frac{1}{2}}}{1 + I^{\frac{1}{2}}} + \sum_j \left\{ \left(\frac{(0.06 + 0.6B_{ij})|Z_i Z_j|}{(1 + \frac{1.5}{|Z_i Z_j|} I)^2} + B_{ij} \right) \left(\frac{|Z_i| + |Z_j|}{2} \right)^2 M_j \right\} \quad (6.60)$$

in which γ is the activity coefficient for the i^{th} species, A the Debye Huckel constant, which is 0.5105 as converted for the molar basis, Z_i the charge on the i^{th} species, B is the interaction term between the anion and cationic species in the solution, I is the ionic strength of the solution and M is the molarity of the salt in the solution.

The interaction term B for lanthanides in the chloride systems were calculated by Bromley [139] as shown in Table 6.2. In this study, the interaction parameters associated with $LnCl^{2+}$ are assumed the same as that of Ln^{3+} as reported by the experimental data presented in the study.

Table 6.2 List of the Bromley interaction parameters for the lanthanide chloride salts, calculated using the equilibrium data published by Bromley[139].

Rare Earth Salt	Interaction Parameter, B	Standard Deviation
$LaCl_3$	0.08221	0.007
$PrCl_3$	0.08121	0.006
$NdCl_3$	0.08021	0.007
$SmCl_3$	0.08121	0.007
$EuCl_3$	0.08521	0.007
$GdCl_3$	0.08721	0.006
$TbCl_3$	0.08221	0.006
$DyCl_3$	0.08121	0.007
$HoCl_3$	0.08021	0.007
$ErCl_3$	0.0974	0.007
$TmCl_3$	0.0963	0.006
$YbCl_3$	0.0960	0.006
$LuCl_3$	0.0967	0.007
YCl_3	0.0982	0.006

The activity coefficients and concentrations in the system in the current study are inter-related, i.e., the activity coefficients in the Bromley model is dependent on the concentration of the species (Eq. 6.24) present in the aqueous solution. Simultaneously, the concentration of the species is dependent on the activity coefficient (Eqs. 6.7 and 6.8).

For the calculation of the concentration of the aqueous species, i.e., $LnCl^{2+}$, $Ln^{3+,}$ and Cl^{-}, as well the activity coefficients of the species, activity coefficients of all the species can be assumed to be unity. Subsequently, the concentration of the species is calculated based on the following equations:

$$[\mathrm{Cl}] = [\mathrm{LnCl}^{2+}] + [\mathrm{Cl}^{-}] \tag{6.61}$$

$$[\mathrm{Ln}] = [\mathrm{LnCl}^{2+}] + [\mathrm{Ln}^{3+}] \tag{6.62}$$

$$\beta = \frac{[\mathrm{LnCl}^{2+}]}{[\mathrm{Ln}^{3+}][\mathrm{Cl}^{-}]} * \frac{1}{\Gamma} \tag{6.63}$$

The quantities $[\mathrm{Cl}]_{\mathrm{total}}$, $[\mathrm{Ln}]_{\mathrm{total}}$, and β are known for the given system, and the ratio of the activity coefficients(Γ) can be calculated based on the initial guess. Therefore, the three unknowns, $[\mathrm{LnCl}^{2+}]$, $[\mathrm{Ln}^{3+}]$, and $[\mathrm{Cl}^{-}]$, can be calculated using the system of three equations. The solution of the equation after simplification and rearranging is:

$$[\mathrm{Ln}^{3+}] = \frac{-(\beta\Gamma([\mathrm{Cl}] - [\mathrm{Ln}])) + 1) + \sqrt{(\beta\Gamma([\mathrm{Cl}] - [\mathrm{Ln}])) + 1)^2 + 4[\mathrm{Ln}] * \beta\Gamma}}{2\beta\Gamma} \tag{6.64}$$

$$[\mathrm{Cl}^{-}] = \frac{-(\beta\Gamma([\mathrm{Cl}] - [\mathrm{Ln}])) + 1) + \sqrt{(\beta\Gamma([\mathrm{Cl}] - [\mathrm{Ln}])) + 1)^2 + 4[\mathrm{Ln}] * \beta\Gamma}}{2\beta\Gamma} + [\mathrm{Cl}] - [\mathrm{Ln}] \tag{6.65}$$

$$[\mathrm{LnCl}^{2+}] = [\mathrm{Ln}] - \frac{-(\beta\Gamma([\mathrm{Cl}] - [\mathrm{Ln}])) + 1) + \sqrt{(\beta\Gamma([\mathrm{Cl}] - [\mathrm{Ln}])) + 1)^2 + 4[\mathrm{Ln}] * \beta\Gamma}}{2\beta\Gamma} \tag{6.66}$$

The calculated concentrations were used to quantify the activity coefficients as described in the Eqs. (6.19) -(6.22). The process was iterated using an iterative loop in the program. For the calculation of the concentrations and the activity coefficients, the iterative program code was developed in Python 2.7.1. The procedural logic for the program is shown in Figure 6.1.

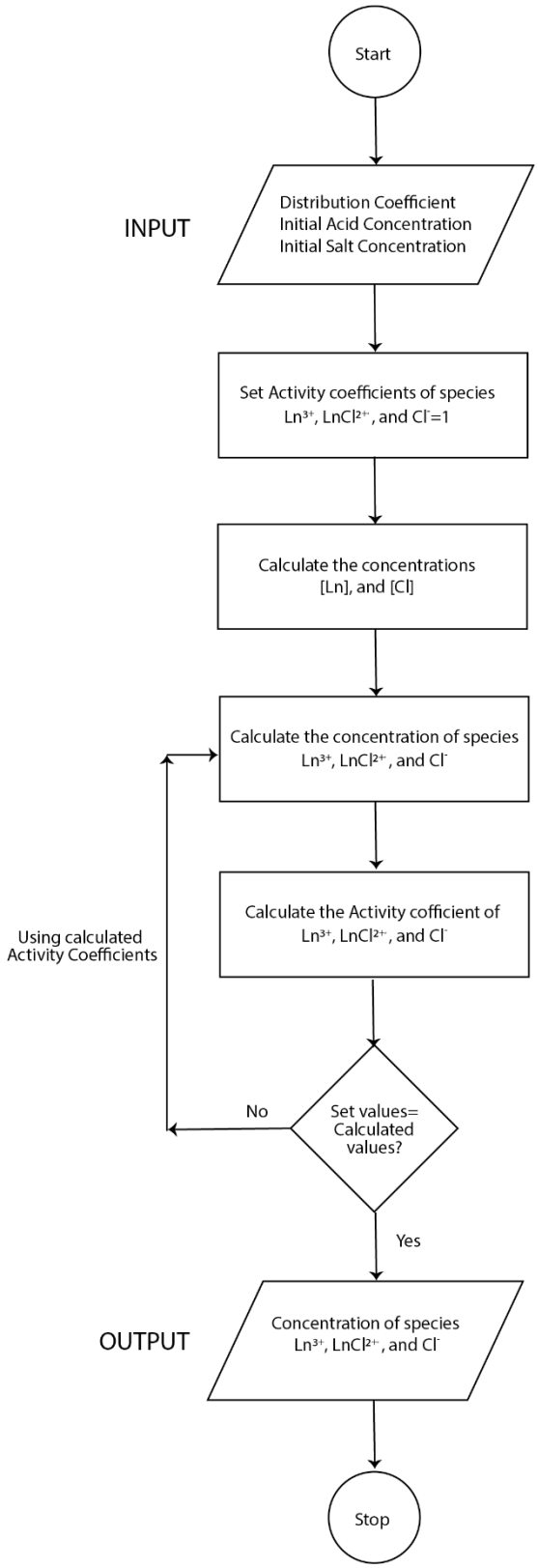
Start
INPUT
Distribution Coefficient
Initial Acid Concentration
Initial Salt Concentration
Set Activity coefficients of species
Ln^{3+}, $LnCl^{2+}$, and Cl^{-}=1
Calculate the concentrations
[Ln], and [Cl]
Calculate the concentration of species
Ln^{3+}, $LnCl^{2+}$, and Cl^{-}
Calculate the Activity cofficient of
Ln^{3+}, $LnCl^{2+}$, and Cl^{-}
Using calculated
Activity Coefficients
No
Set values=
Calculated
values?
Yes
OUTPUT
Concentration of species
Ln^{3+}, $LnCl^{2+}$, and Cl^{-}
Stop

Figure 6.1 Procedural flowchart for the calculation of the concentration and the activity coefficient of the aqueous species.

6.2.3 Equilibrium Constant Calculation

The last parameter in the model, the equilibrium constant, depends on the reaction of metal with the organic extractant and can be estimated by regression of experimental data and curve fitting. As discussed previously, it is assumed in the model that the apparent equilibrium constant is a function of the free extractant concentration, as expressed in Eq. (6.18). Therefore, a plot of log(K') with the log([$(HG)_2$] yields the two quantities log K and λ by the slope and the intercept of the regression equation, respectively.

6.3 Computer Program for Predictive Model

The model was developed in python IDLE 2.7.1. The execution of the model was based on the procedural flowchart shown in Figure 6.2.

The code was developed in three sections, i.e.: 1) a function block for calculation of the activity coefficients, 2) another function block for calculation of the concentration of the aqueous species, and 3) the main block where the distribution function was calculated using the model equation. The main block utilized iterative loops to estimate the value of the distribution coefficient.

The initial system conditions, i.e., the concentration of the salt solution, the initial concentration of the acid, and the free extractant concentration, were utilized as input from the user. The quantities $[H^+]$, $[Cl^-]^T$, $[Ln]^T$, and $[(HG)_2]^O$ were calculated based on the initial guess of the distribution coefficient using the following:

$$[(HG)_2] = \frac{[HG]}{2} - 3[Ln(HG_2)_3] \tag{6.67}$$

$$[H^+] = [HCl] + 3 * [Ln(HG_2)_3] \tag{6.68}$$

$$[Cl] = [HCl] + 3[LnCl_3] \tag{6.69}$$

$$[\mathrm{Ln}] = \frac{1}{1+\mathrm{D}}([\mathrm{LnCl_3}]) \tag{6.70}$$

The concentration of the aqueous species and the activity coefficients are calculated as described in the previous section. The values were subsequently plugged into the model equation, and the distribution coefficient was calculated. The distribution coefficient was incrementally increased from the initial guess (D=0) until the value obtained from the model converged with the set value.

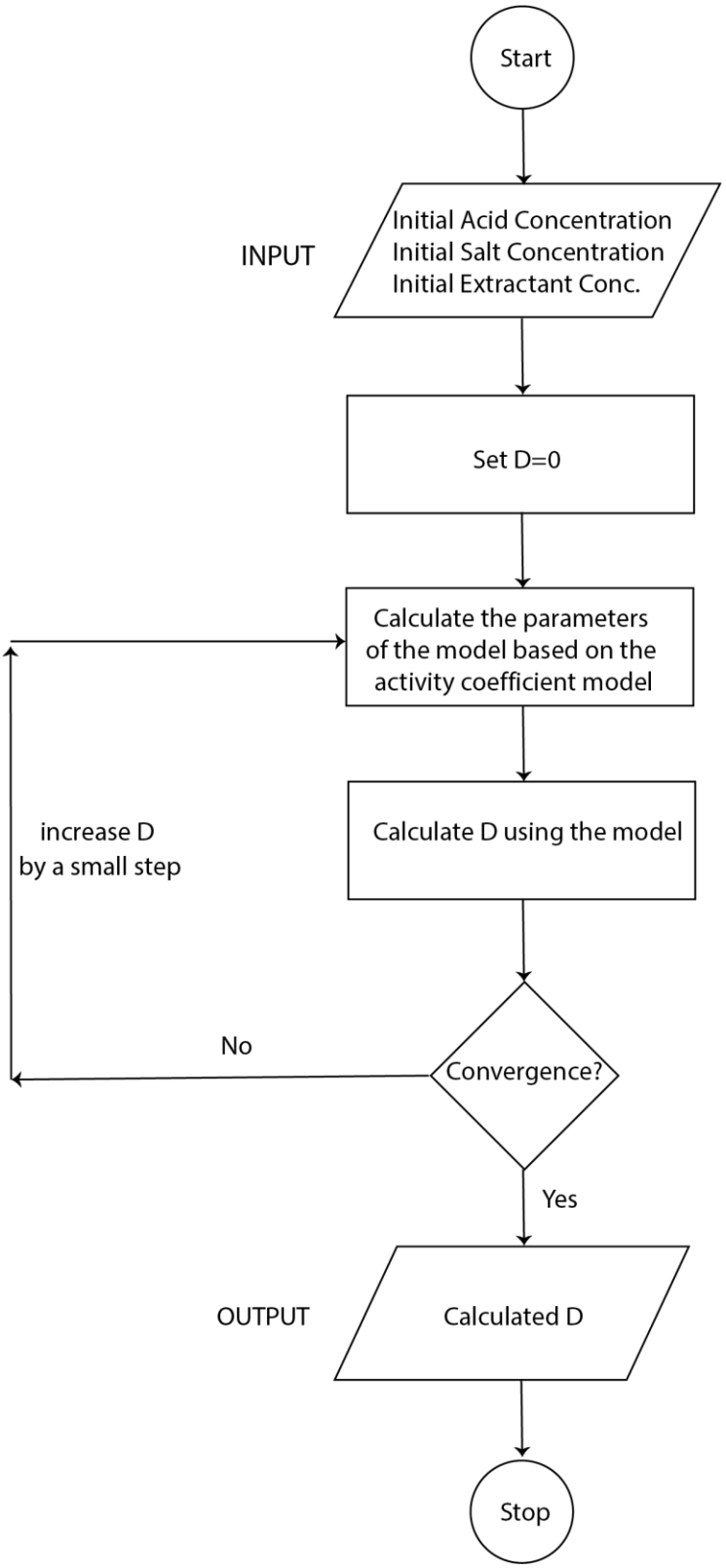

Figure 6.2 Procedural flowchart for the calculation of the distribution coefficient.

6.4 **Results**

The model developed was tested on the $LaCl_3$-HCl-DEHPA system. The equilibrium data was generated for test solutions of different concentrations of lanthanum chloride (0.025M to 0.133M) by 1M solution of DEHPA in kerosene using the extraction method described in the materials and methods section. The apparent equilibrium constant was calculated for each test condition (Table 6.2). It was observed that the apparent equilibrium constant was not constant for all conditions and decreased from 0.79 for a 0.133M solution to 0.22 for a 0.025M solution.

To calculate the equilibrium constant and the constant λ, the variation of Log K' was plotted with the DEHPA concentration in the organic phase (Table 6.3). Using the slope and the intercept of the trendline, it was ascertained that the equilibrium constant (log K) for the reaction is 2.3289 and the constant C calculated to be -4.8279.

Table 6.3 Experimental data for calculation of equilibrium constant and constant λ

$[Ln]_{org}$	$[Ln]_{aq}$	log D	Log $[(HG)_2]$	Log K'
57.53	75.87	-0.12	-0.48	0.79
47.99	46.68	-0.08	-0.46	0.62
43.19	30.65	0.15	-0.43	0.51
35.79	14.66	0.39	-0.41	0.46
20.97	4.18	0.70	-0.36	0.22

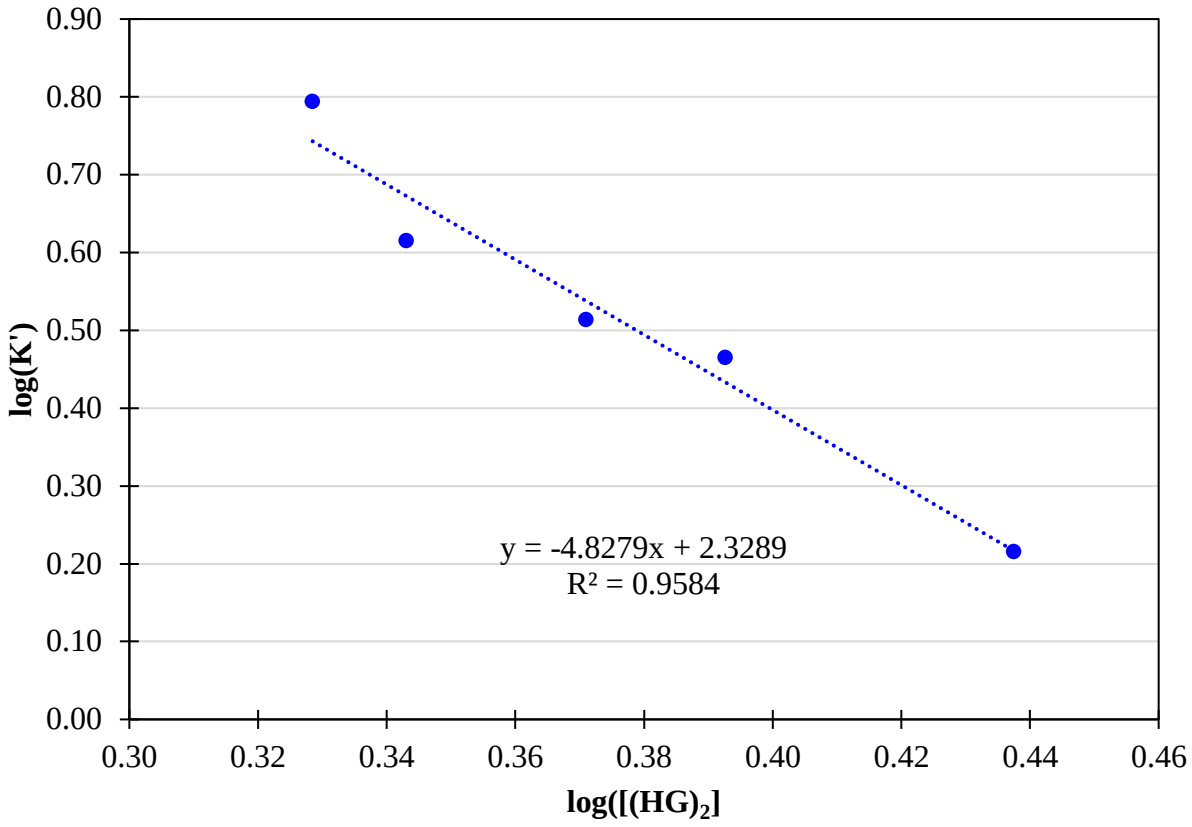

Figure 6.3 Experimental calculation of equilibrium constant and the constant λ using curve fitting.

The model required three initial conditions as input, i.e.: 1) the initial salt concentration, 2) the initial acid concentration, and 3) the initial extractant concentration. As shown in Figure 6.4, the program calculates the distribution coefficient and the set value of the distribution coefficient (initially zero) is increased with each iteration. The program ends when the calculated distribution coefficient becomes equal to the set value of the distribution coefficient. The value of the set distribution coefficient was incrementally increased by a value of 0.001 with each iteration, and the values converged in the displayed example in about 50000 iterations. For a more precise prediction, the increment value can be further reduced. However, the execution of the code will become computationally extensive.

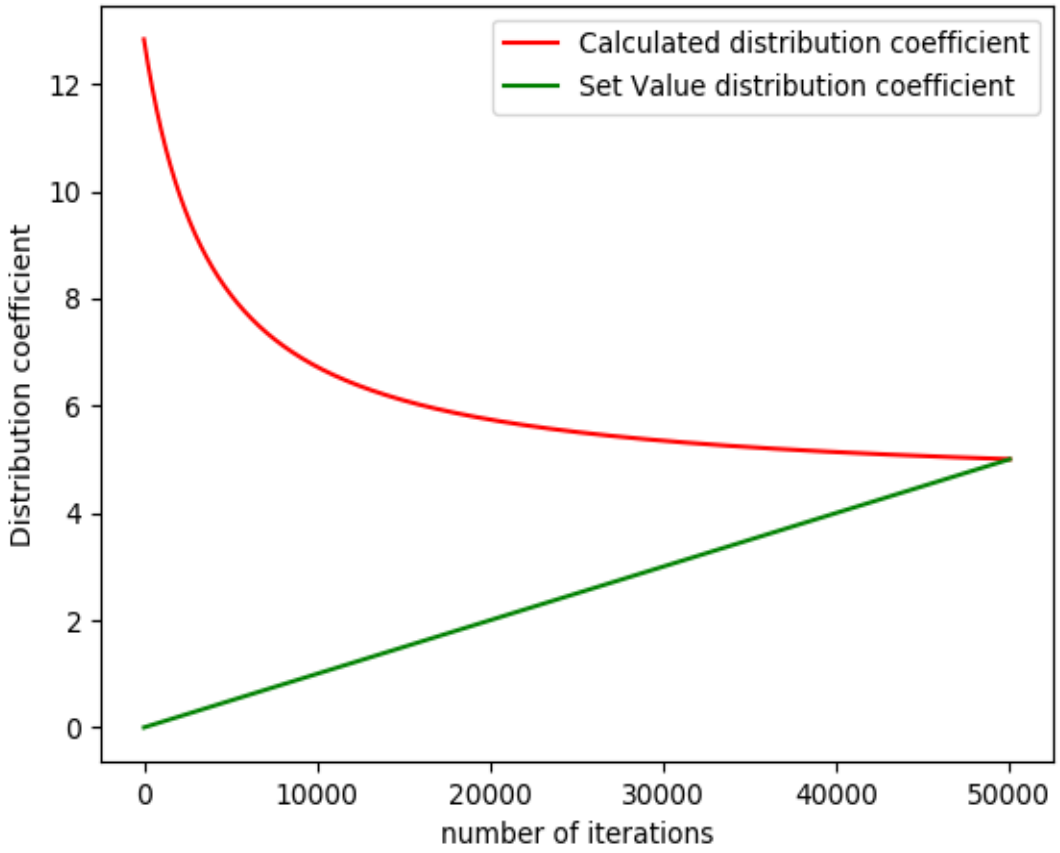

Figure 6.4 Variation of the set value and the calculated value of the distribution coefficient with the number of iterations.

The predictive model was tested on different initial conditions and the values validated by the experimental data. The predicted values followed the measured values very closely, and the correlation coefficient between the two values was 0.996 with an R^2 value of 0.995 (Figure 6.5)

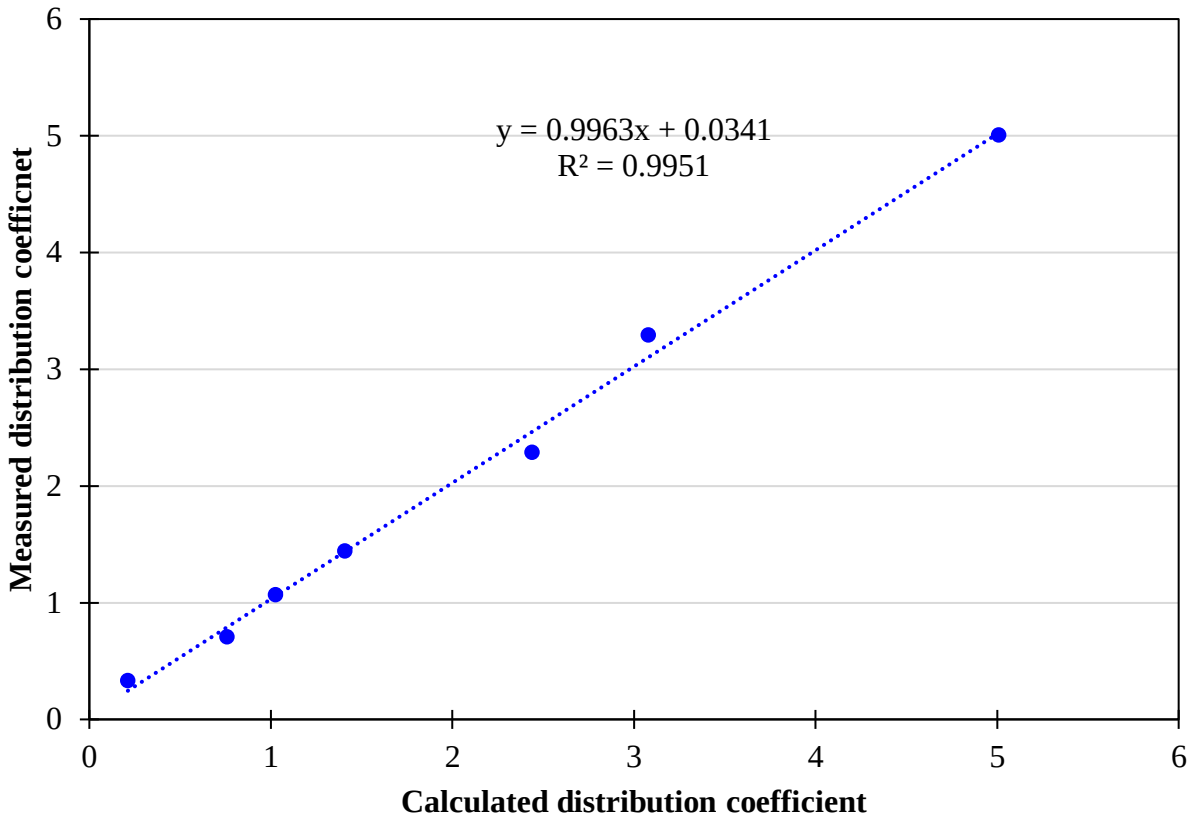

Figure 6.5 Comparison of calculated and predicted distribution coefficient by the model.

6.5 Conclusions

In this chapter, the development of a predictive thermodynamic model was presented and discussed, which used the initial conditions of the extraction system (acid concentration, extractant concentration, and salt concentration) to predict the distribution coefficient of any trivalent metal using a cation exchange extractant. This development is a unique contribution provided by the research effort presented in this chapter. The model considered the mononuclear complexation behavior of lanthanides as well as the non-ideality of the aqueous species by estimation of the activity coefficients using the Bromley approximation. The non-ideality of the organic phase was incorporated in the model using the apparent equilibrium constant of the reaction. The parameters required in the model were calculated for validation purposes for the $LaCl_3$-HCl-DEHPA system. The model was then used for the prediction of distribution coefficients for different initial conditions. The specific developments from the study include:

1. A predictive model was developed using the equilibrium reaction mechanism of solvent extraction and the complexation mechanism of the lanthanide ions in the aqueous system. The model was implemented using a computer program developed in Python 2.7.1 platform and used iterative calculations to estimate the distribution coefficient of the metal.
2. The activity coefficients, along with the concentrations of the aqueous species in the system, were estimated using the Bromley approximation, which uses a single interaction parameter and is accurate in the ionic strengths < 6M. An iterative computer program developed in Python 2.7.1 was used to calculate the quantities based on the approximation.
3. The apparent equilibrium constant of the reaction was calculated using the experimental data. The equilibrium constant and the constant λ in the model were calculated by curve fitting of the experimental data. The value of the equilibrium constant for the $LaCl_3$-HCl-DEHPA system was calculated to be 2.3289, and the λ constant was calculated to be -4.8279.
4. The distribution coefficients predicted by the model were compared to the experimental data. The predicted values were determined to be statistically accurate for the given system.
5. Unlike previous models developed by O Brien[113], Hoh[95] and Nevarez[114] which require certain quantities at equilibrium to predict the distribution coefficient, the model developed from this study requires the initial conditions of the system i.e. salt concentration, acid concentration and extractant concentration, as inputs and therefore can be used for process design and modelling. The model also incorporates the thermodynamic non-idealities in the organic phase by the activity coefficients, which was considered to be constant in the previous model.

7 CONCLUSIONS

Solvent extraction for the purpose of REE recovery from pregnant leach solutions (PLS) obtained from coal-based sources was systematically studied in this research project. The study involved the testing of solvent extraction processes and circuits at both bench-top and pilot plant scales. A novel solvent extraction process (U.S. Utility Patent Application Serial No. 16/534,738) was developed to concentrate the REEs and reject the contaminants from a PLS containing very low concentration of REEs and relatively high concentration of contaminants. The impacts of various process parameters were evaluated through laboratory tests performed on a model solution prepared from salt solutions based on the contents of PLS generated from coal sources. The process developed was tested on a PLS generated from coal-based source on a continuous basis using bench-top and pilot-scale equipment. As part of process enhancement efforts, the impact of tributyl phosphate (TBP) addition to a di-(2-ethylhexyl)phosphoric acid (DEHPA) organic solution on the extraction characteristics of rare earth and associated contaminant metals and the effect on process selectivity was studied in detail using extraction tests and FTIR analysis. Finally, a thermodynamic model was developed for prediction of distribution coefficient of lanthanides from a cation exchange extractant. The model utilized the initial conditions of the system to estimate the lanthanide complexation and the activity coefficients of the species in both aqueous and organic phases to calculate the distribution coefficient. The detailed findings of the dissertation are listed as follows:

1. The extraction tests performed on the test solution indicated that for A;O ratio of 1:1, the optimal decontamination ratio occurred at pH 2.0. The concentration of DEHPA in the organic phase had little effect on the decontamination ratio. Iron rejection from the PLS was enhanced by reducing the iron from ferric to ferrous state by addition of ascorbic acid as a reducing agent. The optimum reduction of iron was calculated at an ORP value of 400 mV.

2. Calcium co-extracted in the organic phase can be selectively scrubbed out using a mild acid. However, the selectivity of calcium rejection diminishes at higher concentrations

of acid. 70% of the calcium co-extracted in the organic phase was rejected using 0.1 M HCl solution while losing 4.2% lanthanum from the solution.

3. Due to the very high relative concentration of contaminants in the PLS, the SX process was performed in two cycles, rougher and cleaner, to reduce the contaminant concentration sufficiently low for the selective precipitation to be viable. PLS from six different coal sources were processed by the SX process to remove the contaminants and the REE were precipitated as oxalates, which were roasted to produce the REO concentrate. Over 97% REO by weight were produced from each of the source tested.

4. Scandium exhibited very poor stripping efficiency using acid stripping from DEHPA, which results in low concentrations of scandium in the REO produced from PLS from coal sources. Two alternative methods for recovery of scandium, saponification of the organic phase, and use of an alternate extractant Cynex 272, were tested in the study. 8.09% stripping efficiency of scandium was achieved using saponification from 2M NaOH. Whereas 69.3% stripping efficiency was achieved using 2M H_2SO_4 acid Cynex 272 solution.

5. The SX process developed was evaluated on a pilot-scale continuous circuit. A 94.5 % by weight REO was produced by treated heap leachate generated from coarse refuse coal of Dotiki coal processing plant.

6. The addition of TBP as a phase modifier had an anti-synergistic effect on the extraction characteristics of REEs, resulting in an increase in the $pH_{0.5}$ of the elements. The extraction tests indicated that the addition of 1% TBP can improve the separation between lanthanum and gadolinium as the $\Delta pH_{0.5}$ for La-Gd pair increased from 0.32 to 0.59. Addition of 2% TBP can improve the separation of lanthanum and yttrium $\Delta pH_{0.5}$ for La-Y pair increased from 0.99 to 1.21, whereas the best separation efficiency for gadolinium-yttrium separation was achieved without TBP addition as the $\Delta pH_{0.5}$ for Gd-Y pair was 0.66 and it decreased to 0.62 upon addition of TBP.

7. The addition of TBP resulted in a similar effect on the extraction curves of contaminant elements. The $pH_{0.5}$ of iron increased from 1.60 to 2.05 upon addition of 1% TBP, while for the same addition, $pH_{0.5}$ of aluminum saw an increase from 1.67 to 1.97. The addition of TBP resulted in improved separation of REEs with iron and aluminum. However, the separation of REEs with calcium got poorer upon the addition of TBP. However, typical acid leachate generated from coal sources contains iron in much higher quantities as compared to calcium, and therefore, the addition of TBP can improve the overall contaminant rejection of the process.

8. FTIR studies revealed that the characteristic peak of the P-O bond shifted from 1033 cm^{-1} to 1048 cm^{-1} when TBP was added to the DEHPA solution. This was theorized to be because of the breaking of the DEHPA dimer, which caused the P-O bond to get shorter. The shift in the peak due to the formation of DEHPA-TBP associated molecule can be used to explain the anti-synergistic effect of TBP on the extraction of metals with DEHPA.

9. A thermodynamic model was developed using the equilibrium reaction mechanism of solvent extraction and the complexation mechanism of the lanthanide ions in the aqueous system. The model incorporated the thermodynamic non-idealities in the aqueous phase by the activity coefficients using the Bromley approximation which uses a single interaction parameter and is accurate in the ionic strengths < 6M. An iterative computer program developed in Python 2.7.1 was used to calculate the quantities based on the approximation. The non-idealities in the organic phase were incorporated by assuming that the ratio of the activity coefficients in the organic phase are a function of the dimeric concentration of the free extractant in the organic phase.

10. The apparent equilibrium constant of the reaction was calculated using the experimental data. The equilibrium constant and the constant λ in the model were calculated by curve fitting of the experimental data. The value of the equilibrium constant for $LaCl_3$-HCl-DEHPA system was calculated to be 2.3289 and λ constant was calculated to be -4.8279.

11. The distribution coefficients predicted by the model was compared to the experimental data and the predicted values were in very close agreement with the experimentally determined values with the correlation coefficient between the predicted and measured values being 0.996.

12. The successful development of a model to predict the distribution coefficients for a solvent extraction system based on feed solution characteristics is a unique contribution that could lead to more efficient process circuit being used and operated. The extensive experimental work typically needed to determine the distribution coefficients for a given system will no longer be needed resulting in a significant reduction in costs and a more detailed set of data being generated.

8 RECOMMENDATIONS FOR FUTURE STUDIES

The current study focused on developing a solvent extraction process for rejection of contaminants from PLS generated from coal-based sources as well as the impact of TBP as a phase modifier on the extraction behavior of REEs as well as contaminants. The impact was studied on three rare earth elements, lanthanum, gadolinium and yttrium, and there is a requirement of additional testing for studying the impact on other rare earth elements. A thermodynamic model incorporating the lanthanide complexation as well as the non-idealities in the aqueous and organic phase was developed to predict the distribution coefficients of the lanthanides using a cation exchange extractants. However, the model is currently developed for a single species and additional efforts should be made for extension of the model for multi-component solutions. Specific suggestions for future studies are as follows:

1. The continuous flowsheet developed for REE recovery from the coal based sources should be tested on PLS from different sources to validate the results obtained from the coal based sources. Additionally, testing on a continuous basis should be performed on use of Cynex 272 and saponification for recovery of scandium from dilute PLS as it has high economic value.

2. The impact of TBP on all the rare earth elements other than lanthanum, gadolinium and yttrium should be studied, with focus on elements having high economic value such as dysprosium and scandium. A systematic study on the impact of other phase modifier such as 1-octanol and Isodecanol will significantly contribute for the process development of REE separation using solvent extraction.

3. The enhanced selectivity for individual REE as well as REE from contaminants should be validated on a continuous basis by running the tests for different concentration of TBP in the organic phase. As the enhanced selectivity of the REE separation would enable the separation to be made in fewer number of stages, there should be a cost-benefit analysis of using TBP as a phase modifier in separation of REEs.

4. The predictive model developed for the single element should be developed further and validated for elements other than lanthanum. There is a requirement for development of a library of values of the equilibrium constant and the constant λ for each metal. The model should be expanded to include multi-species solutions and the impact of different diluent having different polarities in the organic phase on the apparent equilibrium coefficients should be considered.

5. Process models using linear analysis should be developed for predicting the steady state of a continuous solvent extraction plant based on thermodynamically predicted distribution coefficient. The process model can be used to design new SX processes and developing and controlling test systems. The process model coupled with the predictive model for distribution coefficient will be a very useful tool to design a SX process plant without experimental data regarding the metals.

REFERENCES

1. Seredin, V., *A new method for primary evaluation of the outlook for rare earth element ores.* Geology of Ore deposits, 2010. **52**(5): p. 428-433.
2. Zhang, W., M. Rezaee, A. Bhagavatula, Y. Li, J. Groppo, and R. Honaker, *A Review of the Occurrence and Promising Recovery Methods of Rare Earth Elements from Coal and Coal By-Products.* International Journal of Coal Preparation and Utilization, 2015. **35**(6): p. 295-330.
3. Luttrell, G.H., M.J. Kiser, R.-H. Yoon, A. Noble, M. Rezaee, A. Bhagavatula, and R.Q. Honaker, *A Field Survey of Rare Earth Element Concentrations in Process Streams Produced by Coal Preparation Plants in the Eastern USA.* Mining, Metallurgy & Exploration, 2019. **36**(5): p. 889-902.
4. Krishnamurthy, N. and C.K. Gupta, *Extractive metallurgy of rare earths*. 2004: CRC press.
5. Xie, F., T.A. Zhang, D. Dreisinger, and F.J.M.E. Doyle, *A critical review on solvent extraction of rare earths from aqueous solutions.* 2014. **56**: p. 10-28.
6. Abreu, R.D. and C.A. Morais, *Study on separation of heavy rare earth elements by solvent extraction with organophosphorus acids and amine reagents.* Minerals Engineering, 2014. **61**: p. 82-87.
7. Jha, M.K., A. Kumari, R. Panda, J.R. Kumar, K. Yoo, and J.Y.J.H. Lee, *Review on hydrometallurgical recovery of rare earth metals.* 2016. **165**: p. 2-26.
8. Binnemans, K., P.T. Jones, B. Blanpain, T. Van Gerven, Y. Yang, A. Walton, and M. Buchert, *Recycling of rare earths: a critical review.* Journal of Cleaner Production, 2013. **51**: p. 1-22.
9. Binnemans, K., P.T. Jones, K. Van Acker, B. Blanpain, B. Mishra, and D. Apelian, *Rare-Earth Economics: The Balance Problem.* JOM, 2013. **65**(7): p. 846-848.
10. Taylor, S.R., *Abundance of chemical elements in the continental crust: a new table.* Geochimica et Cosmochimica Acta, 1964. **28**(8): p. 1273-1285.
11. Henderson, P., *General geochemical properties and abundances of the rare earth elements*, in *Developments in geochemistry*. 1984, Elsevier. p. 1-32.
12. Taylor, S.R. and S.M. McLennan, *The continental crust: Its composition and evolution*. 1985: Blackwell Scientific Pub.,Palo Alto, CA; None. Medium: X; Size: Pages: 328.
13. Elderfield, H., *The oceanic chemistry of the rare-earth elements.* Philosophical Transactions of the Royal Society of London. Series A, Mathematical and Physical Sciences, 1988. **325**(1583): p. 105-126.
14. Cotton, S., *Lanthanide and actinide chemistry*. 2013: John Wiley & Sons.
15. Küchle, W., M. Dolg, and H. Stoll, *Ab initio study of the lanthanide and actinide contraction.* The Journal of Physical Chemistry A, 1997. **101**(38): p. 7128-7133.
16. Geoffrey N áCloke, F., *Zero oxidation state compounds of scandium, yttrium, and the lanthanides.* Chemical Society Reviews, 1993. **22**(1): p. 17-24.
17. Choppin, G.R. and S.L. Bertha, *Lanthanide complexation: Inner versus outer sphere.* Journal of Inorganic and Nuclear Chemistry, 1973. **35**(4): p. 1309-1312.
18. Moeller, T., *The Chemistry of the Lanthanides*. 1973.

19. Wang, W. and C.Y. Cheng, *Separation and purification of scandium by solvent extraction and related technologies: a review.* Journal of Chemical Technology & Biotechnology, 2011. **86**(10): p. 1237-1246.
20. Li, D., Y. Zuo, and S. Meng, *Separation of thorium(IV) and extracting rare earths from sulfuric and phosphoric acid solutions by solvent extraction method.* Journal of Alloys and Compounds, 2004. **374**(1): p. 431-433.
21. Spedding, F.H., A.F. Voigt, E.M. Gladrow, N.R. Sleight, J.E. Powell, J.M. Wright, T.A. Butler, and P. Figard, *The Separation of Rare Earths by Ion Exchange.1,2 II. Neodymium and Praseodymium.* Journal of the American Chemical Society, 1947. **69**(11): p. 2786-2792.
22. Sui, N., K. Huang, C. Zhang, N. Wang, F. Wang, H.J.I. Liu, and E.C. Research, *Light, middle, and heavy rare-earth group separation: a new approach via a liquid–liquid–liquid three-phase system.* 2013. **52**(17): p. 5997-6008.
23. Parhi, P.K., K.H. Park, C.W. Nam, and J.T. Park, *Liquid-liquid extraction and separation of total rare earth (RE) metals from polymetallic manganese nodule leaching solution.* Journal of Rare Earths, 2015. **33**(2): p. 207-213.
24. Damhus, T., R. Hartshorn, and A. Hutton, *Nomenclature of inorganic chemistry: IUPAC recommendations 2005.* CHEMISTRY International, 2005.
25. Ichihashi, H., H. Morita, and R. Tatsukawa, *Rare earth elements (REEs) in naturally grown plants in relation to their variation in soils.* Environmental Pollution, 1992. **76**(2): p. 157-162.
26. Kynicky, J., M.P. Smith, and C. Xu, *Diversity of rare earth deposits: the key example of China.* Elements, 2012. **8**(5): p. 361-367.
27. Goodenough, K.M., F. Wall, and D.J.N.R.R. Merriman, *The rare earth elements: demand, global resources, and challenges for resourcing future generations.* 2018. **27**(2): p. 201-216.
28. Gupta, T., T. Ghosh, G. Akdogan, and S. Bandopadhyay, *Maximizing REE Enrichment by Froth Flotation of Alaskan Coal Using Box-Behnken Design.* Mining, Metallurgy & Exploration, 2019. **36**(3): p. 571-578.
29. Wallace, M.E. and D.H. Green, *An experimental determination of primary carbonatite magma composition.* Nature, 1988. **335**(6188): p. 343.
30. Xu, C., I.H. Campbell, J. Kynicky, C.M. Allen, Y. Chen, Z. Huang, and L. Qi, *Comparison of the Daluxiang and Maoniuping carbonatitic REE deposits with Bayan Obo REE deposit, China.* Lithos, 2008. **106**(1-2): p. 12-24.
31. Willett, G., R. Duncan, and R. Rankin. *Geology and economic evaluation of the Mt Weld carbonatite, Laverton, Western Australia*. in *International Kimberlite Conference: Extended Abstracts*. 1986.
32. Lottermoser, B., *Rare-earth element mineralisation within the Mt. Weld carbonatite laterite, Western Australia.* Lithos, 1990. **24**(2): p. 151-167.
33. Castor, S.B., *The Mountain Pass rare-earth carbonatite and associated ultrapotassic rocks, California.* The Canadian Mineralogist, 2008. **46**(4): p. 779-806.
34. Dostal, J., *Rare metal deposits associated with alkaline/peralkaline igneous rocks.* Rev. Econ. Geol, 2016. **18**: p. 33-54.
35. Hedrick, J.B., S.P. Sinha, and V.D. Kosynkin, *Loparite, a rare-earth ore (Ce, Na, Sr, Ca)(Ti, Nb, Ta, Fe+3)O3.* Journal of Alloys and Compounds, 1997. **250**(1): p. 467-470.

36. Machacek, E. and N. Fold, *Alternative value chains for rare earths: The Anglo-deposit developers.* Resources Policy, 2014. **42**: p. 53-64.
37. Machacek, E. and P. Kalvig, *Assessing advanced rare earth element-bearing deposits for industrial demand in the EU.* Resources Policy, 2016. **49**: p. 186-203.
38. Jaireth, S., D.M. Hoatson, and Y. Miezitis, *Geological setting and resources of the major rare-earth-element deposits in Australia.* Ore Geology Reviews, 2014. **62**: p. 72-128.
39. Golev, A., M. Scott, P.D. Erskine, S.H. Ali, and G.R. Ballantyne, *Rare earths supply chains: Current status, constraints and opportunities.* Resources Policy, 2014. **41**: p. 52-59.
40. Zhou, B., Z. Li, and C. Chen, *Global potential of rare earth resources and rare earth demand from clean technologies.* Minerals, 2017. **7**(11): p. 203.
41. Randive, K. and S. Jawadand, *Strategic minerals in India: present status and future challenges.* Mineral Economics, 2019: p. 1-16.
42. Vahidi, E., J. Navarro, and F. Zhao, *An initial life cycle assessment of rare earth oxides production from ion-adsorption clays.* Resources, Conservation and Recycling, 2016. **113**: p. 1-11.
43. Yang, X.J., A. Lin, X.-L. Li, Y. Wu, W. Zhou, and Z. Chen, *China's ion-adsorption rare earth resources, mining consequences and preservation.* Environmental Development, 2013. **8**: p. 131-136.
44. Papangelakis, V.G. and G. Moldoveanu. *Recovery of rare earth elements from clay minerals*. in *European Rare Earth Resource Conference*. 2014.
45. Rollat, A., D. Guyonnet, M. Planchon, and J. Tuduri, *Prospective analysis of the flows of certain rare earths in Europe at the 2020 horizon.* Waste management, 2016. **49**: p. 427-436.
46. Humphries, M., *Rare earth elements: the global supply chain*. 2013, Congressional Research Service Washington, DC.
47. Sadri, F., A.M. Nazari, and A. Ghahreman, *A review on the cracking, baking and leaching processes of rare earth element concentrates.* Journal of Rare Earths, 2017. **35**(8): p. 739-752.
48. Voncken, J.H.L., *The rare earth elements: an introduction*. 2016: Springer.
49. Jordens, A., Y.P. Cheng, and K.E. Waters, *A review of the beneficiation of rare earth element bearing minerals.* Minerals Engineering, 2013. **41**: p. 97-114.
50. Houot, R., *Beneficiation of phosphatic ores through flotation: review of industrial applications and potential developments.* International Journal of Mineral Processing, 1982. **9**(4): p. 353-384.
51. Aplan, F., *The processing of rare earth minerals.* Rare Earths: Extraction, Preparation and Applications, 1989: p. 15-34.
52. Gramaccioli, C. and T. Segalstad, *A uranium-and thorium-rich monazite from a south-alpine pegmatite at Piona, Italy.* American Mineralogist, 1978. **63**(7-8): p. 757-761.
53. Kumari, A., R. Panda, M.K. Jha, J.R. Kumar, and J.Y. Lee, *Process development to recover rare earth metals from monazite mineral: A review.* Minerals Engineering, 2015. **79**: p. 102-115.
54. Koch, D., *Rare earth extraction and separation.* Mater. Australas., 1987. **19**(4): p. 12-15.

55. Hart, K. and D. Levins. *Management of wastes from the processing of rare earth minerals*. in *Chemeca 88: Australia's Bicentennial International Conference for the Process Industries; Preprints of Papers*. 1988. Institution of Engineers, Australia.
56. Calkins, G.D. and E.G. Bohlmann, *Processing of monazite sand*. 1957, Google Patents.
57. Abreu, R.D. and C.A. Morais, *Purification of rare earth elements from monazite sulphuric acid leach liquor and the production of high-purity ceric oxide.* Minerals Engineering, 2010. **23**(6): p. 536-540.
58. Bril, K. and P. Krumholz, *Developments in thorium production technology*. 1964, Brazil. Instituto de Energia Atomica, Sao Paulo.
59. Moldoveanu, G. and V. Papangelakis, *An overview of rare-earth recovery by ion-exchange leaching from ion-adsorption clays of various origins.* Mineralogical Magazine, 2016. **80**(1): p. 63-76.
60. Chi, R., J. Tian, X. Luo, Z. Xu, and Z. He, *The basic research on the weathered crust elution-deposited rare earth ores.* Nonferrous Metals Science and Engineering, 2012. **3**(4): p. 1-13.
61. Bautista, R.G., *Separation chemistry.* Handbook on the Physics and Chemistry of Rare Earths, 1995. **21**: p. 1-27.
62. Sato, T., *Liquid-liquid extraction of rare-earth elements from aqueous acid solutions by acid organophosphorus compounds.* Hydrometallurgy, 1989. **22**(1): p. 121-140.
63. Peppard, D., W. Driscoll, R. Sironen, and S. McCarty, *Nonmonotonic ordering of lanthanides in tributyl phosphate-nitric acid extraction systems.* Journal of Inorganic and Nuclear Chemistry, 1957. **4**(5-6): p. 326-333.
64. Seredin, V.V. and S.J.I.J.o.C.G. Dai, *Coal deposits as potential alternative sources for lanthanides and yttrium.* 2012. **94**: p. 67-93.
65. Arya, S., J. Sottile, J.P. Rider, J.F. Colinet, T. Novak, and C. Wedding, *Design and experimental evaluation of a flooded-bed dust scrubber integrated into a longwall shearer.* Powder technology, 2018. **339**: p. 487-496.
66. Arya, S., J. Sottile, and T. Novak, *Development of a flooded-bed scrubber for removing coal dust at a longwall mining section.* Safety Science, 2018. **110**: p. 204-213.
67. Arya, S., T. Novak, K. Saito, A. Levy, and J. Sottile, *Empirical Formulae for Determining Pressure Drop Across a 20-Layer Flooded-Bed Scrubber Screen.* Mining, Metallurgy & Exploration, 2019: p. 1-9.
68. Birk, D.J.C.J.o.E.S., *Quantitative coal mineralogy of the Sydney Coalfield, Nova Scotia, Canada, by scanning electron microscopy, computerized image analysis, and energy-dispersive X-ray spectrometry.* 1990. **27**(2): p. 163-179.
69. Honaker, R.Q., W. Zhang, X. Yang, and M. Rezaee, *Conception of an integrated flowsheet for rare earth elements recovery from coal coarse refuse*. Minerals Engineering, 2018. **122**: p. 233-240.
70. Honaker, R., W. Zhang, J.J.E. Werner, and Fuels, *Acid Leaching of Rare Earth Elements from Coal and Coal Ash: Implications for Using Fluidized Bed Combustion to Assist in the Recovery of Critical Materials.* 2019.
71. Zhang, W., J. Groppo, and R. Honaker. *Ash beneficiation for REE recovery*. in *2015 World Coal Ash Conference, Nashville, TN*. 2015.
72. Zhang, W. and R.Q. Honaker, *Rare earth elements recovery using staged precipitation from a leachate generated from coarse coal refuse.* International Journal of Coal Geology, 2018. **195**: p. 189-199.

73. Yang, X., *Leaching Characteristics of Rare Earth Elements from Bituminous Coal-Based Sources* in *Department of Mining Engineering*. 2019, University of Kentucky: Lexington.
74. Preston, J., P. Cole, W. Craig, and A.J.H. Feather, *The recovery of rare earth oxides from a phosphoric acid by-product. Part 1: Leaching of rare earth values and recovery of a mixed rare earth oxide by solvent extraction.* 1996. **41**(1): p. 1-19.
75. Aly, M.M. and N.A. Mohammed, *Recovery of lanthanides from Abu Tartur phosphate rock, Egypt.* Hydrometallurgy, 1999. **52**(2): p. 199-206.
76. Meyer, L. and B. Bras. *Rare earth metal recycling*. in *Proceedings of the 2011 IEEE International Symposium on Sustainable Systems and Technology*. 2011.
77. Xu, T., X. Zhang, Z. Lin, B. LÜ, C. Ma, and X. Gao, *Recovery of rare earth and cobalt from Co-based magnetic scraps.* Journal of Rare Earths, 2010. **28**: p. 485-488.
78. Rao, Y.R. and S. Acharya, *A rapid titrimetric determination of D2EHPA and M2EHPA.* Hydrometallurgy, 1993. **32**(1): p. 129-135.
79. Alamdari, E.K., D. Darvishi, S. Sadrnezhaad, Z.M.h. Shabestari, A. O'hadizadeh, and M. Akbari. *Effect of TBP as a modifier for extraction of zinc and cadmium with a mixture of DEHPA and MEHPA*. in *SOLE KC, COLE PM, PRESTON JS, ROBINSON D J. Proc Int Conf Solvent Extraction Conference. Johannesburg: S Afr Inst Min & Metall*. 2002.
80. Ferdowsi, A. and H. Yoozbashizadeh, *Solvent Extraction of Rare Earth Elements from a Nitric Acid Leach Solution of Apatite by Mixtures of Tributyl Phosphate and Di-(2-ethylhexyl) Phosphoric Acid.* Metallurgical and Materials Transactions B, 2017. **48**(6): p. 3380-3387.
81. Fatmehsari, D.H., D. Darvishi, S. Etemadi, A.E. Hollagh, E.K. Alamdari, and A. Salardini, *Interaction between TBP and D2EHPA during Zn, Cd, Mn, Cu, Co and Ni solvent extraction: A thermodynamic and empirical approach.* Hydrometallurgy, 2009. **98**(1-2): p. 143-147.
82. Batchu, N.K., C.H. Sonu, and M.S. Lee, *Solvent extraction equilibrium and modeling studies of manganese from sulfate solutions by a mixture of Cyanex 301 and TBP.* Hydrometallurgy, 2014. **144**: p. 1-6.
83. Ghadiri, M., S.N. Ashrafizadeh, and M. Taghizadeh, *Study of molybdenum extraction by trioctylamine and tributylphosphate and stripping by ammonium solutions.* Hydrometallurgy, 2014. **144**: p. 151-155.
84. Azizitorghabeh, A., F. Rashchi, A. Babakhani, and M. Noori, *Synergistic extraction and separation of Fe (III) and Zn (II) using TBP and D2EHPA.* Separation Science and Technology, 2017. **52**(3): p. 476-486.
85. Cheraghi, A., M.S. Ardakani, E.K. Alamdari, D.H. Fatmesari, D. Darvishi, and S.K. Sadrnezhaad, *Thermodynamics of vanadium (V) solvent extraction by mixture of D2EHPA and TBP.* International Journal of Mineral Processing, 2015. **138**: p. 49-54.
86. Sahu, K. and R. Das, *Synergistic extraction of iron (III) at higher concentrations in D2EHPA-TBP mixed solvent systems.* Metallurgical and Materials Transactions B, 1997. **28**(2): p. 181-189.
87. Ahmadipour, M., F. Rashchi, B. Ghafarizadeh, and N. Mostoufi, *Synergistic effect of D2EHPA and Cyanex 272 on separation of zinc and manganese by solvent extraction.* Separation Science and Technology, 2011. **46**(15): p. 2305-2312.

88. Barnard, K., N. Kelly, and D. Shiers, *Chemical reactivity between bis (2-ethylhexyl) phosphoric acid (DEHPA) and tributyl phosphate.* Hydrometallurgy, 2014. **146**: p. 1-7.
89. Sato, T., *The extraction of uranium (VI) from hydrochloric acid solutions by di-(2-ethylhexyl)-phosphoric acid.* Journal of Inorganic and Nuclear Chemistry, 1965. **27**(8): p. 1853-1860.
90. Kraikaew, J., W. Srinuttrakul, and C. Chayavadhanakur, *Solvent Extraction Study of Rare Earths from Nitrate Medium by the Mixtures of TBP and D 2 EHPA in Kerosene.* Journal of metals, materials and minerals, 2005. **15**(2): p. 89-95.
91. Peppard, D., G. Mason, J. Maier, and W. Driscoll, *Fractional extraction of the lanthanides as their di-alkyl orthophosphates.* Journal of Inorganic and Nuclear Chemistry, 1957. **4**(5-6): p. 334-343.
92. Peppard, D.F., J. Ferraro, and G. Mason, *Hydrogen bonding in organophosphoric acids.* Journal of Inorganic and Nuclear Chemistry, 1958. **7**(3): p. 231-244.
93. Baker, H. and C. Baes Jr, *An infra-red and isopiestic investigation of the interaction between di (2-ethylhexyl) phosphoric acid and tri-n-octylphosphine oxide in octane.* Journal of Inorganic and Nuclear Chemistry, 1962. **24**(10): p. 1277-1286.
94. Kosinski, F. and H. Bostian, *Lanthanum solvent extraction mechanisms using di-(2-ethylhexyl) phosphoric acid.* Journal of Inorganic and Nuclear Chemistry, 1969. **31**(11): p. 3623-3631.
95. Hoh, Y.-C., M. Nevarez, and R.G. Bautista, *A Predictive Thermodynamic Model for the Distribution Coefficients of Neodymium in the Nd (No3) 3-HNO3-H2O-1 M HDEHP-Amsco Liquid-Liquid Extraction System.* Industrial & Engineering Chemistry Process Design and Development, 1978. **17**(1): p. 88-91.
96. O'BRIEN, W.G. and R.G. BAUTISTA, *Activity behavior of the NdNO 3--HNO 3--H 2 O--HDEHP--AMSCO System*. 1978, ACS Publications.
97. Ioannou, T.K., *Prediction of equilibrium data for the solvent extraction system SmCl3-NdCl3-CeCl3-HCl-H2O with the extractant DI-(2-ethylhexyl) phosphoric acid in Amsco.* 1970.
98. Noirot, P. and M. Wozniak, *Computing of liquid-liquid equilibria. I. Application of a general chemical model to the extraction of uranium from phosphoric acid by a hydroxyalkyldiphosphonic acid.* Hydrometallurgy, 1985. **13**(3): p. 229-248.
99. Rao, L. and G. Tian, *Complexation of lanthanides with nitrate at variable temperatures: thermodynamics and coordination modes.* Inorganic chemistry, 2008. **48**(3): p. 964-970.
100. Krumholz, P., *Spectroscopic studies on rare-earth compounds—II: A comparative study of the absorption spectra of the neodymium ion in aqueous solution and in crystalline salts.* Spectrochimica Acta, 1958. **10**(3): p. 274-280.
101. Goto, T. and M. Smutz, *Stability constants of lighter lanthanide (III) chloride complexes by a potentiometric method.* Journal of Inorganic and Nuclear Chemistry, 1965. **27**(3): p. 663-671.
102. Khopkar, P. and P. Narayanankutty, *Effect of ionic media on the stability constants of chloride, nitrate and thiocyanate complexes of americium (III) and europium (III).* Journal of inorganic and nuclear chemistry, 1971. **33**(2): p. 495-502.

103. Peppard, D., G. Mason, and I. Hucher, *Stability constants of certain lanthanide (III) and actinide (III) chloride and nitrate complexes.* Journal of Inorganic and Nuclear Chemistry, 1962. **24**(7): p. 881-888.
104. Choppin, G.R. and W.F. Strazik, *Complexes of trivalent lanthanide and actinide ions. I. Outer-sphere ion pairs.* Inorganic Chemistry, 1965. **4**(9): p. 1250-1254.
105. Coward, N.A. and R.W. Kiser, *A Spectrophotometric Study of the Nd3+-NO3- Association1*. The Journal of Physical Chemistry, 1966. **70**(1): p. 213-217.
106. McKay, H. and J. Woodhead, *142. A spectrophotometric study of the nitrate complexes of uranium (IV).* Journal of the Chemical Society (Resumed), 1964: p. 717-723.
107. Ahrland, S. and R. Larsson, *The complexity of uranium (IV) chloride, bromide and thiocyanate.* Acta chem. scand, 1954. **8**(2): p. 1.
108. Sharp, B.M. and M. Smutz, *Stagewise Calculation for Solvent Extraction System Monazite Rare Earth Nitrates-Nitric Acid-Tributyl Phosphate-Water.* Industrial & Engineering Chemistry Process Design and Development, 1965. **4**(1): p. 49-54.
109. Forrest, C. and M. Hughes, *The modelling of equilibrium data for the liquid-liquid extraction of metals Part I. A survey of existing models.* Hydrometallurgy, 1975. **1**(1): p. 25-37.
110. Alstad, J., J. Augustson, T. Danielssen, and L. Farbu. *A comparative study of the rare earth elements in extraction by HDEHP/Shell Sol T from nitric and sulfuric acid solution*. in *Solvent extraction proceedings of the international solvent extraction conference, ISEC 74, Lyon, 8-14th September 1974*. 1974.
111. Goto, T. *CALCULATION OF COUNTER-CURRENT EXTRACTION OF LANTHANIDES WITH A DIGITAL COMPUTER*. in *pp 1011-24 of Proceedings of the International Solvent Extraction Conference. Vol. I and II. London Society of Chemical Industry (1971)*. 1971. Government Chemical Industrial Research Inst., Tokyo.
112. Lloyd, P. and M. Oertel. *A theoretical basis for the evaluation of long chain amine extractants*. in *International Symposium on Hydrometallurgy*. 1963. Gordon and Breach NY.
113. O'Brien, W.G., *Rare earth ion activities by static vapor and specific ion electrode measurements with application to a single component solvent extraction system.* 1974.
114. Nevarez, M. and R. Bautista, *Thermodynamic equilibrium model to predict the cobalt distribution coefficient in the CoCl 2--HCl--H 2 O--TBP liquid--liquid extraction system*. 1976, Ames Lab.
115. Hoh, Y.-C. and R.G. Bautista, *Chemically based model to predict distribution coefficients in the Cu-LIX 65N and Cu-KELEX 100 systems.* Metallurgical Transactions B, 1978. **9**(1): p. 69-75.
116. Giles, A. and C. Aldrich, *Modelling of rare earth solvent extraction with artificial neural nets.* Hydrometallurgy, 1996. **43**(1-3): p. 241-255.
117. Han, K.-S., K. Tozawa, and Y.-S. Kim, *Extraction Behavior and Prediction of Distribution Coefficients for the Lanthanum Chloride--Hydrochloric Acid--Acidic Organophosphorus Compound Systems.* Bull. Res. Inst. Miner. Dressing Metall., 1987. **43**(2): p. 184-194.
118. Ioannou, T.K., R.G. Bautista, and M. Smutz, *CORRELATING MULTICOMPONENT EQUILIBRIUM DATA FOR THE EXTRACTION OF LANTHANIDES WITH DI (2-ETHYLHEXYL) PHOSPHORIC ACID AS THE SOLVENT*. 1972, Ames Lab., Iowa.

119. Han, K. and K. Tozawa, *Thermodynamic prediction of distribution coefficients for the solvent extraction of the rare earth metals*, in *Rare earths*. 1988.
120. Valian, A., J.G. Groppo, C.F. Eble, S.F. Greb, J.C. Hower, and R.Q. Honaker. *SPATIAL AND TEMPORAL TRENDS OF RARE EARTH ELEMENT ABUNDANCE IN ILLINOIS BASIN COAL BEDS*. in *GSA Annual Meeting in Phoenix, Arizona, USA-2019*. 2019. GSA.
121. Wang, L., X. Huang, Y. Yu, and Z. Long, *Kinetics of rare earth pre-loading with 2-ethylhexyl phosphoric acid mono 2-ethylhexyl ester [HEH (EHP)] using rare earth carbonates.* Separation and Purification Technology, 2014. **122**: p. 490-494.
122. Webster, S., *Solvent Extraction Pilot Plant*, S. Kinetics, Editor. 2018: 39 A Hamilton Ave., Cobourg, ON, Canada.
123. Li, X., C. Wei, Z. Deng, M. Li, C. Li, and G. Fan, *Selective solvent extraction of vanadium over iron from a stone coal/black shale acid leach solution by D2EHPA/TBP*. Hydrometallurgy, 2011. **105**(3-4): p. 359-363.
124. Cheng, C.Y., *Purification of synthetic laterite leach solution by solvent extraction using D2EHPA.* Hydrometallurgy, 2000. **56**(3): p. 369-386.
125. Allen, D.M. and H.J. Almond, *Characterisation of aqueous ferric chloride etchants used in industrial photochemical machining.* Journal of Materials Processing Technology, 2004. **149**(1-3): p. 238-245.
126. Dalton, R. and K. Severs, *Advances in solvent extraction for copper by optimized use of modifiers*, in *Mining Latin America/Minería Latinoamericana*. 1986, Springer. p. 67-75.
127. Zhang, W. and R.Q.J.I.J.o.C.G. Honaker, *Rare earth elements recovery using staged precipitation from a leachate generated from coarse coal refuse.* 2018. **195**: p. 189-199.
128. Ochsenkühn-Petropoulou, M.T., K.S. Hatzilyberis, L.N. Mendrinos, and C.E. Salmas, *Pilot-plant investigation of the leaching process for the recovery of scandium from red mud.* Industrial & engineering chemistry research, 2002. **41**(23): p. 5794-5801.
129. Wang, W., Y. Pranolo, and C.Y. Cheng, *Metallurgical processes for scandium recovery from various resources: A review.* Hydrometallurgy, 2011. **108**(1): p. 100-108.
130. Ochsenkühn-Petropulu, M., T. Lyberopulu, and G. Parissakis, *Selective separation and determination of scandium from yttrium and lanthanides in red mud by a combined ion exchange/solvent extraction method.* Analytica Chimica Acta, 1995. **315**(1-2): p. 231-237.
131. Akcil, A., N. Akhmadiyeva, R. Abdulvaliyev, Abhilash, and P. Meshram, *Overview on extraction and separation of rare earth elements from red mud: focus on scandium.* Mineral Processing and Extractive Metallurgy Review, 2018. **39**(3): p. 145-151.
132. Wang, D., J. Wu, Y. Li, S. Weng, P. Wu, and G. Xu, *Mechanism of extractant loss in solvent extraction process (I)-Transfer of saponified D2EHPA from organic phase to aqueous phase and its aggregation behaviour.* Science in China (Scienctia Sinica) Series B, 1995. **11**(38): p. 1281-1287.
133. Kertes, A., *CHEMISTRY OF THE FORMATION AND ELIMINATION OF A THIRD PHASE IN ORGANOPHOSPHORUS AND AMINE EXTRACTION SYSTEMS*. 1968, Hebrew Univ., Jerusalem.

134. Taghizadeh, M., R. Ghasemzadeh, M.G. Maragheh, and S. Ashrafizadeh, *Crud formation in the solvent extraction system Zr (IV), HNO3-D2EHPA.* Mineral Processing & Extractive Metallurgy Review, 2009. **30**(3): p. 260-268.
135. Baes Jr, C., *The synergistic effects in organophosphate extraction systems.* Nuclear Science and Engineering, 1963. **16**(4): p. 405-412.
136. Preez, A.d., J.J.S.E. S Preston, and I. Exchange, *The solvent extraction of rare-earth metals by carboxylic acids.* 1992. **10**(2): p. 207-230.
137. Marcus, Y., *Anion exchange of metal complexes—XV (1): Anion exchange and amine extraction of lanthanides and trivalent actinides from chloride solutions.* Journal of Inorganic and Nuclear Chemistry, 1966. **28**(1): p. 209-219.
138. Fomin, V., B. Kartushova, and T. Budenko, *Determination of stability constants of cefNOa)^-* ions by extraction with tributyl phosphate.* Zhr. Neogh. Khim, 1958. **3**: p. 2117-2127.
139. Bromley, L.A., *Thermodynamic properties of strong electrolytes in aqueous solutions.* AIChE Journal, 1973. **19**(2): p. 313-320.

VITA

Education

Indian School of Mines, Dhanbad

B.Tech in Mineral Engineering, June 2013

Area of Expertise

Mineral processing, Hydrometallurgy, Extractive Metallurgy, Solvent extraction

Research Experience

08/2015-12/2019, Research Assistant, Department of Mining Engineering, University of Kentucky, Lexington, KY, USA

Projects

Design and development of rare earths recovery and production from coal sources. (2016-now)

- Kinetics study of rare earth leaching and process rate control.
- Flowsheet development including size reduction, froth flotation, leaching, solvent extraction, and precipitation to produce high purity rare earth oxide.
- Commissioning and operation of ¼ tph pilot scale facility and its optimization.

Industrial Experience

Process Engineer – Mineral Engineering, Rampura Agucha Mines, India (June 2013- July 2015*)*

- Incharge of process control, including Automation Control for the grinding and flotation circuit for the Lead-Zinc Beneficiation plant for the largest Lead-Zinc producing mine of South-East Asia.

- Part a team of 6 associates and engineers on projects to improve the overall metal recovery of the plant as well improving the quality of final product which included installation of Proflote in flotation circuit, upgrading the design of classifying cyclones.

Summer Intern- BCCL, Coal India Limited (May 2012 to June 2012*)*

Assisted in designing of production reporting sheets and ventilation surveys.

Summer Intern- Vishakhapatnam Integrated Steel (May, 2011 to June, 2011*)*

Studied the working of coke ovens, and coke dry cooling plants.

Publications/Patents

R Honaker, X Yang, A Chandra, W Zhang, J Werner (2018). "Hydrometallurgical Extraction of Rare Earth Elements from Coal." *Extraction 2018*, volume 81, 2309-2322.

R Honaker, A Chandra, J Werner "Continuous Solvent Extraction Process for Generation Of High Grade Rare Earth Oxides from Leachates Generated from Coal Sources" *U.S. Provisional Patent Serial Nos. 62/715,644 and 62/752,633*

Presentations

Chandra, Alind. Honaker, Rick. Werner, Joshua (2019). “Development of Continuous Operation of Recovery of Rare Earth Elements from Coal Based Leachates.” Paper presented at the SME Conference at Denver

Chandra, Alind. Honaker, Rick. Werner, Joshua (2019). “Acid Mine Drainage Treatment by Controlling the Oxidation Reduction Potential and pH of the Solution.” Paper presented at the SME Conference at Denver.

Chandra, Alind. Honaker, Rick. Werner, Joshua (2018). “High Grade Rare Earth Oxides Produced by Solvent Extraction from Leachates Produced from Coal Sources.” Paper presented at the SME Conference at Minneapolis.

Chandra, Alind. Honaker, Rick. (2017). “Contaminant Rejection from Dilute PLS generated from Coal Sources using SX.” Paper presented at the SME Conference at Denver.

Awards and Fellowships

ISEE student scholarship 2016

1st in technical poster contest, Environmental Division 2019 SME

2nd in technical poster contest, Mineral Processing Division 2019 SME

Professional Memberships

Society of Mining, Metallurgy and Exploration